UNIVERSITÉ DE STRASBOURG

Ecole Doctorale des Sciences de la Vie et de la Santé

IGBMC- Institut de génétique et de biologie moléculaire et cellulaire

THÈSE présentée par :

Olga BIELSKA

soutenue le : **21 Mars 2018**

pour obtenir le grade de : **Docteur de l'université de Strasbourg**

Discipline/ Spécialité : Aspects moléculaires et cellulaires de la biologie

The role of PKD in mitochondrial fission during mitosis

THÈSE dirigée par :

Mr RICCI Romeo Directeur de thèse

RAPPORTEURS :

Mme CHACINSKA Agnieszka Rapporteur externe

Mr ROSSIGNOL Rodrigue Rapporteur externe

AUTRE membre :

Mme SUMARA Izabela Examinateur interne

Acknowledgements

I wish to thank my thesis supervisior **Prof. Romeo Ricci** for this opportunity to discover science and magic world of PKD signalling. I am also very grateful for freedom with no limitations in research and for accepting me the way I am.

I am particularly grateful to **Dr. Izabela Sumara** for all your invaluable help in mitosis part of the project and for always useful inputs throughout my PhD. Thank you, Iza!

I would like to thank **Prof. Agnieszka Chacińska** and **Dr. Rodrigue Rossignol** for your kind agreement to be my committee members, to spend your priceless time reading and evaluating this thesis and to come so far to my defense. Thank you very much!

I am very grateful to **Dr. Yansheng Liu** and **Prof. Ruedi Aebersold**, our collaborators, for the the help with mass-spec and continuous readiness to collaborate!

I wish to acknowledge the **IGBMC International PhD Program** and the **LabEx** Sponsorship, which allowed me to conduct this work in one of the best research institutes in France. I am also grateful to **La Ligue contre le cancer**, which supported me financially during the fourth year of my PhD.

My thanks go to **Mustapha, Gilles** and **Pascal** and people from **IGBMC facilities** for their contribution to this project.

I would like to offer my thanks to **all alumni and current members of Ricci and Sumara labs**, whom I met during these four years. My special thanks go to **Zhirong**. Thank you for being there for me and teaching me loads of lab methods. I am also grateful to **Stephane** for his advices, tools and willingness to come to discuss. Thank you **Kevin, Adrien** and **Eric** for your invaluable help with French language, otherwise I would be „lost in translation“ ☺. Thank you **Helena** and **Martita** for supporting me and making positive atmosphere in the lab. Thank you **Gergo** for organizing our best lab retreats. Thanks to **Katka, Charlotte, Arantxa, Sushil, Eva, Zhengzhen** and **Yongrong!**

I wish to thank my friends **Lyuba, Sam, Katie, Gio, Liza** and many many others for these enjoyable years!

Table of contents

Detailed table of contents

1 Abbreviations

ADOA	Autosomal dominant optic atrophy
ADP	Adenosine diphosphate
AMP	Adenosine monophosphate
AMPK	AMP-activated protein kinase
APC/C	Anaphase-promoting complex/Cyclosome
ARF	ADP-rybosylation factor
ATM	Ataxia-telangiectasia mutated kinase
ATP	Adenosine triphosphate
ATR	Ataxia-telangiectasia related kinase
BSE	Bundle signaling element
CAMK	Calcium/calmodulin kinase family (CAMK)
CDK	Cyclin-dependent kinase
CERT	Ceramide transfer protein
CHK1	Checkpoint effector kinase 1
CMT2A	Charcot-Marie-Tooth type 2A
DAG	Diacylglycerol
DDR	DNA-damage response
ER	Endoplasmatic reticulum
GAP	GTPase-activating protein
GDP	Guanosine diphosphate
GEF	Guanine-nucleotide exchange factor
GFP	Green fluorescent protein
HDAC	Histone deacetylase
IB	Insert B
IM	Inner mitochondrial membrane
IMS	Intermembrane space
MEK1	MEK1 mitogen-activated protein kinase kinase
MICOS	Mitochondrial contact site and cristae organizing system

MIM	mitochondrial import (MIM) complex
MnSOD	Mitochondrial superoxide dismutase
MPP	mitochondrial processing peptidase (MPP)
mtDNA	Mitochondrial DNA
mTOR	Mammalian target of rapamycin
NADH	Nicotinamide adenine dinucleotide, reduced
NCR	Non-coding region
NE	Nuclear envelope
NFkB	Nuclear factor kappa-light-chain-enhancer of activated B cells
nPKCs	Novel Protein kinases C
OM	Outer mitochondrial membrane
OXPHOS	Oxidative phosphorylation
PH domain	Pleckstrin homology domain
PI4KIIIβ	Phosphatidylinositol-4 kinase IIIβ
PKC	Protein kinase C
PKD	Protein kinase D
PLC	Phospholipase C
PLD	Phospholipase D
PMA	Phorbol myristate acetate
PP1	Protein phosphatase 1
Raf	RAF proto-oncogene protein kinase
Ras	Rat sarcoma
ROS	Reactive oxygen species
SAM	Sorting and assembly complex
SM	Sphyngomyelin
SUMO	Small ubiquitin-like modifier
TA	Tail-anchored
TGN	Trans-Golgi network
TIM	Translocase of the inner membrane
TOM	Translocase of the outer membrane
VRK1	Vaccinia-related kinase

2 Introduction

2.1 Mitochondria

Mitochondria are specialized organelles, which are responsible for energy production in all eukaryotic organisms. Their origin stems from ancient endosymbionts related to α-proteobacteria (Gray et al., 1999; Lane and Martin, 2010). This fact explains some unique features of this organelle – a double membrane, its own circular genome, its ability to produce ATP via oxidative phosphorylation (OXPHOS). Mitochondrial membranes are morphologically and functionally distinct. The outer mitochondrial membrane (OM) is facing the cytosol and shares the intermembrane space (IMS) with the inner mitochondrial membrane (IM). The inner membrane forms folds or evaginations significantly increasing its surface compared to the outer membrane. These folds (termed "cristae") are compartmentalizing the mitochondrial matrix and contain the respiratory chain complexes. The self-autonomous but yet not self-sufficient mitochondrial genome is present in multiple copies in form of nucleoid structures located in the mitochondrial matrix. Compared to its putative ancestor, mitochondrial DNA (mtDNA) is greatly reduced with the majority of genes transferred to the nucleus. Human mtDNA (Fig. 1) covers around 16,6 kilobases and encodes 37 genes (Anderson et al., 1981; Andrews et al., 1999). These genes can be further translated into 13 proteins, 22 transfer RNAs (tRNAs) and 2 ribosomal RNAs (rRNAs).

Such productivity under limitation in size is explained by the mechanism of mitochondrial transcription, as it is polycistronic (Attardi et al., 1982). Mitochondrial genome replication and transcription is under control of the large (of about 1 kilobase) non-coding regulatory sequence within mtDNA called the mitochondrial displacement loop, i.e. the D-loop. Interestingly, the D-loop is not a double, but a triple-stranded region located in the major non-coding region (NCR). It is formed due to premature termination of mtDNA replication, which accounts for more than 95%

of all replication events (Doda et al., 1981). In that case, nascent mtDNA stably associates with a template, a short DNA chain known as 7S DNA (Brown et al., 1986; Pereira et al., 2008). And this is not the only surprise. Mitochondrial DNA helicase, TWINKLE, has high sequence similarity to the gene 4 protein, a bacteriophage T7 DNA helicase/primase (Spelbrink et al., 2001).

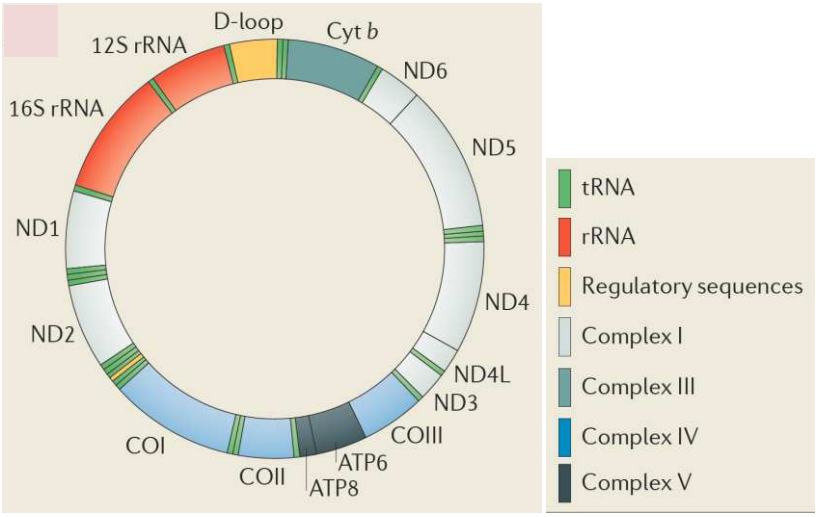

Introductory figure 1. Schematic illustration of mitochondrial genome with annotated genes and the regulatory sequence (D-loop) (Adapted from Mishra and Chan, 2014).

Although considered residual the mitochondrial genome still encodes some vital proteins. These are 13 subunits of OXPHOS protein complexes. The rest of the mitochondrial proteome comprises nuclear-encoded proteins, which are actively transported from the cytosol into mitochondrial compartments (Chacinska, 2017; Mokranjac and Neupert, 2007; Neupert and Herrmann, 2007; Wasilewski et al., 2017). The translocase of the outer membrane (TOM) complex is the main entrance point for mitochondrial precursor proteins into mitochondria. Unlike signal-anchored OM proteins (e.g., TOM20 and TOM70), which target OM through the mitochondrial import (MIM) complex, tail-anchored (TA) proteins (e.g., MFF and Fis1) may not require a dedicated import machinery, but rather rely on their incorporation based on specific lipid compositions within the OM. OM targeting of β-barrel proteins is mediated through the interaction between two big complexes - the sorting and assembly (SAM) complex and the mitochondrial contact site and cristae organizing system (MICOS). Transport of small proteins (e.g., Tim chaperons) into the IMS is mediated by mitochondrial IMS import and assembly (MIA) pathway. Yet the major way to

reach the mitochondrial matrix or IM constitutes the presequence translocase of the inner membrane multi subunit complex (TIM23), which recognizes a positively charged amino-terminal presequence of sorted proteins. This recognition-signal containing this presequence is later cleaved by mitochondrial processing peptidase (MPP). Protein translocation through TIM23 is an ATP-consuming process and is dependent on the presequence translocase-associated motor (PAM) complex. Those proteins that contain a transmembrane domain are sorted laterally by TIM23, but not PAM. Multi-pass transmembrane proteins destined to the IM are translocated by the TIM22 complex. This is the major translocase for metabolite carriers (e.g., ADP/ATP carriers) as well as IM translocase components. Such proteins contain multiple internal import signal sequences. Both TIM22 and TIM23 require $\Delta\Psi$ for efficient integration of carrier proteins. Several studies in yeast suggest that mitochondrial protein import machineries possibly co-evolved with the respiratory chain complexes (Wasilewski et al., 2017).

The respiratory chain complexes are formed from nuclearly encoded proteins and 13 mitochondrial subunits. They arrange into OXPHOS complexes I, II, III, IV, and V, with complex II being the only one entirely transcribed from nuclear genes (Fig. 2).

Complexes I, III, and IV actively transport protons from the mitochondrial matrix to the intermembrane space. This process is called electron transport and is required for generation of a pH gradient and an electrical potential across IM. This electro-chemical gradient creates a passive flow back down the gradient through Complex V (ATP synthase), which rotates the enzyme and powers ATP production in a phosphorylation reaction. ATP molecules travel back to the intermembrane space through the ATP-ADP translocase and then diffuse into the cytosol through the OMM. The OXPHOS pathway is 15-18 times more efficient in generating ATP

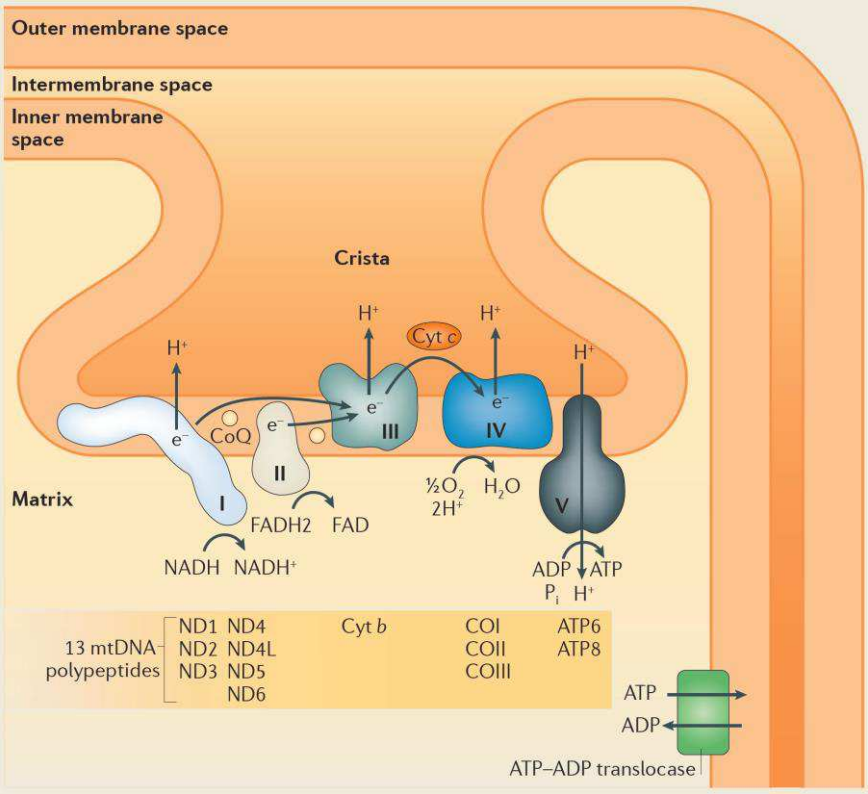

Introductory Fig.ure 2. Schematic illustration of the mitochondrial respiratory chain complexes, mtDNA encoded subunits are listed below. (Adapted from Mishra and Chan, 2014).

compared to glycolysis (Okuno et al., 2011). Thus, mitochondria are often referred to as "power plants" of the cell. But energy production is not the sole function of mitochondria. They also regulate calcium homeostasis, lipid biosynthesis and oxidation, the oxidative status of the cell, self-defense against pathogens, cell division and apoptosis.

2.1.1 Mitochondrial dynamics

While most biology textbooks depict the mitochondrion as a bean-shaped organelle, in reality, depending on the cell type, this form might be adopted by a small population of mitochondria and only at a certain period of time. The dynamic nature of mitochondria was first observed by Lewis as early as 1914 (Lewis and Lewis, 1914). They first described mitochondrial forms as "granule",

"rod" or "thread" and noticed that over time mitochondria may fuse or divide. With this simple observation, the new field of mitochondrial dynamics was born. Yet, only the discoveries of the past decades along with advances in molecular biology and confocal microscopy started to unveil the complexity behind the mitochondrial shape.

As mentioned above, mitochondria can be round and small or tubular or highly fused and branched and change their shape in response to different stimuli. Molecular machines that coordinate these changes rely on large GTPases of the dynamin superfamily. During the fusion process of two mitochondria, the outer mitochondrial membranes participate first followed by the inner mitochondrial membranes (Fig. 3).

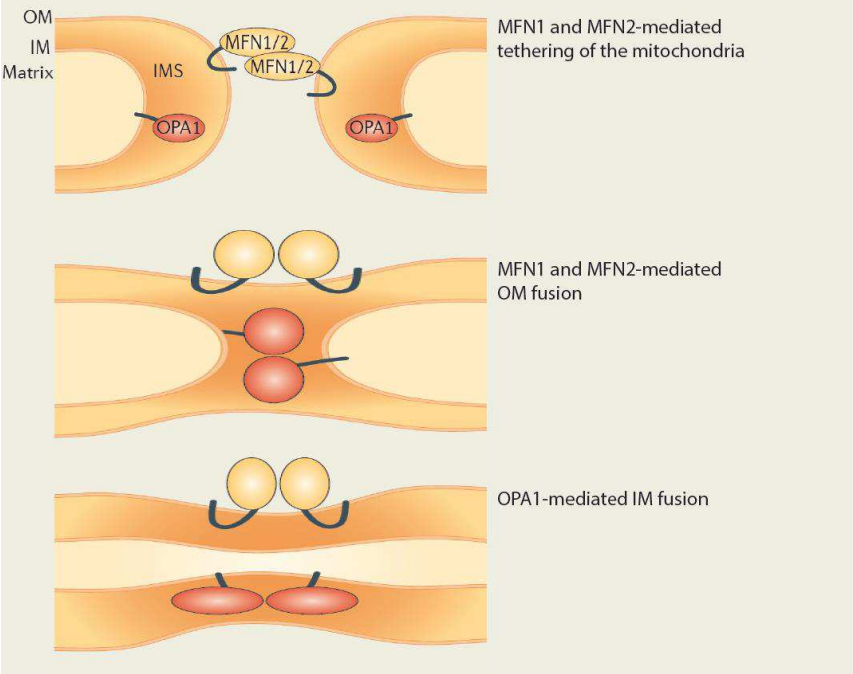

Introductory figure 3. Schematic illustration of the mechanism of mitochondrial fusion in mammalian cells (Adapted from (Mishra and Chan, 2014)

The first step of fusion requires tethering of two dynamin-related GTPases called mitofusins, Mfn1 and Mfn2. Mfn1 is only found on the mitochondrial outer membrane, whereas Mfn2 is located also on the ER. The second step is mediated by the Opa1 GTPase (Olichon et al., 2002; Song et al., 2009). Loss of function studies revealed that upon Mfn1 and Mfn2 deletion mitochondria look grossly

fragmented and show no outer membrane fusion, whereas cells lacking Opa1 can fuse outer mitochondrial membranes but cannot undergo fusion of their inner membranes (Meeusen et al., 2006; Song et al., 2009). Mitochondrial fusion allows separate mitochondria to connect, thereby facilitating exchange of mtDNA molecules and products of their transcription. Cells that are devoid of the mitochondrial fusion machinery (either Mfn1/2 null or Opa1 null) have a severe defect in respiratory capacity (Chen et al., 2005; Song et al., 2009). As each cell contains many copies of mtDNA, it may have mutated and wild-type DNA present at the same time. This feature of the mitochondrial genome is called heteroplasmy, and without active mitochondrial fusion it could entail detrimental effects. But instead, heteroplasmic cells carrying mtDNA with pathogenic mutations show no obvious phenotype until they reach a so called "threshold", which for certain mutations could be up to 90% of mutant mtDNA (Letellier et al., 1994; Rossignol et al., 2003) Thus, mitochondrial fusion ensures stability of mtDNA levels and enables cells to withstand high levels of mtDNA mutations.

In humans, mutations in Mfn2 and OPA1 are causatively associated with two neurodegenerative diseases—Charcot-Marie-Tooth type 2A (CMT2A) and autosomal dominant optic atrophy (ADOA), respectively (Alexander et al., 2000; Delettre et al., 2000; Zuchner et al., 2004). CMT2A is a primary peripheral axonal neuropathy resulting in muscle weakness and atrophy (Zuchner et al., 2004). ADOA is the most common inherited optic neuropathy characterized by progressive loss of vision due to loss of retinal ganglion cells and multiple deficiencies in nerve fibers. During disease progression vision is completely lost (Delettre et al., 2000). Total OPA1 knockout mice are embryonically lethal during organogenesis (E9-E13.5) and OPA heterozygosity in mice results in slower onset of optic nerve degeneration. Heterozygous mice are used as a model for OPA1 ADOA (Chen et al., 2012; Davies et al., 2007; Rahn et al., 2013). Mice homozygously deficient in either of mitofusins cannot survive midgestation and die *in utero* (Chen et al., 2003). Cerebellum-specific deletion of Mfn2 in mice results in neurodegeneration caused by defects in mitochondrial fusion (Chen et al., 2007).

Mitochondrial division (fission) (Fig. 4) constitutes the counterbalance process relying on the function of dynamin DYN2 and dynamin-related protein DRP1 (Lee et al., 2016; Smirnova et al., 2001; Smirnova et al., 1998). These two GTP-ases are present in the cytosol and need specific interactors to be recruited to the outer mitochondrial membrane. DRP1 has four mitochondrial receptors, whereas DYN2, has no to date described mitochondrial interactor. DYN2, unlike DRP1, contains instead a functional PH domain, which is proposed to facilitate its association with the membranes. Four DRP1 receptors differ not only structurally but also functionally. The major receptor is MFF. It recruits oligomeric DRP1 from the cytosol and this recruitment results in mitochondrial fission. Another receptor is Fis1, and it is important for apoptosis induced DRP1-dependent mitochondrial fragmentation. Two adaptor proteins MiD49 and Mid51 are believed to sequester inactive DRP1 dimers onto the mitochondrial surface and thus contribute to mitochondrial fusion. The endoplasmic reticulum (ER) is yet another important player in this process. Similar to mitochondrial fusion, mitochondrial fission is a sequential process.

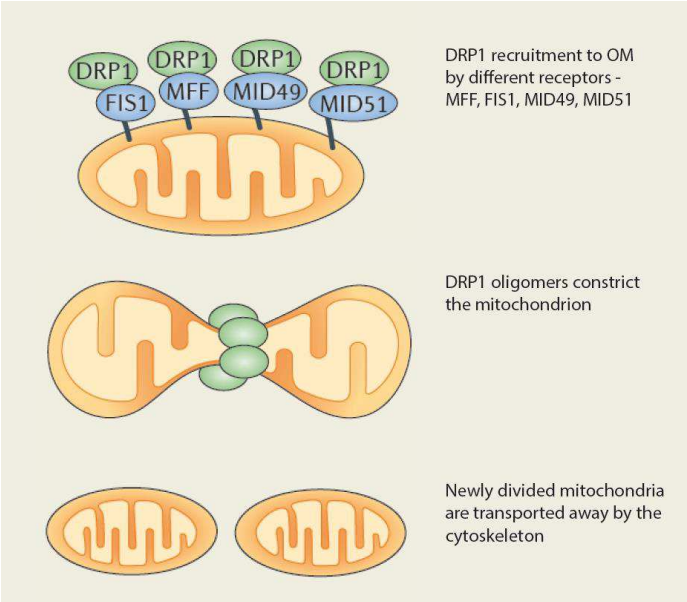

Introductory figure 4. Schematic illustration of the mechanism of mitochondrial fission in mammalian cells (Adapted from (Mishra and Chan, 2014)

The first step of mitochondrial fragmentation is mediated through establishment of contact sites between tubular ER, actin filaments and mitochondria. Subsequently, DRP1 oligomers are

recruited to MFF foci and constrict mitochondria to a diameter of around 50nm. This diameter of mitochondrial tubule is then permissive for assembly of a second constriction GTPase DYN2, which further compresses membranes until fission occurs. Once mitochondria were split, DRP1 oligomers stay on surfaces of both daughter mitochondria, marking the division site.

In humans, autosomal mutations in DRP1 result in compromised neurologic development and death in infancy (Waterham et al., 2007). MFF deletion causes Leigh-like encephalopathy, optic atrophy and peripheral neuropathy (Koch et al., 2016). Mutations in DYN2 are linked to centronuclear myopathy 1, which is characterized by progressive muscular weakness and wasting. Like mtDNA diseases, this disorder may have a neonatal onset or might be present in childhood or adolescence or may not even become evident until the third decade of life (Bitoun et al., 2009; Bitoun et al., 2007; Bitoun et al., 2005).

In mice, complete DRP1 deficiency causes early embryonic lethality (E10.5 - E12.5) associated with severe developmental abnormalities, specifically in the forebrain. Neuron-specific DRP1 deletion results in brain hypoplasia and death within a day after birth (Ishihara et al., 2009). Total MFF knockout mice suffer from severe dilated cardiomyopathy and die prematurely of heart failure at 13 weeks of age. Closer analysis of heart tissue samples from mutant mice revealed reduced mitochondrial mass, diminished respiratory chain activity along with an increase in stress markers and autophagic flux. Interestingly, these defects in mitochondrial function could be completely rescued by complementary deletion of Mfn1, arguing that unopposed mitochondrial fusion is the main cause of the observed phenotype (Chen et al., 2015).

Another interesting discovery concerning mitochondrial dynamics came from recent studies in mammalian cells. It has been shown, that mitochondrial division occurs in vicinity to replicating nucleoids (Fig. 5).

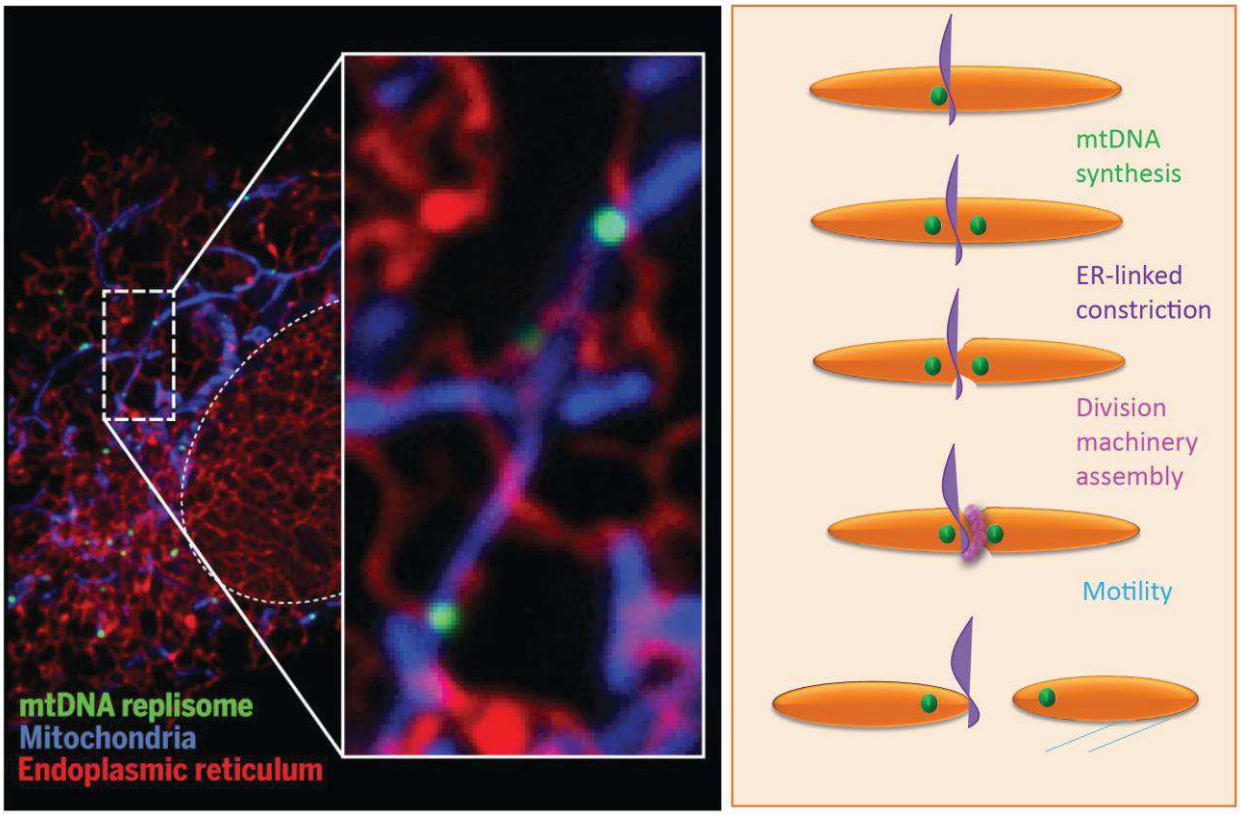

Introductory figure 5. Schematic illustration of the mechanism of ER-associated mitochondrial division (ERMD). On the left, fluorescence microscopy image of human osteosarcoma U2OS cell with ROI (inset) magnification of several ER-mitochondria contacts (ER in red, mitochondria in blue). A subset of these contacts is located in vicinity to replicating nucleoids (POLG2, green). On the right, same process is schematically explained with a brief description of each step: mitochondria are orange, ER is violet, fission machinery is purple and microtubules are blue. (Adapted from (Lewis et al., 2016)).

The tubular ER plays a major role in this process marking the sites of mitochondrial division and thus participating in mtDNA segregation (Lewis et al., 2016). Duplication of mtDNA occurs asynchronously with the nuclear genome, so that mitochondria can regulate their mtDNA copy numbers even in post-mitotic cells. Blockage of mitochondrial fission through downregulation of DRP1 or, to a lesser extent, MFF results in nucleoid enlargement and their clustering within fused mitochondrial tubules (Ishihara et al., 2015). As resulting gigantic nucleoids ("mito-bulbs") cannot divide, their copy number is greatly diminished and eventually lost after several cell divisions. And vice versa, down-regulation of Mfn1/Mfn2 or OPA1 causes mitochondrial fragmentation with a partial to a complete loss of mtDNA (Chen and Chan, 2010; Chen et al., 2005; Chen et al., 2007; Davies et al., 2007). In both cases, mtDNA depletion precedes defects in oxidative

phosphorylation and mitochondrial dysfunction with severe impacts on cell physiology. Thus, mitochondrial fission and fusion events need to be tightly balanced to ensure proper distribution and maintenance of the mitochondrial genome.

How can mitochondria travel from the site of division to the place of energy demand? In metazoans, mitochondria are transported along microtubules with the help of motor proteins (Ball and Singer, 1982; Heggeness et al., 1978). Co-polymers of alpha- and beta-tubulins are used as sliding tracks, on which kinesins transport mitochondria towards the plus-end (towards cell periphery, anterograde) (Nangaku et al., 1994), whereas dyneins can move mitochondria in the antiparallel direction - towards the minus-end (to the nucleus, retrograde)(Tanaka et al., 1998). Disruption of the cytoskeleton structure with microtubule-depolymerizing agents such as colcemid or nocodazole causes disorganization of the mitochondrial network. Depending on the cell type, intermediate filaments and actin could also cooperate in mitochondrial transport. For example, in neurons actin filaments play an important role in recruitment of mitochondria to the presynaptic active zone (Saxton and Hollenbeck, 2012; Sheng and Cai, 2012). The search for a linker between mitochondria and the transport machinery in Drosophila neurons revealed another adaptor protein named Milton (Stowers et al., 2002). Milton binds kinesin (Glater et al., 2006) and the OMM integral protein Miro (Fransson et al., 2003; Fransson et al., 2006), thus connecting cytoskeleton and mitochondria. Miro is a large atypical Rho GTPase that has two Ca^{2+}-sensing EF-hand domains and can bind kinesins and dyneins trough Milton or directly in a Ca^{2+}-depending manner (Fransson et al., 2006; Macaskill et al., 2009; Russo et al., 2009) , thus providing selectivity against the direction and duration of the mitochondrial movement.

2.2 Mitosis

Mitochondrial fragmentation also occurs during mitosis. Mitosis or cell division is the end-product of self-replication, a process of critical importance for any cellular organism. Mitosis occurs only in eukaryotes, while prokaryotes divide through binary fission. Despite the significant complexity compared to bacteria, the outcome is the same – one parental cell divides into two daughter cells, which carry the exact copies of genetic material. Depending on the cell type, the duration of the cell cycle can vary. Some cells, like embryonic cells divide very rapidly, while others may be slow. Cancer cells, which are often used as research models, generally need around 24 hours to complete a single cell cycle. Mitosis is the shortest phase of a cell cycle, while interphase, a period between two mitotic events, is the phase, in which cells spend most of their time.

The interphase can be further subdivided into separate phases. All phases have more than a simple descriptive character and do possess actual functional consequences. Right after mitosis cells enter the phase of initial growth (G1) followed by a phase of nuclear DNA synthesis (DNA replication) and chromosome duplication (S). In S phase diploid cells become tetraploid and enter the second growth phase (G2). During G2 cells start to prepare for the most dynamic phase in its life – mitosis (M) (Fig. 6). The amount of genomic DNA is frequently used as a marker to roughly estimate the stage of cell cycle. Each phase is under strict enzymatic and metabolic control and has its own checkpoints. If the latter cannot be satisfied, cells cannot proceed to the next step. In this way, cells ensure that upon mitosis, daughter cells will receive enough cellular resources and, most importantly, intact genetic material.

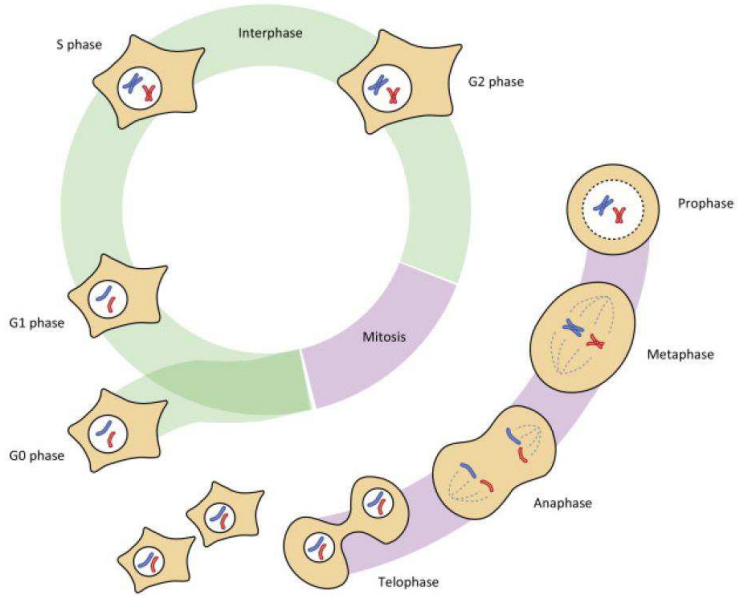

Introductory figure 6. Schematic illustration of the cell cycle of mammalian cells (Adapted from (Jongsma et al., 2015).

There are two major checkpoints during cell cycle– the first one occurring before S-phase and DNA replication (G1/S DNA damage checkpoint) and the second one before mitosis (G2/M DNA damage checkpoint). Both checkpoints are executed by signaling cascades orchestrated by ataxia-telangiectasia mutated (ATM)/ ataxia-telangiectasia related (ATR) kinases and checkpoint effector kinases CHK1/CHK2. ATR/ATM and p53 together with adaptor proteins can sense different kinds of DNA damage, including double-strand breaks, stalled replication forks, ultraviolet-induced thymine dimers, single-base alterations and mismatches (Saldivar et al., 2017). If during the G1/S checkpoint DNA is damaged, cells will try to repair the damage, thus blocking cell cycle progression. If the damage is irreparable cells may enter a special stage called G_0 or quiescence, which means that it will not progress into cell cycle, or it may choose to undergo apoptosis. Mechanistically, ATM/ATR phosphorylated CHK kinases as well as INK4 and CIP/KIP proteins will prevent the formation of active G1 cyclin-CDK complexes, whereas p53 stabilization will induce transcription of p53 target genes and activation of p53-dependent DDR pathways (Lakin and Jackson, 1999). During early G1, cyclin D can bind and activate CDKs 4/6 stimulating phosphorylation of its targets – retinoblastoma (RB) family of proteins (RB, p107 and p130). G1 cyclins belong to two families of cyclins – the D family (cyclins D1, D2 and D3) and the E family

(cyclins E1 and E2) (Sherr, 1993). As cells progress to G1, cyclin E form complexes with CDK2, inducing hyperphosphorylation and inhibition of RB proteins. As a consequence, E2F transcription factors become re-activated and induce expression of S phase cyclins, CDKs, DNA repair and replication genes (Lukas et al., 1999). During early S phase, cyclins D is degraded, and CDK2 forms complexes with cyclin A. Complexes of CDK2 with cyclin A2 and cyclin E trigger replication of DNA and duplication of centrosomes. At the end of S phase cyclins E become degraded and cyclin A associates with CDK1 and CDK2, as synthesis of mitotic cyclin B progresses. Formation of active cyclinB-CDK1 complexes marks entrance into mitosis.

Mitosis is further divided into five stages, each step with its unique and at the same time highly conserved characteristics (Fig. 6). During each of them, the cytoskeleton, chromosomes, organelles and the plasma membrane udergo dynamic spatio-temporal organization. All these events are under the precise control of mitotic kinases, phosphatases, ubiquitin ligases and deubiquitinating enzymes. There are many kinases with important roles in mitosis. Those include CDKs, Polo-like kinases (Plk 1-4), Aurora kinases (A, B, C) , NIMA-related kinases, Bub kinases, Haspin and Mps/TTK (Gelens et al., 2018). Mitotic kinases together with ubiquitin E3 ligases such as SCF (skp/cullin/F-box) (Bai et al., 1996) and the APC/C (Anaphase-promoting complex/Cyclosome) (King et al., 1995) complexes orchestrate mitotic initiation, progression and exit, respectively. Mitosis starts with prophase, when chromosomes condense, but sister chromatids remain held together by cohesin (Tanaka et al., 1999; Uhlmann et al., 1999; Waizenegger et al., 2000). During this stage, the nuclear envelope loosens and eventually dismantles. This step is important for proper chromosomal alignment during the following stages and is characteristic for most eukaryotes. Such type of mitosis is called ‘open mitosis’, while fungi and some algae, like Dinoflagellates, keep their nuclear membrane intact, following a ‘closed mitosis’ respectively. Mechanistically mitotic entry is regulated by Aurora A (Barr and Gergely, 2007; Glover et al., 1995), which already in G2 forms a complex with its auxiliary factor Bora and activates Plk1 (Bruinsma et al., 2014; Sunkel and Glover, 1988). Plk1 activity is necessary for mitotic spindle assembly (Sumara et al., 2004). Aurora A also drives centrosome maturation by

recruiting Centrosomin, LATS2, TACC and NDEL1 (Hannak et al., 2001; Mori et al., 2007; Toji et al., 2004). The second phase is called prometaphase, where spindle microtubules start to search and probe for attachment to kinetochores, special molecular motors, present at the centromeric region of each chromosome. Aurora B kinase as a catalytic subunit of the chromosome passenger complex (CPC) localizes to the region between kinetochores and is responsible for correction of mis-attachments and regulation of chromosome bi-orientation through phosphorylation of kinetochore substrates (Emanuele et al., 2008; Liu et al., 2009; Tanaka et al., 2002; Welburn et al., 2010). In metaphase, chromosomes align in the middle of the cell along the equatorial plane. This aspect is very important and is controlled by the Spindle assembly checkpoint (SAC). SAC reassures proper attachment of kinetochores to the mitotic spindle and corrects chromosomes alignment. Unsatisfied SAC may delay anaphase onset until all chromosomes are attached by microtubules emanating from the opposite poles of the cell. Main components of the SAC are Aurora B, Bub1, Bubr1, Bub3, Mad1, Mad2 and Cdc20. SAC auxiliary proteins include Mps1, the ROD-ZW10 complex, p31comet, Trip, PP1 and PPc2A (Musacchio, 2011, 2015). SAC promotes the formation of an inhibitory complex named the Mitotic Checkpoint Complex (MCC). The MCC consists of Bubr1, Mad2, Bub3 and Cdc20 and targets the APC/C (Gelens et al., 2018; Izawa and Pines, 2015). APC/C is a large (around 1,5 MDa) ubiquitin ligase complex responsible for triggering anaphase onset and mitotic exit through polyubiquitination and subsequent proteasomal degradation of Securin and Cyclin B (Herzog et al., 2009; King et al., 1995). MCC-mediated inhibition of the APC/C stabilizes these substrates, effectively preventing chromosome segregation. Once SAC is satisfied, APC/C becomes activated and mitosis progresses to anaphase. In anaphase, sister chromatids are no longer tightly bound to each other, as APC/C-mediated Securin degradation releases Separase, a protease that cleaves the cohesin rings (Waizenegger et al., 2000). Sister chromatids are moved towards the opposite poles, creating a separate set of chromosomes for future daughter cells. Mitotic exit is marked by inactivation of mitotic kinases through action of phosphatases and

APC/C-mediated degradation of mitotic cyclins (Wurzenberger and Gerlich, 2011). Mitosis culminates with the telophase, when the chromosomes go through decondensation and nuclear envelope starts to reform. Unlike nuclear envelope breakdown in prophase, nuclear reassembly in telophase is largely controlled by phosphatases. The exact mechanisms just started to be unveiled, but some key players are already known, mainly protein phosphatase 2A (PP2A) and protein phosphatase 1 (PP1). Histones, chromatin-binding proteins and lamins are among the targets of these phosphatases (Asencio et al., 2012; Fischle et al., 2005; Vagnarelli et al., 2011; Ye et al., 1997). At this stage cells proceed to cytokinesis, which is not a stage of mitosis, but rather the end stage of cell cycle. In cytokinesis, the membrane and protein complexes at the junction between daughter cells sever by the actin-myosin contraction ring through formation of a cleavage furrow. The final stage of cytokinesis is marked by formation of a midbody. i.e. Flemming body, after Walter Flemming, who discovered it in 1891 (Paweletz, 1967). The midbody has a diameter of 1μm and is located in the place of the cleavage furrow. It contains spindle microtubules and various proteins involved in cell division and is important for the completion of the final abscission step (Hanai et al., 2016). If cytokinesis does not occur, mitosis results in endomitosis, and the cell ends up having two separate nuclei, which is quite common for some specialized cells like hepatocytes or megakaryocytes.

2.2.1 Organelle remodeling and inheritance in mitosis

While most research in the mitotic field is focused on mechanisms of proper chromosome segregation, it is worth to note that during evolution cells developed ways to control equal organelle distribution to two daughter cells. A recent study in yeast showed that during cell division all intracellular components, except for the microtubule-organizing center, are equally partitioned between mother cells and daughter buds (Menendez-Benito et al., 2013). Small organelles like peroxisomes can be easily distributed. But what happens to the larger and more

complex organelles, such as ER, mitochondria, and Golgi? The simple answer would be – they have to be disassembled and fragmented. But they also have to keep the interaction-position memory to be properly reassembled upon completion of mitosis. They should also not stochastically float in the cytoplasm interfering with segregating chromosomes and the spindle apparatus. Thus, there must be mechanisms that reassure correct disassembly and nonrandom positioning perhaps implementing checkpoints that could keep mitosis on hold until all requirements are satisfied.

Studies in mammalian cells showed that ER and Golgi networks, which share a similar cisternae-tubule-stacks architecture, with ER being the largest membranous organelle, undergo dramatic morphological changes during mitosis. Despite the similarities, their remodeling during mitosis is controlled by distinct mechanisms involving different kinases/phosphatases and substrate proteins.

In prophase, the peripheral continuous network of ER segments into tubules (Puhka et al., 2007) or cisternae (Lu et al., 2009; Poteryaev et al., 2005) or a mixture of both depending on the cell type (Puhka et al., 2012). The nuclear envelope (NE), which is considered to be a part of the ER, breaks down allowing chromosomes to interact with spindle microtubules. Key players in this process are vaccinia-related kinase (VRK1), which phosphorylates the barrier to autointegration factor (BAF) to initiate the NE breakdown and PP2A that opposes VRK1 phosphorylation, thus allowing proper nuclear assembly during mitotic exit (Asencio et al., 2012). Cytoplasmic microtubule motors kinesin-1 and dynein coordinate ER transport away from the midzone, whereas the ER integral protein STIM1 stimulates elongation of ER tubules interacting with growing plus ends of the microtubules (Grigoriev et al., 2008; Lane and Allan, 1999; Wozniak et al., 2009). What happens then to the resident proteins? Soluble fraction becomes exposed to the cytosol, whereas the transmembrane complexes integrate into dispersed peripheral parts of the ER (Yang et al., 1997). Yet in prometaphase, ER reforms the interconnected network, without subdivision in

rough ER (RER) or smooth ER (SER) or NE, and remains so until the end of mitosis (Ellenberg et al., 1997).

In contrast, the Golgi ribbon becomes fragmented into tubule-reticular elements and vesicles, which remain dispersed throughout the entire mitotic phase. The destiny of Golgi-resident proteins and Golgi fragments is however under debate. Some research teams reported merging events between fragmented Golgi units and ER (Thyberg and Moskalewski, 1992; Zaal et al., 1999), whereas others claim a distinct fate for ER and Golgi clusters or vesicles (Hammond and Glick, 2000; Jesch et al., 2001; Shima et al., 1997). Golgi stack remodeling is initiated and controlled by a distinct set of kinases – mitogen-activated protein kinase kinase (MEK1) (Acharya et al., 1998) Polo-like kinase (Plk1) (Sutterlin et al., 2001), Cyclin B-CDK1 kinase (Harding et al., 2003) and Aurora A (Lim et al., 2010). These kinases regulate conversion of pericentriolar Golgi stacks into mitotic blobs through distinct cascades involving golgins (Barr and Short, 2003) and Golgi reassembly-stacking proteins (GRASPs), the key factors maintaining the Golgi apparatus integrity (Barr et al., 1997; Wang et al., 2003). MEK1 potentiates the fragmentation through CDK1-ERK2-GRASP55/GM130 (Feinstein and Linstedt, 2007; Lowe et al., 1998) and, as recently shown, Myt1 (Villeneuve et al., 2013), while Plk and CDK1 directly phosphorylate GRASP65 (Kano et al., 2000; Lin et al., 2000; Preisinger et al., 2005; Sutterlin et al., 2001). Golgi disassembly also triggers Src activation and Aurora A phosphorylation, which results in Aurora A recruitment to the centrosomes. Centrosomal localization of Aurora A is required for proper spindle formation and faithful chromosome segregation. Thus, the importance of mitotic Golgi fragmentation should not be underestimated, as its failure results in G2/M or early mitotic arrest, directly indicating the existence of a 'Golgi mitotic checkpoint' (Sutterlin et al., 2002; Wei et al., 2015). This hypothesis was further corroborated by Guizzunti et al. showing that inhibition of Golgi fragmentation potentiates SAC and blocks bipolar spindle formation (Guizzunti and Seemann, 2016).

2.2.2 Mitochondrial dynamics in mitosis

What about mitochondrial networks? How are they distributed during mitosis? Initial attempts to address these questions gave mixed results. Through studies in yeast, several mutations were identified to be important for mitochondrial morphology and inheritance. A screen performed in yeast revealed that null mutants in Mmm1, Mdm10 and Mdm12 displayed altered mitochondrial morphology, a significant decrease in mtDNA numbers and slow growth rates in response to different carbon sources (Okamoto and Shaw, 2005). Identified genes were further assigned to be important components of the ERMES/MDM complex, which acts as a linker between ER and mitochondria, and also as MDM12-MMM1 subcomplex, involved in OM beta-barrel assembly pathway downstream of SAM. Yet all of the known proteins belonging to the yeast mitochondrial fission machinery (Dnm1, Fis1, Mdv1 and Caf4) were shown to be irrelevant for mitochondrial inheritance or cell viability (Bleazard et al., 1999; Otsuga et al., 1998). These results were counterintuitive, as mitochondrial fission was documented to be important during meiosis in yeast (Gorsich and Shaw, 2004). Despite the fact that strains lacking proteins important for mitochondrial fission or fusion or even both could complete meiosis and form spores, closer analysis revealed numerous morphological defects in mitochondrial morphology of the mutants. Specifically, mitochondria failed to fragment, formed aggregates and eventually were not equally distributed. This resulted in some spores receiving virtually no nucleoids, which correlated with decrease in spore size (Gorsich and Shaw, 2004). These findings suggested the regulation of mitochondrial dynamics as a quality control for distribution of mtDNA during cell division.

Yet the question remained open. What could be the regulation mechanisms ensuring proper mitotic distribution of mitochondria and mtDNA specifically in mammalian cells? The group of Katsuyoshi Mihara was amongst the first to analyze remodeling and inheritance of mitochondrial networks in human cells during mitosis (Taguchi et al., 2007). They showed that tubular networks of interphasic HeLa cells start to fragment in prophase with marked increase in fragmentation in

metaphase and gradual decrease in late telophase. They also reported about a stochastic segregation of mitochondria between daughter cells, which upon entering the interphase reformed tubular structure of mitochondria, similar to the one in parental cell. Mechanistically, mitochondrial mitotic fragmentation was dependent on activatory DRP1 phosphorylation at S616 (human; Ser585 in rat DRP1 used in the study) by CDK1/CyclinB. These findings were further extended in another study which showed that mitotic kinase Aurora A phosphorylates a small Ras-like GTPase RalA on S194, driving its mitochondrial localization (Kashatus et al., 2011). On the mitochondrial surface RalA interacts with its binding protein RalBP1 forming an active complex with phosphorylated DRP1 in a MFF-dependent manner. Stable downregulation of either RalA or RalBP disrupted mitochondrial fission and segregation, which resulted in significant decrease in cellular ATP levels and cell death.

During mitosis, DRP1 oligomerization and activation is regulated not only through CDK1. A SUMO protease, SenP5, relocalizes from nucleoli and cytosol, where it resides during interphase, to OM during early prophase before NE breakdown. There it deSUMOylates many mitochondrial proteins including DRP1, which coincides with an increase in mitochondrial fragmentation. SENP5 desumoylation of DRP1 during mitosis increases DRP1 oligomerization, facilitating mitochondrial fission. Silencing of SenP5 blocked cells in prometaphase (Zunino et al., 2009). These data are somewhat contradictory to the fact that even in the absence of DRP1 cells still can undergo mitosis, yet with significant defects in mitochondrial segregation. This was especially evident in highly polarized cells, when one daughter cell would receive a large aggregated mitochondrial cluster, whereas the other - very few mitochondria (Ishihara et al., 2009). This discrepancy could be explained by suspecting additional mitochondrial substrates, beyond DRP1, to be involved in the regulation of a potential mitochondrial mitotic checkpoint. Besides, the same group reported previously that SenP5-mediated de-sumoylation during the interphase promoted mitochondrial elongation, whereas downregulation of SenP5 resulted in fragmented mitochondria (Zunino 2007), which indicates a more complex scenario, involving additional factors.

But these are not the only conflicting results in the field. The mitochondrial transport concept, according to which mitochondrial movement in mitosis is relying on microtubules, has been recently challenged. In agreement with this new concept mitotic mitochondria passively dissociate from spindle microtubules and diffuse to the cell periphery. This process, named 'mitochondrial shedding', was driven by CDK1 and Aurora A, although the mechanism remained elusive (Chung et al., 2016). Yet another compelling study shows the opposite (Kanfer et al., 2015). According to Kanfer et al. mitochondria interact with plus ends of microtubules and are actively transported towards the daughter cell periphery in telophase. This process was shown to be mediated by Miro and the cytoskeletal-associated protein CENP-F. Depletion of CENP-F or Miro decreases mitochondrial spreading and leads to defects in cytokinesis.

Compared to our knowledge about mitotic ER or Golgi disassembly, much less is known about mechanisms that govern mitochondrial partitioning in mitosis. While a handful of studies focuses on DRP1 posttranslational modifications, practically nothing is known about its main interacting partner MFF or other DRP1 receptors. Since mitochondria undergo significant changes in their morphology this opens many questions as to how their function stays preserved and what the respective molecular mechanisms are?

2.3 MFF

MFF stands for mitochondrial fission factor, a new name assigned to C2orf33 in a first functional study for this protein performed in the laboratory of Alexander M. van der Bliek. Their work aimed at identification of novel regulators of mitochondrial dynamics. An initial high-throughput siRNA-based screen was carried out in Drosophila DS2R+ cells resulting in the identification of CG30404/Tango11 as a protein required for mitochondrial fragmentation that is highly conserved in other metazoans. Interestingly, the name "Tango11" was assigned to CG30404 after it was

picked up as a hit in another siRNA screen dedicated to find proteins involved in transport and Golgi organization (TANGO proteins, Bard et al., 2006). A BLAST search revealed C2orf33 as a human homologue of CG30404/Tango11 and further functional validation was performed in human cells (Gandre-Babbe and van der Bliek, 2008; Otera et al., 2010).

In humans, MFF is encoded by a nuclear gene located on the q-arm of chromosome 2 (2q36.3) and its mRNA is alternatively spliced into nine different isoforms. However not all of these mRNA isoforms are translated into well annotated proteins. Only five isoforms are documented to encode functional proteins. These isoforms differ by the middle part of the protein corresponding to exons 5, 6, and 7. Except for isoform 1, all isoforms lack exon1 and are translated from an alternative translation initiation codon starting in exon 2. Human MFF exons 5, 6, and 7 are not conserved in Drosophila, but vertebrates have mostly similar patterns of MFF alternative splicing. This implies a functional importance for these exons depending on tissue specificity and the cellular context. MFF is ubiquitously expressed throughout different tissues with particularly high levels in heart, brain, muscle, kidney and liver (Gandre-Babbe and van der Bliek, 2008), organs that have especially high metabolic rates and energy demands. Mouse tissue profiling using a polyclonal MFF antibody revealed the presence of different MFF isoforms of distinct molecular weights (Ducommun et al., 2015). While all tissues displayed short variants, aforementioned organs additionally contained a long variant. The largest variant was notably present in brain and skeletal muscle.

Although the crystal structure of MFF is yet to be discovered, the overall domain architecture is deduced from its sequence analysis and truncation studies. MFF is a single-pass tail-anchored (TA) mitochondrion outer membrane (MOM) and peroxisomal protein. Comparative sequence analysis of human and other metazoan MFF orthologs revealed common features of the MFF polypeptide. At the amino-terminus, there are three short repeat motifs (R1 – R3), which comprise a minimal sufficient DRP1 binding region in MFF (Liu and Chan, 2015), whereas R1–R2 are absolutely required for the interaction (Otera et al., 2010). These short repeats (R1 – R3) are

followed by a disordered region and an amino acid stretch with a strong coiled coil (CC) forming propensity that is responsible for MFF homo-oligomerization. The sequence is ended by a single helical hydrophobic transmembrane segment (TMS) at the carboxyl-terminus (Fig. 7) that serves as a membrane anchor into mitochondria and peroxisomes (Gandre-Babbe and van der Bliek, 2008; Otera et al., 2010).

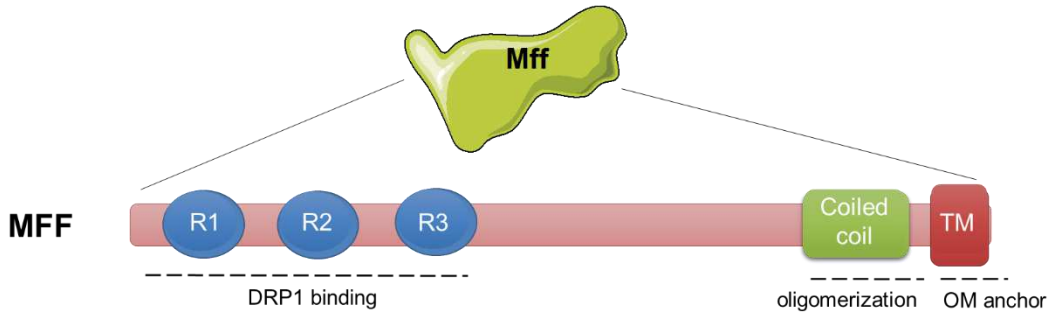

Introductory figure 7. Schematic illustration of the functional domain structure of MFF. Starting from the amino-terminus three short repeat motifs (R1 – R3, in blue), which constitute the DRP1 binding region, followed by a disordered segment and coiled coil (CC) domain (in green). At the carboxyl-terminus MFF sequence contains a transmembrane segment (TM, in red) that serves as a membrane anchor into mitochondria and peroxisomes.

The mechanism of this dual mitochondrial and peroxisomal targeting of MFF remains unclear. Studies on other MOM TA proteins such as Fis1 and Bcl family proteins imply that the TMD amino acid sequence may contain key structural characteristics necessary for direct membrane targeting. There is no obvious sequence conservation in their tail region, but some common features include moderate hydrophobicity of the TMD, flanked by positively charged amino acids and its relatively short length. Thus, TA can act by itself as a destination determinant without having a concrete consensus motif needed for recognition by a translocase complex (Kemper et al., 2008; Merklinger et al., 2012). Yet the unique host membrane lipid composition is also believed to contribute to the selectivity of MFF recruitment (Krumpe et al., 2012).

2.3.1 MFF function

MFF was initially discovered as a protein that localizes to mitochondria and peroxisomes and plays an important role in their division (Gandre-Babbe and van der Bliek, 2008). The knockdown of MFF resulted in elongated mitochondria, whereas transient overexpression caused increased mitochondrial fragmentation. These effects were dependent on DRP1 as fragmentation induced by MFF overexpression was abolished in cells with a DRP1 knockdown. Microscopy analysis revealed increased recruitment of DRP1 to mitochondrial surface in control cells compared to MFF RNAi cells, where DRP1 foci were largely cytoplasmic. Moreover, DRP1 foci were co-localizing with MFF puncta on mitochondria thus suggesting that MFF could act as a DRP1 receptor. These findings were also corroborated by subcellular fractionation, co-immunoprecipitations of cell lysates and pulldowns of recombinant proteins *in vitro* (Otera et al., 2010). Although this interaction is proven to be direct, it could be detected only after chemical crosslinking, implying its short-lived or unstable nature. Moreover, a point mutation resulting in a single amino acid substitution in DRP1 (A395D), which was discovered in a patient with encephalopathy due to defective mitochondrial and peroxisomal fission (Fahrner et al., 2016; Waterham et al., 2007), completely abrogated DRP1-MFF interaction. This mutation negatively affects DRP1 higher order assembly, indicating that already pre-assembled tetrameric DRP1 complexes, rather than monomers or dimers, interact with MFF. This hypothesis was recently tested and confirmed experimentally using different mutated and truncated versions of MFF and DRP1 (Liu and Chan, 2015). According to their findings, the minimal regions sufficient for interactions are the stalk domain in DRP1 and two repeats (R1-R2) within the short N-terminus of MFF. Interestingly insert B region in DRP1 prevents a stable complex formation between DRP1 and MFF and its deletion greatly enhances the DRP1-MFF interaction. All mutations that affected DRP1 tetramerization also resulted in failure to interact with MFF but not MiD51. As higher order assembly is required for fission activity of DRP1, this explains why DRP1 recruitment by MFF

results in mitochondrial fission, whereas alternative receptors MiD49 and MiD51 rather sequester inactive DRP1 dimers on the mitochondrial surface. Altogether these findings strengthen the primary role of MFF as a DRP1 receptor.

Recent studies indicate that ER is an active player in mitochondrial division. ER tubules appear to mark future fission sites, collaborate in constriction of mitochondrial tubules and remain in a close proximity during the entire fission process (Friedman et al., 2011). Particularly, DRP1 was shown to localize to ER-mitochondrial constriction sites in a MFF-dependent manner. ER-mediated constriction precedes MFF-DRP1 complex formation and acts independently of both MFF and DRP1. It remains a puzzling question whether and how ER could specifically recruit MFF to ER-marked mitochondria division sites. It also has been shown, that localization of MFF is adjacent and dependent on nucleoids (Lewis et al., 2016).

2.3.2 MFF regulation

Despite its fundamental importance in mitochondrial dynamics the posttranslational modifications of MFF still remain largely unexplored. Regulation by phosphorylation is of particular interest because of its reversible nature and big potential for future therapeutics, as many pharma companies have large libraries of protein kinase inhibitors.

While most attention has been drawn to DRP1, which was found to be phosphorylated, ubiquitinated, S-nitrosylated, SUMOylated, O-Glc-N-acylated, only two very recent studies addressed MFF regulation so far. Both studies independently discovered MFF phosphorylation by AMPK under energy stress conditions (Ducommun et al., 2015; Toyama et al., 2016). Phosphorylation of MFF at S155 and S172 by AMPK in response mitochondrial poisons led to increased DRP1 recruitment to mitochondria accompanied by a significant mitochondrial

fragmentation. Authors of these studies speculate that these phosphorylations are key events in facilitating disposal of damaged mitochondria through mitophagy.

2.4 DRP1

Dynamin-related proteins were discovered as regulators of mitochondrial fission in yeast (Dnm1p) (Otsuga et al., 1998) and mammals (DRP1) (Smirnova et al., 1998), followed by a complementary study on the C.elegans DRP1 ortholog (Labrousse et al., 1999). It has been described that mutations in human DRP1 caused elongation and redistribution of mitochondria to perinuclear clusters (Smirnova et al., 1998), while the morphologies of other organelles remained unaffected. Yeast mutants in Dnm1p (Otsuga et al., 1998) caused tubular mitochondrial networks to fuse and to collapse on one side of the cell.

Based on the size of the GTPase domain, Dynamin-related proteins are usually classified as 'large GTPases' (~300 amino acids), compared to very diverse small GTPases such as Ras-like GTPases or α-subunits of G-proteins or the translational GTPases (Praefcke and McMahon, 2004). Other distinguishing features are their oligomerization-dependent GTPase activation mode and low affinities to GTP. This family belongs to the vast Dynamin superfamily together with mitochondrial fusion GTPases (Opa1, Mitofusins 1/2) and yeast Vps1p (Ekena and Stevens, 1995; Nothwehr et al., 1995) and Mgm1p (Backer, 1995; Meeusen et al., 2006; van der Bliek, 1999).

Recent success in DRP1 crystallization as well as functional mutagenesis studies allow us to better understand its structure–activity relationship. Structurally, DRP1 is built up of four identifiable domains: the GTPase domain, the bundle signaling element (BSE), the stalk, and the insert B (IB) region (Fig. 8) (Ferguson and De Camilli, 2012; Frohlich et al., 2013; Wenger et al., 2013).

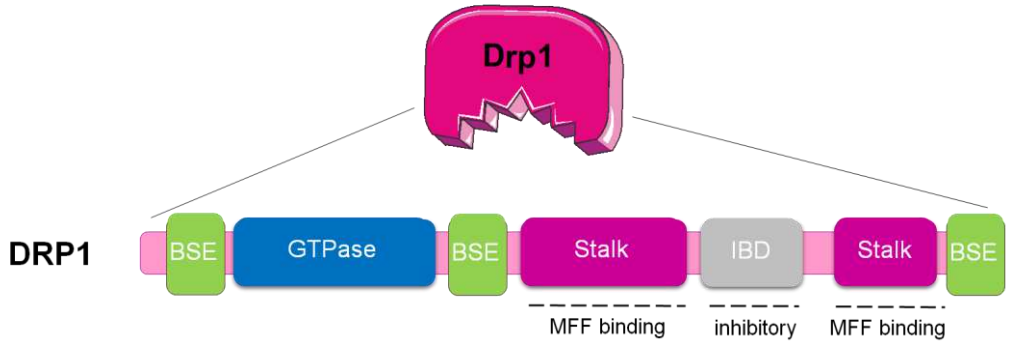

Introductory figure 8. Schematic illustration of the functional domain structure of DRP1. Starting from the amino-terminus bundle signaling element (BSE, in green) are followed by GTPase domain, then BSE and the stalk (in purple). The Salk region is required for MFF binding. The insert B domain (IBD) is highlighted in grey, which is proven to play an inhibitory role in MFF-DRP1 interaction. IBD is followed by the stalk and BSE domains.

A central beta-sheet of eight beta-strands inside of eight alpha helices comprise the amino-terminal GTPase domain of DRP1. BSE is assembled via its hydrophobic core into a three helix bundle (Chappie et al., 2009; Chappie et al., 2011): a1-BSE is localized to the very amino-terminus of DRP1, a2-BSE follows the GTPase domain, and a3-BSE spans the very carboxy-terminus of DRP1. BSE is believed to act as a transmitter of conformational changes from the GTPase domain to the stalk. The stalk is formed of antiparallel four-helix bundles. The IB domain is predicted to be unstructured and positions itself inside of the stalk sequence. Interestingly, the canonical dynamin contains a PH domain that is formed on an equivalent sequence position (Faelber et al., 2011; Ford et al., 2011), thus raising the possibility that it acts as a putative membrane interaction site (Mears et al., 2011). However, human DRP1 mutagenesis studies did not confirm this hypothesis (Strack and Cribbs, 2012; Zhang et al., 2011).

2.4.1 Structural insights in MFF-DRP1 interaction

DRP1 is a cytosolic GTPase, which can assemble in high-order oligomers and transiently bind OMM (Smirnova et al., 1998). This recruitment is mediated by four mitochondrial receptors for DRP1 – MFF (Otera et al., 2010), Fis1 (Suzuki et al., 2003), MiD49 and MiD51(Loson et al., 2013;

Osellame et al., 2016; Palmer et al., 2013). MFF-mediated recruitment stimulates formation of DRP1 helical rings that induce GTP-dependent constriction of mitochondria. Inversely, MiD proteins sequester DRP1 complexes on mitochondrial surfaces without subsequent fission step, thereby inducing mitochondrial fusion. Why do MFF-DRP1 and MiD49/51-DRP1 interactions result in such diametrically opposed outcomes? Several studies aimed at finding putative structural basis for this paradox using mutagenesis-based in vitro approaches, overexpression experiments and yeast two-hybrid assay (Fan et al., 2015; Strack and Cribbs, 2012; Zhang et al., 2011).

Initial studies to detect MFF-DRP1 complex either in cells or *in vitro* were unsuccessful, and only the use of cross-linking reagents allowed to confirm the interaction (Otera et al., 2010; Strack and Cribbs, 2012). However, yeast Dnm1 binds its receptor, Mdv1, with much higher affinity. This interaction is mediated through Dnm1 IB domain, which is recognized by the B-propeller domain of Mdv1 (Bui et al., 2012). The deletion of the IB domain in human DRP1 or its replacement with different linkers did not affect any DRP1 functions such as GTP hydrolysis, membrane constriction (*in vitro*) and mitochondrial recruitment (in cells). DRP1 lacking the IB domain (ΔIB) displayed enhanced interaction with MFF (Liu and Chan, 2015) and its expression in cells enhanced fragmentation of mitochondria as compared to expression of wild-type DRP1 (Strack and Cribbs, 2012), thus suggesting an auto-inhibitory role of the IB domain. In fact, its removal from DRP1 allows detection of DRP1–MFF complex formed *in vitro* in the absence of cross-linkers (Liu and Chan, 2015).

Truncation experiments also revealed that the GTPase domain is stimulatory but not required for DRP1-MFF interaction. Moreover, removal of all domains except for the Stalk domain (ΔGTPaseΔBSEΔIB) did not vastly affect DRP1 interaction with MFF compared to DRP1ΔIB alone (Liu and Chan, 2015). Thus, the DRP1 stalk domain and the MFF R1 and R2 motifs are the minimal regions required for the DRP1–MFF interaction. Specifically, Arg-376 in the DRP1 stalk domain was determined to be necessary for this interaction. When Arg-376 was mutated to glutamate, the

obtained DRP1 R376E mutant resided exclusively in cytosol and induced mitochondrial elongation even in combination with overexpressed MFF. Moreover, DRP1 R376E did not co-immunoprecipitate with MFF, but retained its ability to form dimers (Strack and Cribbs, 2012). Detailed analysis of similar mutants led to identification of regions in DRP1 that completely abrogated interaction with MFF, but not MiD proteins. Functionally, those mutations also abolished DRP1 oligomerization, thus pointing at the fundamental difference in the ability of MFF to recruit oligomeric and highly active DRP1. Inversely, MiD proteins physically associated with inactive dimeric DRP1 from the cytosolic pool (Liu and Chan, 2015).

In summary, the ability to specifically recruit higher-order oligomers of DRP1 defines the role of the receptor and, thus, the outcome of DRP1-recruitment to the mitochondrial surface.

2.5 The protein Kinase D (PKD) family

In a phosphoproteomic approach, MFF among many other candidate proteins has recently been identified as a potential target of PKD (Franz-Wachtel et al., 2012).

The PKD family of Ser/Thr kinases comprises three members: PKD1, PKD2 and PKD3 encoded by three distinct genes (Prkd1, Prkd2 and Prkd3) cloned in early 1994 by the teams of Prof. Enrique Rozengurt in the USA and Prof. Klaus Pfitzenmaier in Germany. Initially, PKDs were assigned to the atypical PKC family, named PKCmu (PKD1) and PKCnu (PKD3) based on domain similarities with PKCs. However, a closer analysis of the structure of the kinase domain revealed their close relationship to Calcium/calmodulin kinase family (CAMK) and now PKDs are classified as members of the CAMK group of kinases. Like PKCs, PKD kinases have two cysteine-rich repeats (C1a and C1b) in their N-termini. These repeats have the ability to bind diacylglycerol (DAG) and phorbol esters (pharmacological DAG mimetics). Interestingly, the C1b repeat is responsible for 95% of DAG binding, whereas the non-consensus residues in C1a repeat mainly contribute to

maintaining the protein's structural fold and participate in PKD homo and hetero-dimer formation (Aicart-Ramos et al., 2016; Chen et al., 2008; Rey and Rozengurt, 2001). The cysteine-rich domains are followed by a central lipid-binding plekstrin-homology (PH) domain, which plays an autoinhibitory role, as its deletion or mutation results in PKD activation (Iglesias and Rozengurt, 1998). The PH domain is not characteristic for PKCs, which have instead a pseudosubstrate motif. Finally, the kinase domain is located closer to the carboxyl-terminus and, as mentioned above, has high similarity to CAMK I and CHK2 kinases. The kinase domain of PKD in the resting state is believed to form a loop, covered by the autoinhibitory PH domain, which corresponds to the so called "closed" conformation. (Feng et al., 2007) (Fig. 9).

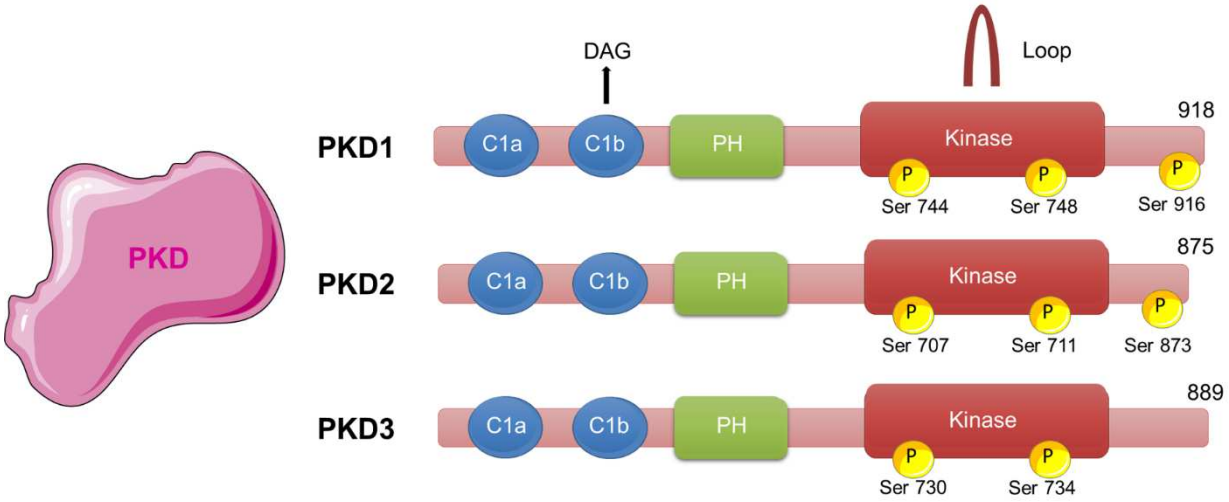

Introductory figure 9. Schematic illustration of the functional domain structure of PKD kinases. Starting from the amino-terminus cystein rich domains (C1a and C1b, in blue), which are important for DAG binding, followed by the autoinhibitory plekstrin homology domain (PH, in green) and the kinase domain (in red). Activatory phosphorylation events by upstream kinases or transphosphorylation are indicated for each PKD member. The length of aminoacids is indicated at the carboxyl-terminus.

All three PKD family members are ubiquitously expressed, but their protein levels may vary depending on the cell type. For example, pancreatic beta cells have high PKD1 and medium PKD3 expression, whereas PKD2 levels are comparably low (Sumara et al., 2009). Inversely, in T

lymphocytes PKD2 seems to be the predominantly expressed (Matthews et al., 2010; Navarro et al., 2014; Spitaler et al., 2006).

2.5.1 PKD regulation

PKD activity increases in response to stimulation of G-protein-coupled receptors (mainly Gq) and receptor tyrosine kinases by growth factors, peptide hormones, neurotransmitters and other stimuli. These signals converge in a local increase in DAG concentration and/or activation of novel PKCs, which include the δ, ε, η, and θ isoforms, and also require DAG for activation.

There are several ways of DAG generation. It can be produced directly by phospholipase C (PLC) β or PLCγ (Navarro et al., 2014; Wang, 2006; Xu et al., 2015) or indirectly by combined forces of phospholipases D (PLDs) (Roth, 2008) and lipid phosphate phosphatases (Lipins) (Brindley et al., 2009) through hydrolysis of phosphatidylcholine (PC) or by sphingomyelin synthase (SMS) that converts ceramide and phosphatidylcholine to sphingomyelin and DAG (Villani et al., 2008). Regardless of biogenesis mechanism, DAG cannot freely travel within the cell and remains membrane bound, thus acting as a platform recruiting and activating nPKCs and PKDs (Baron and Malhotra, 2002).

Novel PKCs exert positive regulation of PKD through direct phosphorylation at Ser744 and Ser748 located in the catalytic domain activation loop (A-loop), which results in an "open" (active) conformation. In response to oxidative stress, tyrosine kinases, such as SFK, activate PKD1 by targeting Tyr463 for phosphorylation within the PH domain, priming PKD for sequential phosphorylation by PKCδ (Storz et al., 2003). Homo- and hetero-dimerization is believed to be another important step in PKD activation (Bossard et al., 2007) as it allows for trans-phosphorylation i.e. self-activation and signal amplification. Therefore, continuous phosphorylation by PKCs results in a formation of an active pool of PKDs that can amplify the

signal through trans-phosphorylation. And vice versa, the kinase-dead construct of PKD (PKD-KD) with a single amino-acid substitution of a critical lysine residue in the ATP binding site in the kinase domain (K618N) (Liljedahl et al., 2001) displays a dominant-negative effect in cells with low PKD expression level (Bossard et al., 2007). Far less is known about negative regulators of PKD activity. Stress induced kinase p38delta (MAPK13) specifically phosphorylates PKD1 on Ser397 and Ser401 most likely stabilizing the inhibitory effect of the PH domain (Sumara et al., 2009).

2.5.2 PKD function

PKDs mediate the action of a whole plethora of extracellular and intracellular signals, so it is no surprise that PKDs are key players in many cellular processes. PKDs are shown to regulate cell motility (Cowell et al., 2009; Jaggi et al., 2005), survival upon oxidative stress (Cowell et al., 2009; Storz et al., 2003), transcription (Dequiedt et al., 2005; Jensen et al., 2009; Song et al., 2006; Xu et al., 2007), immune responses (Aicart-Ramos et al., 2016; Ittner et al., 2012; Ren et al., 2009; Zhang et al., 2017) (Fig. 10). But probably its role in vesicle fission and cargo transport from the trans-Golgi network was one of the most prominent findings (Baron and Malhotra, 2002; Bossard et al., 2007; Hausser et al., 2005). All PKD isoforms are required for vesicle scission and secretion from the TGN (Bossard et al., 2007). At the TGN, PKDs phosphorylates multiple targets, such as Phosphatidylinositol-4 kianse IIIbeta (PI4KIIIβ) (Hausser et al., 2005), ceramide transfer protein (CERT) (Fugmann et al., 2007; Hanada et al., 2009; Olayioye and Hausser, 2012) and oxysterol-binding protein (OSBP)(Nhek et al., 2010). PKD phosphorylation of PI4KIIIβ potentiates Phosphatidylinositol-4 phosphate (PI4P) production and thus creation of the lipid environment, which is favorable for recruitment of the vesicle fission machinery and

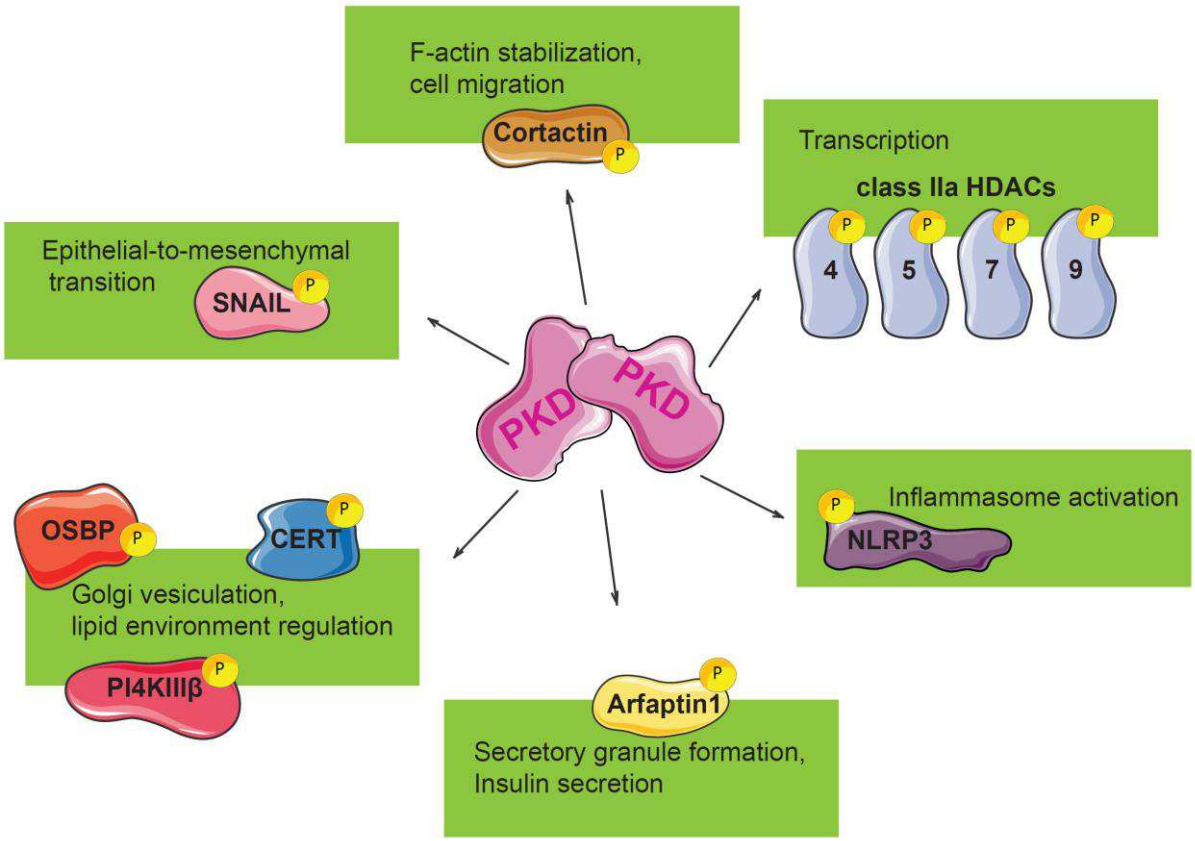

Introductory figure 10. Schematic illustration of PKD regulated processes through phosphorylation of different protein substrates.

many lipid and sterol transfer proteins. CERT acts as a shuttle for ceramide from ER to Golgi, which could be used to enhance DAG generation as a by-product of sphingomyelin synthesis (Hanada et al., 2009; Kudo et al., 2010; Villani et al., 2008). OSBP acts in tandem with CERT transferring cholesterol species to Golgi membranes (Alphey et al., 1998; Olayioye and Hausser, 2012). Cholesterol–sphingomyelin complexes then facilitate protein and lipid cargos sorting and vesicle budding from the TGN (Graham and Burd, 2011; Subathra et al., 2011; Villani et al., 2008). Normally DAGs are minor components of cell membranes (about 1 mole% of the total lipids). DAG accumulation leads to profound effects on membrane curvature thanks to physical properties that favor negatively curved membranes thus reducing the energetic barrier to membrane fission

(Goni and Alonso, 1999; Roth, 2008). In this way, PKD is not only getting activated by DAG but also potentiates DAG signaling through OSBP and CERT.

The work in my host laboratory made a significant contribution to deciphering of the roles of PKD1 in the secretory pathways in pancreatic β cells. While focusing on stimulated secretion, our lab discovered that PKD is required for insulin secretion (Sumara et al., 2009). Through phosphorylation of a small BAR-domain containing protein Arfaptin-1, PKD regulates proper insulin granule formation and its scission from TGN (Gehart et al., 2012). PKD activity is also required for insulin granule quality control and degradation limiting starvation-induced lysosomal insulin disposal and mTORC1-dependent inhibition of autophagy (Goginashvili et al., 2015). These findings are now corroborated *in vivo* in mouse models and, more importantly, lysosomal insulin degradation seems to contribute to β cell failure in type 2 diabetes (Pasquier et al. 2017, in revision).

2.5.3 PKD role in mitochondrial homeostasis

To date, there is no clear evidence describing a possible role of PKD in mitochondrial function. Several studies reported a pro-survival function of PKD in oxidative stress (Cowell et al., 2009). According to their findings reactive oxygen species (ROS) activate PLD1, which converts phosphatydilcholine into phosphatidic acid (PA). Accumulated PA acts as a substrate for PA phosphatases (lipins)-catalysed DAG production on the mitochondrial surface. DAG stimulates the recruitment of PKD1 and its activation by PKCδ and Src family kinase (SFK) (Doppler and Storz, 2007). PKD1-dependent activation of the IKKα/β–Nemo complex in the cytoplasm leads to Iκb degradation and nuclear translocation of NF-κB (Storz et al., 2005). NF-κB induces the transcriptional pro-survival program including the expression of mitochondrial MnSOD. Increased protein levels of MnSOD correlated with a decrease in mitochondrial ROS. The authors

showed that PKD1 was required in this oxidative stress response, yet PKD1 targets leading to activation of the IKKα/β–Nemo complex have not been identified thus far.

A recent study proposed a mechanism for PKD-dependent mitochondrial fragmentation in response to α1-adrenergic stimulation in H9c2 cardiac myoblasts and rat neonatal cardiomyocytes. GqPCR stimulation resulted in PKD activation and its translocation to the OM, where it phosphorylated DRP1 at Ser637 thereby stimulating mitochondrial fission, superoxide generation, and apoptotic signaling (Jhun et al., 2018). Yet another group one year earlier presented the opposite results (Brand et al, 2016). According to their findings, in cardiomyocytes RhoA acts downstream of G-protein coupled receptors and is protective against ischemia/reperfusion injury. PKD acts as a downstream mediator of RhoA signaling, stimulating mitophagy and preventing apoptosis (Xiang et al., 2013). Surprisingly, both groups agree on PKD-mediated fragmentation in a DRP1-dependent manner although proposed molecular mechanisms and, importantly, the outcomes (survival versus apoptosis) differ and require further corroboration.

2.5.4 The role of PKD in mitosis

Although the PKD family is a subject of intensive investigation in the context of secretion, inflammation and cancer, data confirming a role of PKD in mitosis roles remain vague. Papazyan et al. was first to describe enhanced PKD activity in mitotic cells and its mitotic localization to centrosomes, spindles and midbody (Papazyan et al., 2008). Although no direct function or targets were discovered, this study proposed an active participation of all three PKD kinases in cell division.

Interestingly, the group of Angelika Hausser recently proposed an upstream role for PKD in MEK-mediated mitotic Golgi remodeling (Kienzle et al., 2013). They showed that siRNA downregulation

of PKD proteins in HeLa cells prevented mitotic Golgi fragmentation and this defect could be rescued by overexpression of a constitutively active form of MEK1. Moreover, PKDs were required for HeLa cells to progress to mitosis and PKD depletion resulted in a G2/M arrest with no cells able to proceed to prometaphase. These findings are in line with previous observations linking Golgi complex hypervesiculation and overexpression of constitutively active PKD in HeLa cells (Bossard et al., 2007) and strict requirement for PKD activity in nocodazole-induced Golgi dispersal (Fuchs et al., 2009). Moreover, PKD was shown to interact with ADP-ribosylation factor 1 (ARF1) (Pusapati et al., 2010), the activity of which was shown to be important in mitotic Golgi remodeling (Altan-Bonnet et al., 2003; Xiang et al., 2007). Another group reported perturbed microtubule nucleation and dynamics during mitosis in cells devoid of PKD3 (Zhang et al., 2016). PKD1 but not PKD2 showed partial redundancy with PKD3 in microtubule regulation. Yet the study did not describe any target substrate and/or possible mechanisms.

2.6 AMP-activated kinase (AMPK)

AMPK is yet another kinase the function of which has been linked to mitochondrial function and dynamics. AMPK is a Ser/Thr heterotrimeric kinase complex, which is composed of a catalytic subunit (α), a scaffolding subunit (β) and a regulatory subunit (γ) (Fig. 10).

In humans, these ubiquitously expressed subunits are encoded by seven separate genes: *PRKAA1* and *PRKAA2* (encoding α1 and α2), *PRKAB1* and *PRKAB2* (β1 and β2) and *PRKAG1*, *PRKAG2* and *PRKAG3* (γ1, γ2 and γ3). Like PKDs, AMPK kinases belong to the CAMK kinase superfamily and display similar basophilic substrate motif specificity.

AMPK has an established role as a stress kinase complex that can sense a decrease in cellular energy. Thus, AMPK can be activated by a variety of stimuli that deplete intacellular ATP ranging from nutrient starvation to mitochondrial poisons or hypoxia. These so called “energy stress”

signals converge into changes of intracellular AMP and/or ADP ratios. AMP and ADP can directly interact with the AMPK regulatory γ subunit, leading to a conformational change that shields the phosphorylation at Thr172 within the activation loop of AMPK from phosphatases (Oakhill et al., 2011; Xiao et al., 2011). There are two kinases that can positively regulate AMPK by inducing Thr172 phosphorylation. One of them is tumor suppressor kinase LKB1 (Hawley et al., 2003; Shaw et al., 2004), whereas the second one is highly homologues to LKB1, the calcium/calmodulin-dependent CAMKKβ kinase (Hawley et al., 2005). Notably, this phosphorylation is critically important for AMPK kinase activity and is often used as a surrogate marker for AMPK activation. Structurally, the amino-terminus of the catalytic α subunit of AMPK starts with the kinase domain, which is neighboring the autoinhibitory domain (AID). AID interferes with the active kinase conformation, and its deletion increases AMPK basal activity even in the absence of AMP (Fig. 11) (Goransson et al., 2007; Pang et al., 2007).

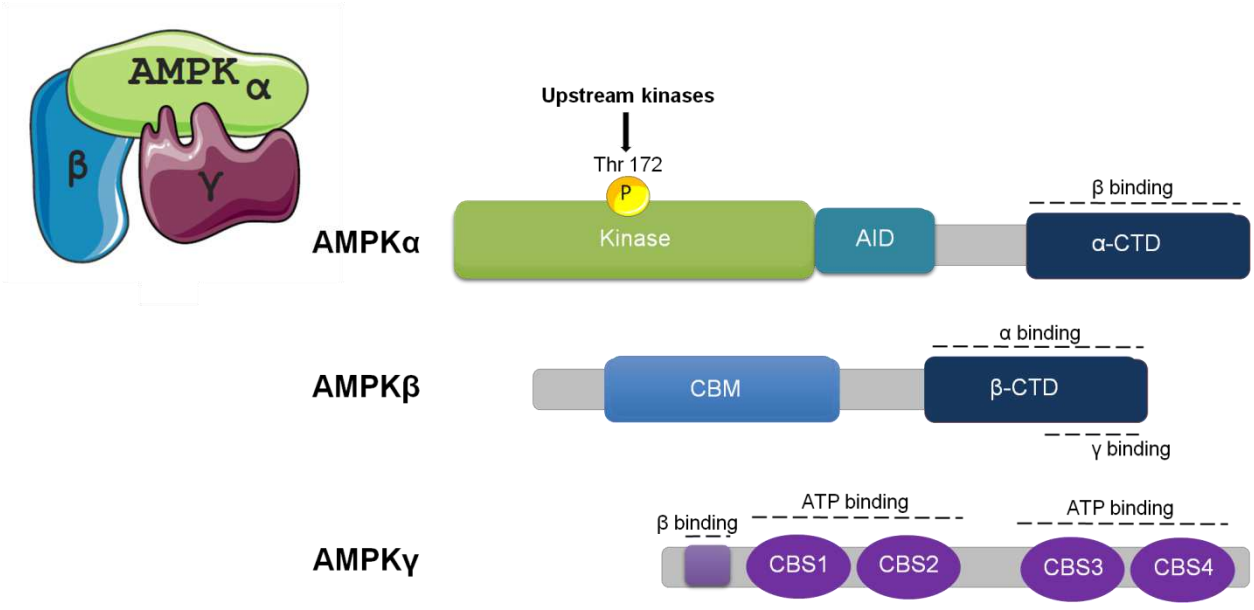

Introductory figure 11. Schematic illustration of the functional domain architecture of AMPK complex members. Starting from the amino-terminus catalytic AMPKalpha subunit, which contains a kinase domain (in green), followed by the autoinhibitory domain (AID, light blue) and C-terminal domain. AMPK beta contains a glycogen binding domain at the amino-terminus (in blue) and an AMPKalpha binding c-terminal domain (CTD, in dark blue). The amino-terminus of the short isoform of AMPK gamma contains a AMPK beta binding region (light violet) and four ATP binding units (CBS, violet), which form two "Bateman domains".

AID is followed by a globular region, which forms the C-terminal domain (CTD). CTD of the α subunit is involved in the homotypic interaction with the CTD of the β subunit (Crute et al., 1998; Hudson et al., 2003). Apart from the α subunit binding site, the β-CTD also contains the γ subunit interaction part, thus providing a structural basis for the formation of the αβγ complex. The amino-terminus of the β subunit contains the myristoylation site, which is shown to be necessary for potentiating Thr-172 phosphorylation by bound nucleotides (Oakhill et al., 2010; Oakhill et al., 2011) and for nucleo-cytoplasmic shuttling (Suzuki et al., 2007). The short isoform of the γ subunit is the most prevalent in tissues. It has the amino-terminus starting with the interaction site for the β subunit, followed by four tandem cystathione β-synthase (CBS) repeats (Viana et al., 2007; Xiao et al., 2007). These four CBS repeats participate in the formation of two "Bateman domains", which have regulatory function for binding of adenine nucleotides (King et al., 2008; Rudolph et al., 2007; Scott et al., 2004; Xiao et al., 2007).

When activated, AMPK stimulates catabolic pathways resulting in ATP production and inhibits ATP-consuming anabolic pathways. Since its discovery in 1973 (Beg et al., 1973; Carlson and Kim, 1973) AMPK became a subject of numerous investigations highlighting its unique metabolic switch-like functions and diverse cellular substrates. In response to lack of nutrients, AMPK blocks cellular growth and proliferation through inhibition of the mTORC1 pathway. Mechanistically, it phosphorylates the tumor suppressor TSC2 and the mTORC1 component Raptor (Gwinn et al., 2008; Inoki et al., 2003). AMPK also stimulates lipolysis through phosphorylation of HSL, glycolysis through phosphorylation of PFKFB2, fatty acid β-oxidation through phosphorlytation of ACC2. Conversely, it inhibits synthesis of proteins through phosphorylation of TSC2 and Raptor, fatty acids through phosphorylation of ACC1, and glycogen through phosphorylation of GYS1/2. When nutrients are scarce, AMPK positively regulates macroautophagy, a multistep process of "self-degradation" in which cellular organelles or cytoplasmic material become degraded into metabolites. In this case, AMPK phosphorylates ULK1 kinase, which is upstream of PIK3C3 in the regulatory chain of autophagophore formation, and AMPK inhibits mTORC1, which is a negative regulator of ULK1 (Kim et al., 2011). As mentioned above, AMPK also plays an important role in

mitochondrial quality control. AMPK activates mitophagy of malfunctioning mitochondria by phosphorylation of ULK1. Cells lacking either AMPK or ULK1 display defects in mitophagy and macroautophagy (Egan et al., 2011). At the same time, AMPK can induce mitochondrial biogenesis through a PGC-1α-mediated transcriptional program. Thus, through activation of AMPK, old mitochondria are replaced by newly generated ones. Recently, AMPK has been described to regulate mitochondrial fragmentation in response to energy stress (Toyama et al., 2016). Mechanistically, AMPK phosphorylates MFF at Ser155/Ser172, which increases the ability of MFF to recruit DRP1 to the mitochondrial surface and stimulates mitochondrial fission in response to mitochondrial poisons or pharmacological AMPK activators. Authors speculate that this AMPK-dependent mechanism should facilitate mitophagy (Toyama et al., 2016).

Since the discovery of AMPK as a downstream target of tumor suppressor LKB1 and a potent inhibitor of mTORC1, numerous laboratories started to unravel its function in cancer and cell cycle progression. Thus, AMPK was reported to directly mediate at least some of LKB1 tumor suppressing functions through direct regulation of p53 (Jones et al., 2005) and the CDK inhibitor p27 (Bjorklund et al., 2010; Liang et al., 2007). It was also discovered that the most common anti-diabetic medication metformin, which is on the market for several decades, activates AMPK through LKB1 (Shaw et al., 2005; Zhou et al., 2001). Mechanistically, metformin as well as its analog phenformin (Dykens et al., 2008) inhibit Complex 1 of the mitochondrial respiratory chain and reduces cellular ATP levels (Owen et al., 2000). Other AMPK agonists, such as AICAR, act as AMP mimetics (Corton et al., 1995), or in case of A-769662 and Salicylate as allosteric regulators of the AMPK complex (Goransson et al., 2007).

2.7 The crosstalk between PKD and AMPK

The regulatory relationship between PKD and AMPK remains unexplored. To date there is only one study addressing this question in the context of the insulin pathway in C2C12 skeletal muscle cells (Coughlan et al., 2016). According to their findings, PKD acts as a negative regulator of AMPK and insulin signaling in muscle. In response to phorbol esters (DAG-mimetics) PKD was shown to phosphorylate S491 in AMPK, which resulted in a 60% drop in AMPK activity. PKD activity attenuation with the novel specific inhibitor CRT0066101 or through siRNA mediated knockdown of PKD1, abrogated S491 phosphorylation and completely restored AMPK activity. Interestingly, AMPK and PKD share similar substrate specificity (L/VXRXXS/T) and even phosphorylate similar substrates (class IIa HDACs). Moreover, very recently AMPK was shown to phosphorylate MFF (Toyama et al., 2016) on same sites as those identified in a phosphoproteomic screen for PKD targets (Franz-Wachtel et al., 2012).

3 Aims of the project

Recently, mitochondrial dynamics has attracted a lot of attention because of its involvement in metabolic reprogramming of transformed cells. Cancer cells have reportedly high levels of mitochondrial fragmentation, which have been positively correlated with high proliferation rates and metastasis potential. Inhibition of mitochondrial fission by targeting fission mechanoenzyme DRP1 by pharmacological agents or RNA interference has been proven to be a valid strategy to slow down the tumor growth.

Pancreatic ductal adenocarcinoma is one of the most aggressive cancers and has been recently characterized with high levels of Protein kinase D (PKD) expression and elevated mitochondrial fragmentation. In several cancer models, PKD inhibition resulted in a decrease in cancer cell proliferation or cell cycle arrest. The PKD kinase family members are well known as decisive players in DAG-mediated membrane fission process at the trans-Golgi network. Interestingly, recent evidence indicates that mitochondrial OM lipids can be also a source for DAG production. Newly generated DAG is believed to promote mitochondrial fission.

Therefore, we hypothesized that PKD kinases may extend their DAG-dependent fission function beyond the Golgi ribbon. So the aims of my project were to confirm the initial hypothesis of requirement of PKD for mitochondrial fission in cancer cells and to identify the molecular mechanism, by which PKD(s) may govern this process.

4 Materials and Methods

3.1 Reagents

Rotenone (Ref. R8875), Carbonyl cyanide 3-chlorophenylhydrazone, CCCP (Ref. C2759), Antimycin A from Streptomyces sp. (Ref. A8674), Thymidine (Ref. T1895-5G), Nocodazole (Methyl Carbamate, Ref. M-1404), Taxol (Paclitaxel, Ref. T-7191), Monastrol (Ref. M8515), RO-3306 (Ref. SML0569), 4′,6-Diamidino-2-phenylindole dihydrochloride (DAPI) (Ref. D8417) were purchased from Sigma-Aldrich. CRT 0066101 (Ref. 4975), kb ND 142-70 (Ref. 3962), CID 755673 (Ref. 3327), A 769662 (Cat. No. 3336), Metformin hydrochloride (Cat. No. 2864), AICAR (Cat. No. 2840) were purchased from Tocris Bioscience. STLC (S-Trityl-L-cysteine, Ref. ALX-105-011-M500) was purchased from Enzo Life Sciences. MitoTracker Red CMXRos (Ref. M7512) was from Life Technologies.

3.2 Plasmids

Human MFF isoform2 of 291a.a., (Q9GZY8, uniprot.org) and MFF isoform4 of 218a.a., (Q9GZY8, uniprot.org) were amplified from HeLa cDNA by PCR. A single FLAG tag along with KOZAK sequence was inserted in frame at the N-terminus of MFF. Human MFF WT and 3S3A, 3S3D, 3S3E mutants were cloned into pcDNA™3.1/Zeo(+) (Invitrogen) and pEGFP-N1 (Clontech) empty vectors using ligation-independent cloning (LIC). Mouse MFF isoform4 (Q6PCP5, uniprot.org) with N-terminal FLAG-tag in pIRESneo3 vector (Clontech) (Otera et al., 2010) was a kind gift from H. Otera (Kyushu University). pEGFP-N1-hPKD1WT/CA/KD constructs were described previously (Gehart et al., 2012). Human MFF WT ΔTMD (transmembrane domain deleted) was generated by PCR as described previously (Otera et al., 2010) and cloned into pGEX6P1 empty vector (GE Healthcare Life Sciences) expressing N-terminal fused GST tag followed by the PreScission protease cleavage site. Human and mouse MFF phosphorylation sites A/D/E mutants were

generated by PCR using LIC or overlap PCR strategies and cloned into pcDNA™3.1/Zeo(+) or pGEX6P1 empty vectors using LIC.

3.3 Antibodies

Rabbit polyclonal MFF antibodies were produced and purified by IGBMC Antibody facility against following antigens: human recombinant MFF ΔTMD (for total MFF antibody), phospho-peptide – GRLKRER**pS**MSENAVR (for phospho-Ser155 MFF antibody), phospho-peptide – NPHHDNVRYGI**pS**NLDAAIEGC (for phospho-Ser275 MFF antibody). Mouse monoclonal anti-Flag, mouse monoclonal anti-GFP and mouse monoclonal anti-GST antibodies were produced by IGBMC Antibody facility.

Following antibodies were commercial: mouse anti-TUBULIN (Ref. T9026) from Sigma-Aldrich; rabbit anti-phospho-PKD/PKCμ (Ser916) antibody (Ref. 2051), rabbit anti-phospho-PKD/PKCμ (Ser744) antibody (Ref. 2054), rabbit anti-phospho-(LXRXXSer/Thr) PKD Substrate antibody (Ref. 4381), rabbit anti-PKD1 antibody (Ref. 2052), rabbit anti-PKD2 antibody (Ref. 8188), rabbit anti-PKD3 antibody (Ref. 5655), rabbit anti-phospho-AMPKalpha (Thr172) antibody (Ref. 2535), rabbit anti-AMPK antibody (Ref. 2532), rabbit anti-phospho-ULK1 antibody (Ser555) (Ref. 5869), rabbit anti-ULK1 antibody (Ref. 4776), rabbit anti-phospho-ACC1 antibody (Ser79) (Ref. 11818), rabbit anti-ACC1 antibody (Ref. 4190), rabbit anti-VINCULIN antibody (8188) were from Cell Signaling technology; rabbit anti-mouse PKD2 antibody (Ref. A300-073A-T) was from BETHYL; rabbit anti-PKD1 antibody (C-20) (Ref. sc-639) and rabbit anti-TOM20 (Ref. sc-11415) were from Santa Cruz Biotechnology; mouse anti-Flag M2 antibody (Ref. F1804) and rabbit anti-GAPDH (Ref. G9545) were from Sigma-Aldrich.

3.4 Mice

PKD1 floxed (PKD1fl/fl) and PKD3 floxed (PKD3fl/fl) mice were described previously (Fielitz et al., 2008; Zhang et al., 2017). PKD1fl/fl mice were provided by E.N. Olson (University of Texas Southwestern). PKD3fl/fl mice were provided by M. Leitges (Biotechnology Centre of Oslo). As PKD1 knockout mice are embryonically lethal (Fielitz et al., 2008) we generated PKD1-PKD3 fl/fl mice by crossing PKD1fl/fl mice and PKD3fl/fl mice on C57BL/6J background. Mice were housed on a 12-h light/dark cycle and received standard chow diet in the animal facility of the IGBMC in compliance with the European legislation on care and use of laboratory animals.

3.5 PKD1/PKD3 DKO MEFs generation

Mouse embryonic fibroblasts (MEFs) were isolated from 12.5-day-old embryos of PKD1-PKD3 fl/fl mice. Early (1-4) passages were frozen. To generate the PKD1-PKD3 DKO MEFs, early passage PKD1-PKD3 fl/fl MEFs were infected with retroviral vector pZip-Neo-SV(X)1 containing SV40 large T antigen (Addgene: 1776) (Jat et al., 1986) (a kind gift from H. Groenemeyer, IGBMC). Infected cells were selected for viral integration using 0.5 mg/mL neomycin (G418) for 3 days until there were no cells remained on the control plate. Transformed PKD1-PKD3 fl/fl MEFs were propagated and later infected with Adeno-associated viruses encoding either eGFP (control) or Cre-eGFP (AAV-CMV-eGFP or AAV-CMV-Cre-eGFP) using rAAV2/DJ vectors from AAV Helper Free System (Cat. No. VPK-430-DJ) from Cell Biolabs. Briefly, 40 µL of the virus (AAV-CMV-eGFP or AAV-CMV-Cre-eGFP) were added in in the new media in 1 well of a 6 well plate, containing cells at 20-30% confluency. After 48h the cells were split in 10cm dish and allowed to grow until confluent. To ensure the purity, infected cells were selected for GFP or Cre-GFP expression using FACS. Efficient PKD1/3 deletions were validated by western blot and by genotyping PCR.

3.6 Cell culture

All cell lines were purchased from ATCC (unless specified otherwise) and maintained at 37 °C in 5% CO_2 humidified incubator. NIH 3T3 mouse fibroblasts were grown in high glucose (4.5 g/L) DMEM supplemented with 10% newborn calf serum and gentamycin (40 µg/ml). HeLa Kyoto human cervix carcinoma cells were grown in high glucose DMEM-GlutaMAX supplemented with 10% fetal calf serum, 1mM sodium pyruvate and gentamycin. PANC-1 human pancreatic ductal adenocarcinoma cells were grown in high glucose DMEM-GlutaMAX supplemented with 10% fetal calf serum, 1mM sodium pyruvate and gentamycin. HEK 293T human embryonic kidney cells were grown in low glucose (1 g/L) DMEM supplemented with 10% fetal calf serum and 1% penicillin/streptomycin. Phoenix™ Eco (Orbigen, a gift from H. Groenemeyer, IGBMC) human embryonic kidney retrovirus packaging cell line was grown in high glucose DMEM-GlutaMAX supplemented with 10% fetal calf serum and gentamycin. WT and MFF -/- MEFS (Loson et al., 2013) were grown in high glucose DMEM-GlutaMAX supplemented with 10% fetal calf serum, 1mM sodium pyruvate and gentamycin and were a kind gift from D. Chan (CalTech). PKD1-PKD3 fl/fl and PKD1/PKD3 DKO MEFS were grown in high glucose DMEM-GlutaMAX supplemented with 10% fetal calf serum, 1mM sodium pyruvate and gentamycin.

3.7 Cell cycle synchronization

HeLa cells were synchronized in different stages of cell cycle by double Thymidine block in S-phase protocol. Briefly, 2 mM Thymidine was added twice for 16 hours with three times wash with warm media and Thymidine-free 8 hours incubation in between. After the second Thymidine block was complete, cells were released in thymidine-free media and collected at time points indicated. HeLa cells were synchronized in mitosis using Nocodazolee for 8 hours or 14 hours at 3 µM final concentration, Taxol for 16-18 hours at 1 µM, STLC for 18 hours at 5 µM, Monastrol for 16 hours at 100 µM. HeLa cells were synchronized in G2 using RO-3306 for 20 hours at 5 µM final concentration.

3.8 Cell treatments

To activate AMPK, HEK293T WT and AMPK α1/α2 DKO were stimulated for 1 hour with mixture of 2mM AICAR/ 100mM A-769662 or 1mM Metformin or 1 μM Rotenone. For PKD inihibition and oxidative stress experiments NIH 3T3 cells were pre-treated with solvent (control#1) or PKD inhibitors for 1h before addition of second solvent (control#2) or 1 μM Rotenone for 5 hours incubation. For requirement of PKD in mitotic MFF phosphorylation, HeLa cells were treated with Taxol or Nocodazole for 14 hours followed by addition of solvent (control) or PKD inhibitor for 6 hours or co-treated with Nocodazole/Taxol and CRT/solvent for 16 hours. For requirement of PKD in mitotic MFF phosphorylation, HeLa cells were synchronized in S phase by double Thymidine block and treated with solvent (control) or three PKD inhibitors or AMPK inhibitor for 2 hours. PANC-1 cells were treated with solvent (control) or PKD inhibitor for 14 hours.

3.9 Cell transfection and virus production

Transient transfections of Hela cells were done with JetPEI (Polyplus Transfection) according to the manufacturer's instructions. Transient transfections of HEK293T and NIH3T3 cells were done with JetPEI (Polyplus Transfection) or Lipofectamine 2000 (Life Technologies). Cell lysates were harvested 24-36 hours after transfection. Retroviral infections were performed using Phoenix™ Eco (Orbigen) packaging cell line using JetPEI transfection reagent following the manufacturer instructions. Lentiviral infections were performed as described previously (Gehart et al., 2012; Zhang et al., 2017). Briefly, HEK293T cells were used as a packaging cell line using JetPEI (Polyplus Transfection). Transfection mixture for 10cm dish contained 12 μg of Lenti-mix plasmids (3 μg pVSVG, 3 μg pMDL and 3 μg pREV) along with 3 μg of plasmid expressing gene of interest. 16h post-transfection media was replaced by fresh one. Virus-containing supernatant was collected 24h, 36h and 48 h after transfection, sterile-filtered through 0.45 μm Millex-HV Syringe Filters (Millipore) and used immediately or stored at 4 °C. NIH 3T3 cells were infected with 10% (v/v) lentivirus-contained supernatant in NIH3T3 media supplemented with 1 μg/ml polybrene (Santa

Cruz, Ref. sc-134220). Stable re-expression of mouse PKD1 or PKD2 into NIH3T3 PKD1/3 DKO cells was performed using lentivirus-mediated transduction with pBOB vector. Mouse PKD2 knockdown in NIH3T3 WT, NIH3T3 PKD1/3 DKO cells or PKD1/3 DKO MEFs was achieved by lentiviral transduction of mPKD2 shRNA constructs in pLKO.1 puro (Sigma Aldrich) (for sequences, please see table below). Infected cells were selected for viral integration using 0,5ug/ml Puromycin (Sigma) for 3 days until there were no cells remaining on the control plate. The PKD2 knockdown efficiency was assessed by Western blotting.

3.10 Gene silencing by siRNA

Human PKD2 and PKD3 mRNAs were silenced in HeLa cells using on-target siRNAs from Dharmacon. Cells were transfected with Oligofectamine (Invitrogen) according to the manufacturer's instructions at final siRNA concentration of 60nM. Knockdown efficiency was verified by western blotting. Cells were analyzed by western blot or fluorescence 48 or 72 hours after siRNA transfection as indicated in text or figure legends.

3.11 RNA extraction and cDNA synthesis

RNA was extracted from HeLa cells using TRI Reagent (Molecular Research Center, Ref. TR118) following the manufacturer's protocol. cDNA was reverse transcribed from 2 µg of isolated RNA using oligo-dT primers and SuperScript III First-Strand Synthesis SuperMix (Invitrogen) according to the manufacturer's instructions.

3.12 Genotyping and sequencing

PKD1 fl/fl MEFs genotyping was performed with Taq polymerase (Roche) using the following primers:

Primer	Sequence
PKD1_ff_geno_fwd	5' GCCCACAGCTATTGTTCCTAA 3'
PKD1_ff_geno_rev	5' GGATAAAGTGATCAAGCAGCA 3'
PKD1_del_geno	5' CCTTTAATCTGAGCACTTGG 3'
Cre_geno_fwd	5' GCGGTCTGGCAGTAAAAACTATC 3'
Cre_geno_rev	5' CAAAACAGGTAGTTATTCGGATCATC 3'

Sequencing of NIH3T3 PKD1/3 DKO clones

Regions covering the gRNA targeted sites in exon1 of mouse PRKD1, PRKD2, PRKD3 genes were amplified by PCR with Phusion DNA Polymerase (Thermo Fisher Scientific) using following primers:

Primer	Sequence
mPRKD1_geno_F	5' AGTTTGGTGGTTCTTCT 3'
mPRKD1_geno_R	5' ACTGTCATCGCAAGAAG 3'
mPRKD2_geno_F	5' TTCTTCCAACCTTCCAATC 3'
mPRKD2_geno_R	5' AAAACAACAAGCAGCGAC 3'
mPRKD3_geno_F	5’ ACCAGGATATTTGAGTACAAGG 3’
mPRKD3_geno_R	5’ ACGTTAAAGAAGCAAGCCAC 3’

Obtained PCR products were gel-purified using NucleoSpin Gel and PCR Clean-up Kit (Macherey-Nagel) and amplified with new primer pairs containing pUC57 (GenScript) overlap sequences:

Primer	Sequence
mPRKD1_geno_F	5' CGAATGCATCTAGATATCGGATCCAGTTTGGTGGTTCTTCT 3'
mPRKD1_geno_R	5' GCCTCTGCAGTCGACGGGCCCGGGACTGTCATCGCAAGAAG 3'
mPRKD2_geno_F	5' CGAATGCATCTAGATATCGGATCCTTCTTCCAACCTTCCAATC 3'
mPRKD2_geno_R	5' GCCTCTGCAGTCGACGGGCCCGGGAAAACAACAAGCAGCGAC 3'
mPRKD3_geno_F	5' CGAATGCATCTAGATATCGGATCCACCAGGATATTTGAGTACAAGG 3'
mPRKD3_geno_R	5' GCCTCTGCAGTCGACGGGCCCGGGACGTTAAAGAAGCAAGCCAC 3'

Obtained PCR products were gel-purified and cloned in pUC57 vector using LIC. Single colonies were mini-prepped using NucleoSpin Plasmid Kit (Macherey-Nagel) and sent for sequencing. For each gene at least 5 colonies were mini-prepped.

3.13 shRNA sequences

Mouse shPKD2 #1	5'- CGGCCTCAACCTTGGAGCGATAAGCTCGAGCTTATCGCTCCAAGGTTGAGGTTTTTG -3'
Mouse shPKD2 #2	5'- CCGGGAAACTGCTCAAGGGTCTATTCTCGAGAATAGACCCTTGAGCAGTTTCTTTTTG -3'

3.14 Generation of KO cell lines using CRISPR/Cas9 system

PKD 1/3 DKO NIH3T3 cell lines were generated using CRISPR/Cas9 genome editing system (Ran et al., 2013) using vectors described in (Zhang et al., 2017). Mouse PKD1, PKD2 and PKD3 guide RNA sequences targeting the exon 1 (as described in Results section) were designed using the online tool at **crispr.mit.edu** and cloned into pX330-P2A-EGFP by T4-ligase mediated cloning. 24 hours after transfection GFP positive cells were single-sorted into 96-well plates by FACS. Single clones were examined by microscopy and screened for PKD proteins by western blot. All chosen clones were validated for efficient knockout by western blot and sequencing.

AMPK α1/α2 DKO HEK293T cell lines were generated using CRISPR/Cas9 genome editing system as described previously (Toyama et al., 2016) except for pX330-P2A-EGFP and pX330-P2A-RFP vectors were used instead of pX462 vector with puromycin selection. 24 hours after transfection GFP positive cells were single-sorted into 96-well plates by FACS. Single clones were examined by microscopy and screened for AMPK α1/α2 proteins by western blot.

3.15 Western blot analysis

Cells were washed with ice-cold PBS on ice and cell lysates for western blotting were prepared using lysis buffer (50 mM Tris-HCl pH7.5, 150 mM NaCl, 1% Triton X-100, 1 mM EDTA, 1 mM EGTA, 2 mM Sodium pyrophosphate $Na_4P_2O_7$, 1 mM Sodium vanadate $NaVO_4$ and 50 mM Sodium fluoride NaF) supplemented with protease inhibitors (Complete Protease Inhibitor Cocktail, Roche)) and incubated on ice for 10 minutes. After centrifugation at 16 000g for 10 minutes at 4°C cleared supernatant was transferred to the new tubes and was used immediately or flash-frozen in liquid nitrogen and stored at -80°C until used. Total protein was measured using the Bradford method by Bio-Rad Protein Assay kit (Bio-Rad). Samples (100µg of total protein content) were boiled in 1x Laemmli Sample Buffer and resolved on 8%, 10%, 11% or 12% acrylamide gels using standard Tris-Glycine SDS-PAGE. Proteins were transferred to PVDF membranes (Millipore) and blotted with antibodies listed in the Antibodies section. For membrane blocking and primary antibody dilution 1% BSA (v/v) in PBST was used. All incubations with primary antibodies were performed for 16 hours at 4 °C. Blots were developed using SuperSignal West Pico (Pierce, Ref. 34580) or Luminata Forte Western HRP substrate (Merck Millipore, Ref. WBLUF0500).

3.16 Immunoprecipitation

Cells were washed with ice-cold PBS on ice and cell lysates for immunoprecipitation were prepared using IP buffer (50 mM Tris-HCl pH7.5, 50 mM NaCl, 0.5% Triton X-100, 0.5% NP40, 5 mM EDTA, 5 mM EGTA, 1 mM Sodium vanadate $NaVO_4$ and 10 mM Sodium fluoride NaF) supplemented with protease inhibitors (Roche) and incubated on ice for 10 minutes. After centrifugation at 16 000g for 10 minutes at 4°C cleared supernatant was used immediately or flash-frozen in liquid nitrogen and stored at -80°C until used. Lysates were equilibrated to volume and concentration. For Flag-MFF immunoprecipitation, ANTI-FLAG M2 Affinity Agarose Gel (Sigma, Ref. A2220) was used. For GFP-PKD or GFP-MFF immunoprecipitation, GFP-Trap-A beads (ChromoTek) were used. Samples were incubated with the beads for 2 or 16 hours at 4°C. For

endogenous MFF immunoprecipitation, home-made polyclonal rabbit anti-MFF antibody was incubated with lysates at concentration of 1µg for 500 µg of total lysate for 16 hours. Affi-Prep Protein A Resin (Bio-Rad) was used to precipitate formed antibody-protein complexes for 2 hours at 4°C. In all cases, the beads were washed four times with IP buffer and then either directly eluted in 1.5x Laemmli Sample Buffer or eluted with FLAG-peptide (only for FLAG-IPs). Eluted samples were boiled in 1.5x Laemmli Sample Buffer for 5 minutes and resolved by SDS-PAGE gel. Samples were analyzed by western blot as described above.

3.17 Flow cytometry

For cell cycle analysis, cells were resuspended and fixed in 70% ice-cold ethanol for 1h on ice followed by staining with propidium iodide (PI) solution (Sigma, Ref. P4170). The DNA content was determined using a BD FACSCalibur™ Cell Analyzer (BD Biosciences). To measure mitochondrial ROS, NIH 3T3 cells were treated with PKD inhibitor or vehicle control in combination with Rotenone for 4h30min, then DCF probe was added for 30min at 5µM. All incubations were performed at 37°C. After treatment was finished, cells were trypsinized, washed and resuspended in PBS. The ROS production was then assessed by measuring DCF probe retention (Ex/Em: ~492–495/517–527 nm).

3.18 *In silico* PKD substrate identification

MFF was identified as a potential PKD substrate by phospho-proteomic study in human cells (Franz-Wachtel et al., 2012). In that study, several MFF phosphosites were discovered to be differentially phosphorylated in HEK293T cells upon expression of constitutively active form of human PKD1, out of which several contained optimal PKD consensus motif (I/L/VXRXXpS/T). Sequence analysis of MFF orthologues in different species revealed high level of conservation of these sites in vertebrates. Further search showed that pS155 and pS172 (both within optimal PKD

motifs) were highly enriched in phospho-proteomic studies performed on cancer cells (Britton et al., 2014; Mertins et al., 2016; Yi et al., 2014) and, intriguingly, in mitosis (Kettenbach et al., 2011; Olsen et al., 2010).

3.19 Recombinant protein expression and purification

Recombinant MFF proteins were purified as described previously (Otera et al., 2010) Briefly, N-terminally GST-tagged human MFF ΔTMD WT and mutant proteins were expressed in protease deficient BL21DE3 E.coli strain using pGex-6P1 vectors. Bacteria were grown in 2xLB at 37 °C until log phase (OD600 = 0.5). Thereafter cultures were transferred to 20 °C incubator and MFF expression was induced by addition of 0.5 mM isopropyl-β-D-thiogalactopyranosid (IPTG) for 16h. Bacteria were pelleted at 5 000 g for 15 minutes. Cell pellet was resuspended in lysis buffer (PBS, 1% Triton X100, 1% NP40, 1mM DTT, Lysozyme (100 ug/ml) (Sigma, Ref. 62970), protease inhibitors (Roche), incubated on ice for 30 minutes and sonicated. Lysate was cleared by centrifugation at 15 000g for 30 minutes at 4 °C. Obtained supernatant was incubated for 16 h with 500 µl of Glutathione Sepharose 4B (GE Healthcare) protein purification resin (per 500 mL of bacterial culture used) on orbital shaker at 4°C. Beads were washed four times with 10 ml of lysis buffer and resuspended in 1mL of lysis buffer containing 2 units/µl PreScission™ Protease (GE Healthcare). GST-tag cleavage was performed for 16 h at 4°C and protease was removed by addition of 50 µl of fresh GSH-resin and centrifugation. Obtained supernatant was dialysed, aliquoted and stored at -80°C in PBS containing 2mM DTT, 20% Glycerol and protease inhibitors (Roche).

3.20 *In vitro* kinase assay

Kinase assays were performed as described previously (Gehart et al., 2012; Hausser et al., 2005; Sumara et al., 2009) with minor modifications. Briefly, for non-radioactive kinase assay, 1 µg of

recombinant GST-tagged human MFF ΔTMD WT and mutant proteins were incubated with 25ng of recombinant human PKD1 (Enzo, Ref. BML-SE348-0005) in Kinase Buffer (50mM Tris pH 7.4, 10mM MgCl2 and 2mM DTT). The reaction started with addition of 200 μM cold ATP and maintained at 30°C. After 30 minutes, 2x SDS-sample buffer was added to terminate the assay. Immediately, samples were loaded and resolved on 12% SDS-PAGE gel. Gel was transferred to PVDF membrane (Millipore) and analyzed as described in western blot section.

For radioactive kinase assay, all steps were similar but 2μCi [γ-32P]-ATP was used instead of cold ATP. SDS-PAGE gel containing radioactive samples was fixed and stained with Coomassie Brilliant Blue staining solution, followed by four steps in Coomassie Destain solution (water, methanol and acetic acid in a ratio of 50/40/10 (v/v/v)). After destaining gel was dried on a gel vacuum drier and analyzed by autoradiography exposing to Hyperfilm MP (Amersham).

3.21 Mass-spectrometry analysis

Mass-spectrometry analysis was performed blinded in collaboration with Dr. Yansheng Liu in Rudolf's Aebersold laboratory (ETH Zurich). Briefly, non-radioactive kinase reactions containing recombinant human MFF with or without recombinant human PKD, were digested with trypsin and analyzed by LC-MS/MS on Oribtrap XL. MaxQuant software (Ver.1.5.2.8) was used to process obtained raw files. Database was searched in MaxQuant using Andromeda peptide search engine against the human Swiss-Prot database. Viewer in MaxQuant was used for visualization of identified hits together with the raw data. Mass spectrometry results were analyzed using Skyline (MacCoss Lab Software).

3.22 Fluorescence and light microscopy

Cells were seeded on glass coverslips (9-12 mm) and let to attach overnight. Next day, after treatment was finished cells were briefly washed with PBS at room temperature and were fixed

in 4% paraformaldehyde (Electron Microscopy Sciences) in PBS for 15 min. After fixation step, cells were permeabilized for 5 min in PBST (PBS, 0.1% Triton X-100 (v/v)). Cells were incubated in blocking solution (5-10% normal goat serum in PBST) for 30minutes, and then in primary antibody for 1 hour at room temperature or for 16 hours at 4°C. Cells were washed three times with PBS and incubated with secondary antibodies for 1 hour at room temperature. Cells were washed three times with PBS and nuclei were counterstained with DAPI (1 μg/ml). Coverslips were mounted with Moviol (Calbiochem). Images were acquired using Confocal Laser Scanning Microscope Leica TCS SP8X (Leica) or Zeiss epifluorescence microscope with 100x NA1.32 or 63x NA1.4 objectives. Light microscopy images with differential interference contrast (DIC) were taken using 10x, 20x and 40x objectives on EVOS XL Core Cell Imaging System (Invitrogen).

3.23 Quantification of relative pS172 MFF signal intensity

Total pS172 MFF signal intensity in HeLa cells at different stages of cell cycle was measured in relation to the total pS172 background threshold signal intensity in the same region. For each cell cycle stage, 10 cells were analyzed per group, 100 cells per experiment.

3.24 Electron Microscopy

Qualitative analysis of mitochondrial morphology in NIH 3T3 cells treated with solvent (control) or PKD inhibitor (CRT) for 6 hours has been performed by TEM. Briefly, cells were fixed in 1% glutaraldehyde in 200mM HEPES (pH 7.4) for 3 hours at room temperature and then stored HEPES buffer alone at 4°C until Epon (Epon812) embedding. Semi-thin sections (60 nm) were stained with 1 % Osmium tetroxide and 1% Uranyl Acetate. Images were taken on TEM CM12 100Kv (FEI) equipped with CCD ORIUS 1000 Gatan camera. Images were taken at a magnification of 7500x and exported as tif files for analysis in Fiji (ImageJ).

3.25 Quantifications and statistics

In NIH 3T3 cells mitochondria were visualized either by staining with 100nM MitoTracker Red (Molecular probes) or immunostained with mitochondrial outer membrane marker TOM20. In HeLa cells mitochondria were visualized by immunostaining with TOM20 or directly using GFP marker (HeLa-MTS-eGFP). Cells were counted and categorized in three separate groups according to mitochondrial morphology. First group, defined as "fragmented", contained cells with a majority of mitochondria being round shaped and small (longer axis less than 5 μm); "intermediate" were cells with a majority of mitochondria being tubular and 5-10 μm long; "fused" contained cells with a majority of mitochondria being more than 10 μm long and/or highly interconnected. Total cell counts were converted into percentage of cells and obtained values were transformed into square root numbers, which were used for analysis of normality of distribution. As distribution was normal, two-way ANOVA with Dunnett's post-hoc multiple comparisons test was performed using GraphPad Prism (GraphPad). When two groups were compared, unpaired Student t-test was used for analysis. The data were expressed as mean ± SD and difference was considered as significant, when p-values were: $*p < 0.05$, $**p < 0.01$, and $***p < 0.001$, $****p < 0.0001$.

5 Results

5.1 MFF is a *bona fide* PKD substrate

In order to find substrates of PKD that may mediate its effects on mitochondrial dynamics and function, we first screened amino acid sequences of human proteins, which regulate mitochondrial dynamics for optimal PKD consensus phosphorylation motifs (L/we/VXRXXS/T). Out of DRP1, DYN2, Mff, Fis1, MiD49, MiD51 only Mff contained several potential PKD phosphorylation sites (Ser155, Ser172, uniprot: Q9GZY8). These potential sites are highly conserved in vertebrates and are present in all five described MFF isoforms.

We subsequently cross-validated our hit using a recently published unbiased phospho-proteomic screen aimed at identification of potential PKD substrates in human cells (HEK293T)(Franz-Wachtel et al. (2012)). This study identified Mff as a protein specifically phosphorylated upon expression of a constitutively active form of PKD. Moreover, the identified MFF phosphorylation sites were significantly down-regulated upon a decrease in PKD1 activity and were in line with the PKD target motif strongly indicating that MFF could be a direct PKD substrate.

To test the possibility that MFF is a substrate of PKD, we first examined whether PKD and MFF could interact in cells. We used human PKD1, which is a founder kinase of the PKD family and is highly homologous to PKD2 and PKD3. To that end, we performed co-immunoprecipitation experiments overexpressing Flag-tagged human MFF (hMFF) along with GFP or GFP-tagged wild type human PKD1 (GFP-hPKD1) in HEK293T cells, which were also used for the PKD phosphoproteome study. MFF co-immunoprecipitated with PKD1 in both conditions – when we immunoprecipitated MFF (Flag-hMFF) using a Flag M2 affinity gel and when we immunoprecipitated GFP-hPKD1 using GFP beads. No interaction was detected between GFP and Flag-hMFF in any of tested conditions (Fig. 1).

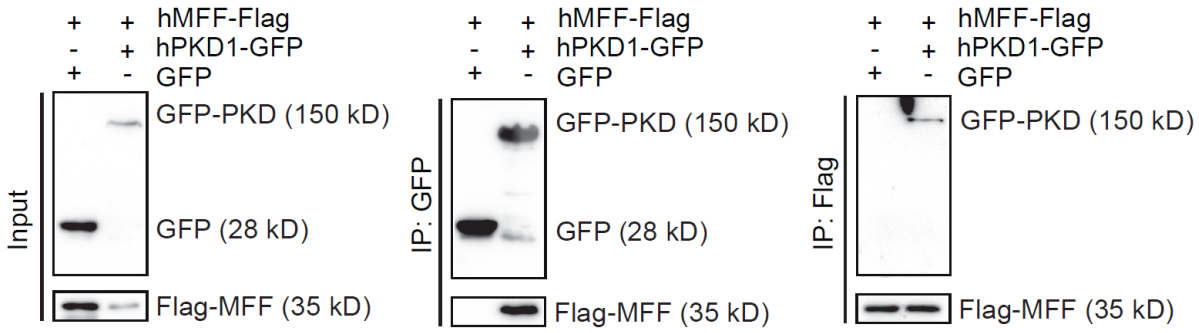

Figure 1. PKD interacts with MFF. Immunoblotting of elutions and inputs of co-immunoprecipitation of exogenous FLAG-tagged MFF with GFP-tagged PKD1 and reverse co-immunoprecipitation of exogenous GFP-tagged PKD1 with FLAG-tagged MFF from HEK293T cells. Antibodies against GFP and FLAG were used to detect respective proteins. Representative result of three independent experiments.

Next, we asked whether PKD could directly phosphorylate MFF in cells. To test this possibility, we tried to detect phosphorylation of MFF in cells using a commercially available PKD consensus phospho-motif antibody, which is designed to recognize a phosphorylated serine or threonine residues found within the PKD motif (LXRXXS/T). This antibody is proved to be a useful tool in identification of a broad spectrum of potential PKD substrates (Doppler et al., 2005). To that end, we co-expressed wild type (WT), constitutively active (CA) or kinase-dead (KD) GFP-hPKD1 together with Flag-hMFF in HEK293T cells. Subsequently, we immunoprecipitated MFF and quantified its phosphorylation using the PKD consensus phospho-motif antibody. Expression of CA-PKD resulted in a strong phosphorylation of MFF, while WT-PKD and KD-PKD induced a weak phosphorylation comparable to the GFP control (Fig. 2). This background signal could be explained by the basal activity of several endogenous PKD kinases, as HEK293T cells express all three PKD family members. Thus, we confirmed that PKD can phosphorylate MFF in human cells.

Alternatively, this phosphorylation still could be indirect or attributed to the activity of kinases acting downstream of PKD, but sharing similar substrate. The best way to exclude this possibility is to perform *in vitro* kinase assay with recombinant PKD and MFF.

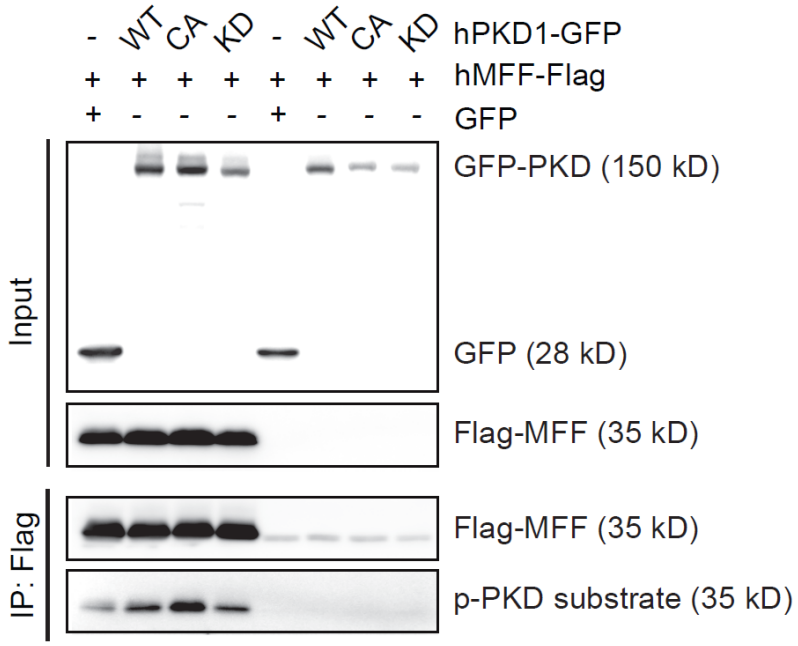

Figure 2. PKD phosphorylates MFF. Immunoblotting of elutions and inputs of FLAG immunoprecipitations from HEK293T cells ectopically co-expressing pcDNA-FLAG (vector control) or FLAG-tagged MFF with EGFP or EGFP-tagged wild type (WT)-, constitutively active (CA)- or kinase-dead (KD) PKD1. Antibodies against FLAG, phospho-PKD substrate motif and GFP were used to detect respective proteins. Representative result of three independent experiments.

Thus, we produced and purified recombinant human MFF with a truncated transmembrane segment from E.coli as described previously (Otera et al., 2010). This recombinant human MFF protein was also used to immunize rabbits in order to generate a polyclonal antibody against MFF in collaboration with the IGBMC Antibody facility. We subjected recombinant MFF to an *in vitro* kinase assay along with fully recombinant hPKD1-GST. Using the PKD phospho-motif antibody, we showed that recombinant human PKD1 phosphorylated MFF, thus confirming that MFF is a direct PKD target (Fig. 3A). This was also confirmed by a radioactive kinase assay. Moreover, a novel specific PKD inhibitor (Harikumar et al., 2010), when added to the kinase reaction, could completely block MFF phosphorylation, as well as PKD autophosphorylation, thus confirming dependence of this phosphorylation on PKD activity (Fig. 3B).

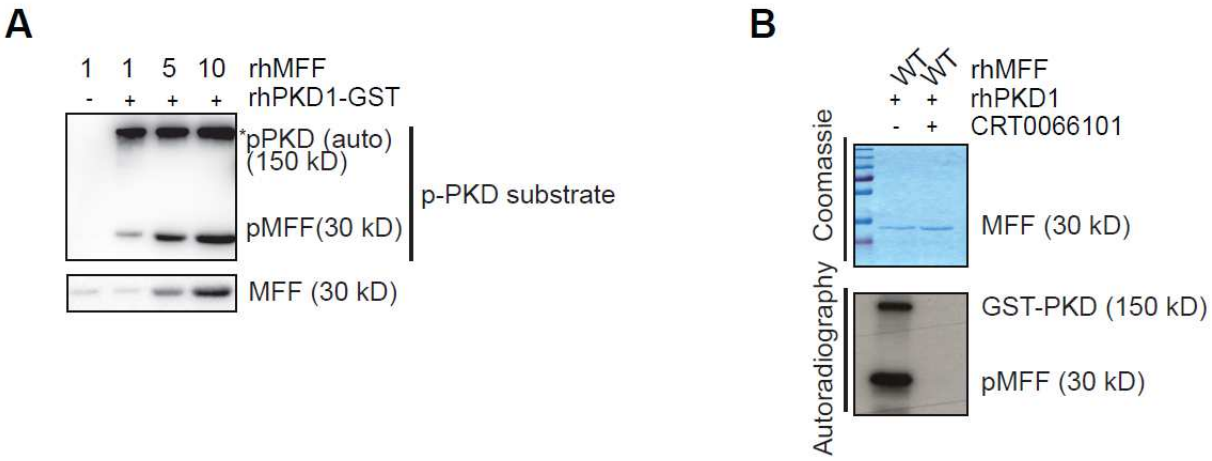

Figure 3. PKD can directly phosphorylate MFF. (A) Immunoblotting of reactions of *in vitro* kinase assay. Increased amounts (1, 2, 5 μg) of recombinant human MFF (rhMFF) were incubated with or without 50 ng recombinant human PKD1 (rhPKD1) at 30 °C for 30 minutes. Antibodies against phospho-PKD substrate motif and total MFF were used to detect respective proteins. Asterisk(*) indicates the auto-phosphorylation of PKD1. (B) Input and autoradiography of radioactive *in vitro* kinase assay. Wild type recombinant human MFF (rhMFF) (1μg) was incubated with 50 ng of recombinant human PKD1 (rhPKD1) with or without 1μM PKD inhibitor CRT0066101 at 30 °C for 30 minutes. Representative results of three independent experiments.

Initial mutagenesis of serine from the first predicted PKD site in MFF (Ser155) into non-phosphorylatable alanine (Ser155Ala) completely abolished phosphorylation of MFF in cells expressing CA-PKD and in a non-radioactive *in vitro* kinase assay, as it was judged by abrogation of PKD phospho-motif antibody signal (Fig. 4A, B, C). Yet, we noticed that upon non-phosphorylatable Ser172Ala mutation Flag-hMFF no longer migrated on SDS-PAGE as two distinct bands, but only displayed a faster-migrating lower band. This observation could indicate that phosphorylated Ser172 corresponds to a slower migrating MFF, and it could be an additional PKD phosphorylation site, although not recognized by the PKD phospho-motif antibody. To test this hypothesis, we subjected recombinant wild type and Ser155A MFF proteins to radioactive *in vitro* kinase assay along with recombinant hPKD1-GST. As predicted, the mutation of Ser155 decreased the phosphorylation level of MFF compared to control, but did not abolish it (Fig. 4D). These results indicated that apart from Ser155, MFF protein contained additional PKD phosphorylation sites.

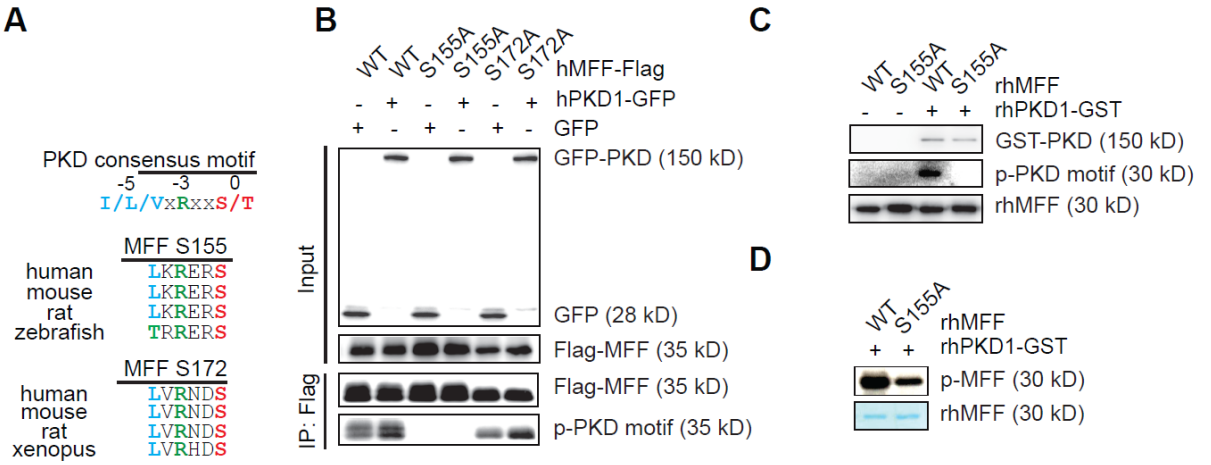

Figure 4. PKD mediated phosphorylation of MFF mutants (A) ClustalW alignment of two conserved sites that match the PKD optimal phosphorylation motif within human MFF protein sequence as well as of MFF from indicated species. The phosphorylation site is marked in red and its amino acid position within the full length protein is indicated. (B) Immunoblotting of whole-cell lysates of HEK293T cells co-expressing FLAG-tagged wild type (WT) or Ser155Ala (S155A) or Ser172Ala (S172A) mutant MFF with EGFP or EGFP-tagged constitutively active PKD1. Antibodies against FLAG, phospho-PKD substrate motif and GFP were used to detect respective proteins. (C) Immunoblotting of i*n vitro* kinase assay with wild type (WT) or serine to alanine (S155A) mutant recombinant human MFF (rhMFF) (1µg) with or without 50ng of recombinant GST-tagged wild-type human PKD-1 (rhPKD1-GST). Antibodies against total MFF, phospho-PKD substrate motif and GST were used to detect respective proteins. (D) Input and autoradiography of radioactive *in vitro* kinase assay. Wild type (WT) or serine to alanine (S155A) mutant recombinant human MFF (rhMFF) (1µg) was incubated with 50 ng of recombinant GST-tagged wild-type human PKD-1 (rhPKD1-GST) at 30 °C for 30 minutes. Representative results of three independent experiments.

As the MFF phosphorylation signal was quite strong, we could not exclude the possibility that beyond Ser155 and Ser172, there could be multiple other phosphorylation sites on MFF. The best way to detect all other sites would be to do the mass-spectrometry analysis of an *in vitro* kinase reaction. In collaboration with the laboratory of Prof. Rudolf Aebersold at ETH Zurich using a blinded and unbiased approach, we identified four potential PKD phosphorylation sites with Ser155 coming out as the strongest hit (Fig. 5). We were not able to detect Ser172 in our kinase assay possibly due to inaccessibility of this site after trypsin digestion. We combined identified sites with sites previously reported in the PKD substrate phosphoproteomic study, creating a list of six potential phosphorylation sites for site-directed mutagenesis (Y39;T112;S155;S172;S275;T280).

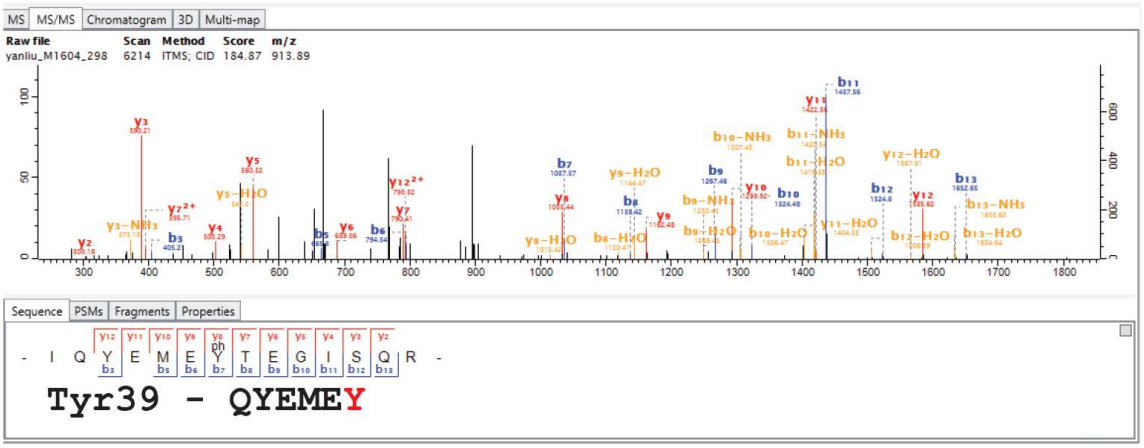
MS MS/MS Chromatogram 3D Multi-map
Raw file Scan Method Score m/z
yanliu_M1604_298 6214 ITMS; CID 184.87 913.89
Sequence PSMs Fragments Properties
- I Q Y E M E pY T E G I S Q R -
Tyr39 - QYEMEY

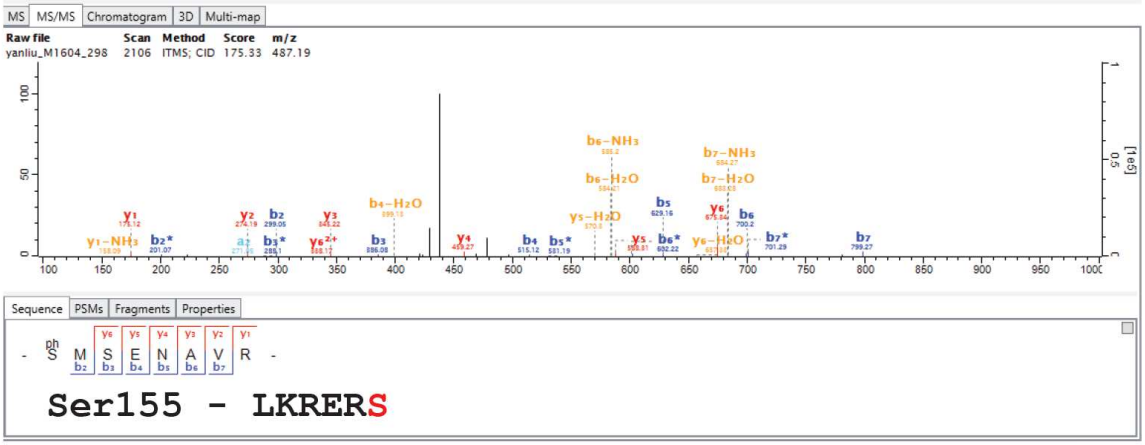
MS MS/MS Chromatogram 3D Multi-map
Raw file Scan Method Score m/z
yanliu_M1604_298 2106 ITMS; CID 175.33 487.19
Sequence PSMs Fragments Properties
- pS M S E N A V R -
Ser155 - LKRERS

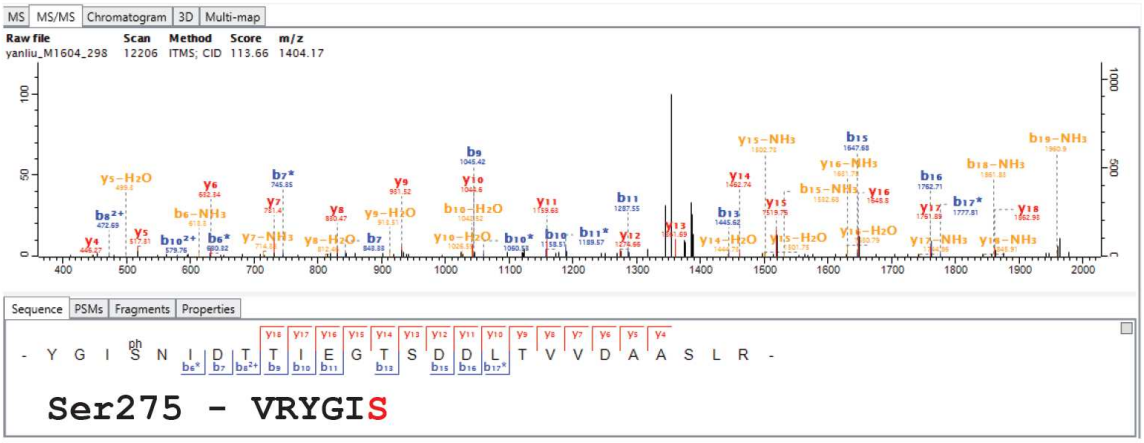
MS MS/MS Chromatogram 3D Multi-map
Raw file Scan Method Score m/z
yanliu_M1604_298 12206 ITMS; CID 113.66 1404.17
Sequence PSMs Fragments Properties
- Y G I pS N I D T T I E G T S D D L T V V D A A S L R -
Ser275 - VRYGIS

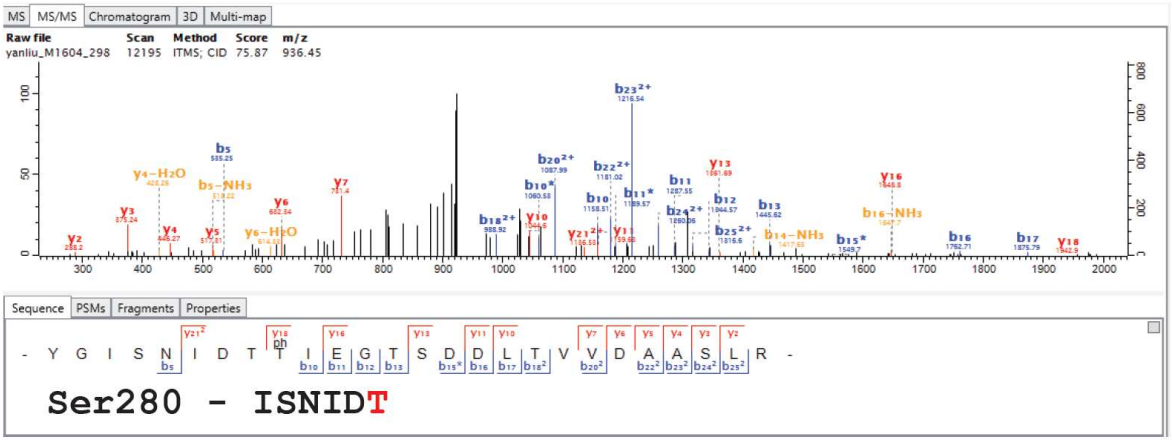
MS MS/MS Chromatogram 3D Multi-map
Raw file Scan Method Score m/z
yanliu_M1604_298 12195 ITMS; CID 75.87 936.45
Sequence PSMs Fragments Properties
- Y G I S N I D T T pI E G T S D D L T V V D A A S L R -
Ser280 - ISNIDT

Figure 5. The MaxQuant spectrum of PKD phosphorylation sites in MFF identified by mass-spectrometry. Products of *in vitro* kinase assay (10 µg of recombinant human MFF with 500 ng of recombinant human PKD1) were digested with trypsine (Roche Diagnostics) and subjected to LC-MS/MS analysis by Oribtrap XL. The raw files were processed with MaxQuant software (version 1.5.2.8). Peptide identification was performed using Andromeda search engine against the human SwissProt database. The identified peptides were further visualized by Viewer in MaxQuant and analyzed in Skyline software. The phosphorylation site is marked in red and its amino acid position within the full length of human MFF protein is indicated.

We prepared series of non-phosphorylatable MFF point mutants, which we expressed as recombinant proteins and subjected sequentially to a radioactive *in vitro* kinase assay. As a positive control, we used a recombinant human Arfaptin1, a target we have recently discovered in our laboratory (Gehart et al., 2012)(Fig. 6).

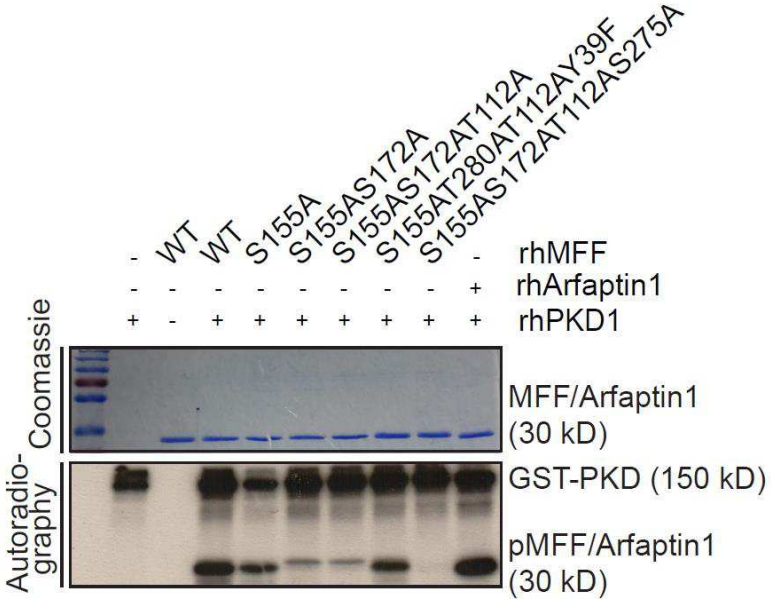

Figure 6. PKD mediated phosphorylation of MFF mutants Input and radiography of radioactive *in vitro* kinase assay. Human recombinant wild type (WT) MFF or serine to alanine MFF mutants (rhMFF) or Arfaptin1 (1µg each) was incubated with or without 50ng of recombinant GST-tagged wild-type human PKD-1 (rhPKD1-GST) at 30 °C for 30 minutes. Representative result of three independent experiments.

Only one of the mutants displayed no phosphorylation signal, thus indicating that mutations represented all potential PKD sites. This mutant contained Ser155, Ser172 and Ser275 all mutated

to alanine and also one site that did not affect the signal (Thr112A), as another mutant protein, which contained mutated Thr112, but not Ser275 still displayed a phosphorylation signal (Fig. 6).

Next, we performed the radioactive kinase assay but now with single, double and triple mutants of identified sites (Fig. 7A). From this result, we could deduce that Ser155 and Ser172 were the major phosphorylation sites with a minor contribution of Ser275. In collaboration with the IGBMC Antibody facility, we generated MFF Ser155 and Ser275 phosphospecific antibodies, which we used to confirm the phosphorylation sites in a non-radioactive kinase assay (Fig. 7B).

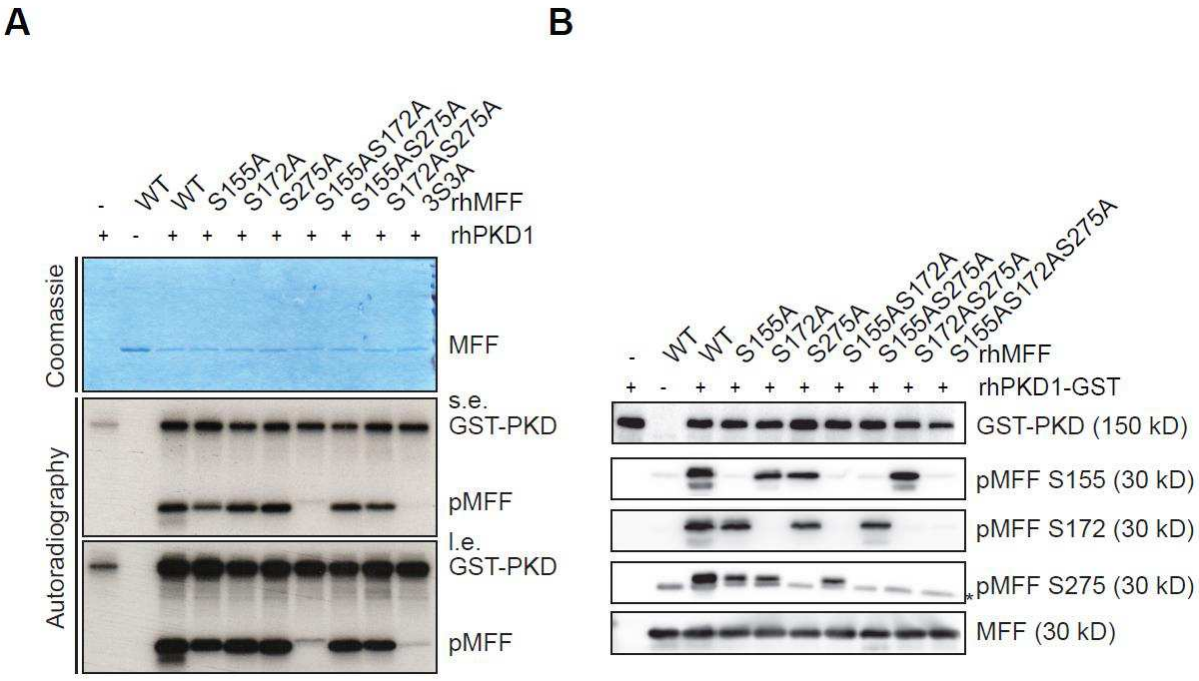

Figure 7. PKD directly phosphorylates MFF at Ser155/Ser172/Ser275 (A) Input and autoradiography of radioactive *in vitro* kinase assay. Human recombinant wild type (WT) MFF or serine to alanine MFF mutants (rhMFF) were incubated with or without 50ng of recombinant GST-tagged wild-type human PKD-1 (rhPKD1-GST) at 30 °C for 30 minutes. (s.e.) indicates short exposure, (l.e.) indicates long exposure. (B) Immunoblotting of reactions of *in vitro* kinase assay. Human recombinant wild type (WT) MFF or serine to alanine MFF mutants (rhMFF) were incubated with or without 50ng of recombinant GST-tagged wild-type human PKD-1 (rhPKD1-GST) at 30 °C for 30 minutes. Antibodies against PKD1, phospho-Ser155, phospho-Ser172, phospho-Ser275 and total MFF were used to detect respective proteins. Asterisk(*) indicates the non-phosphorylated form of MFF recognized by phospho-Ser275 antibody. Representative results of three independent experiments.

Serine to alanine mutations completely abolished binding of the commercial MFF pSer172 antibody as well as the home-made pSer155 antibody. Although home-made pSer275 antibody

nicely recognized the phospho-signal, it could still detect non-phosphorylated recombinant MFF, which migrated as a lower band on SDS-PAGE.

5.2 PKD phosphorylates MFF independently of AMPK

We next asked the question as to whether these phosphorylation events occured in cells. To this end, we overexpressed wild type Flag-hMFF or non-phosphorylatable MFF mutants together with EGFP or EGFP-PKD-CA in HEK293T cells (Fig. 8).

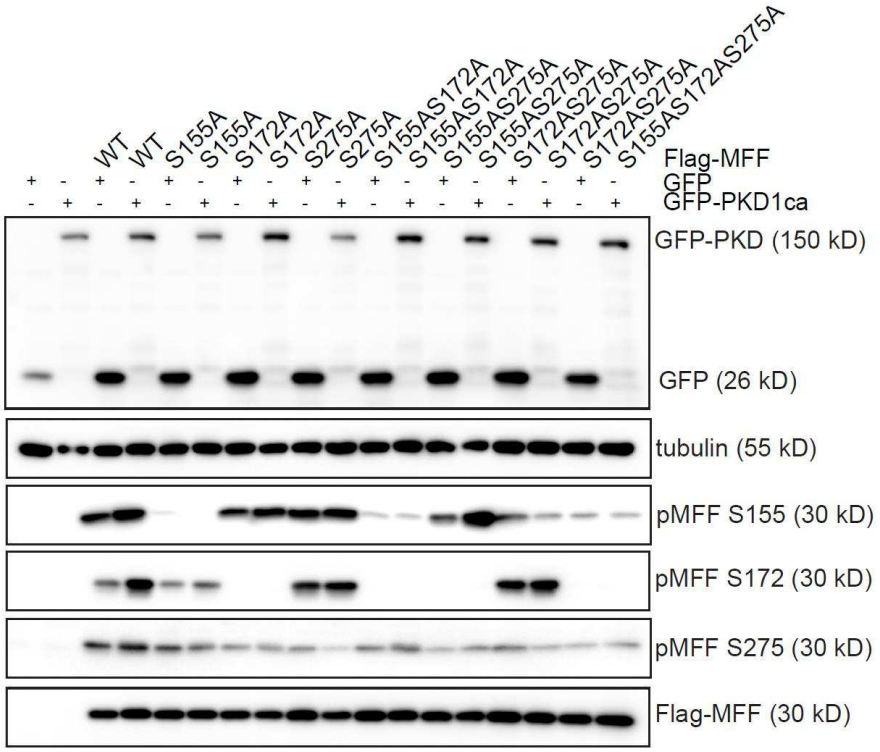

Figure 8. PKD phosphorylates MFF at Ser155/Ser172/Ser275 in cells. Immunoblotting of cell lysates from HEK293T cells ectopically co-expressing pcDNA-FLAG (vector control) or FLAG-tagged wild type (WT) MFF or serine to alanine MFF mutants with EGFP or EGFP-tagged constitutively active (CA) PKD1. Antibodies against FLAG, phospho-MFF (Ser155), phospho-MFF (Ser172), phospho-MFF (Ser275), tubulin and GFP were used to detect respective proteins. Representative result of three independent experiments.

As expected, we observed increased phosphorylation of exogenous wild-type MFF when co-expressing EGFP-PKD-CA, but not the EGFP construct. Yet, the difference was not striking.

This could be explained by high basal phosphorylation of MFF by endogenous PKDs or by the activity of another kinase. Recently, AMP-activated protein kinase (AMPK) was reported to phosphorylate MFF at the same two sites (Ser155 and Ser172) in response to energy stress (Toyama et al., 2016). Could AMPK activity interfere with PKD activity? Or could AMPK compete for the same sites on MFF with PKD? To address these questions, we generated HEK293T cells, which were lacking both catalytic subunits of AMPK (AMPKα1/α2 dKO), thus rendering AMPK complex into an inactive state using CRISPR/Cas9 technology (Fig. 9A). These cells showed neither AMPKα1/α2 proteins nor AMPK activity in response to different established AMPK activators, which was verified by western-blotting with widely used commercial AMPK-specific antibodies and AMPK-specific substrate antibodies (pACC, pULK1). In stark contrast to wild type cells, AMPKα1/α2 dKO completely lacked phosphorylation of Ser79 of ACC and Ser555 of ULK1 (genuine AMPK sites on established AMPK substrates) (Fig. 9C) and, more importantly, Ser172 of MFF in response to rotenone (Fig. 9D). Interestingly, when we probed blots for pSer275 MFF (the genuine PKD site on MFF, not described for AMPK), we could also detect induction of this phosphorylation by Rotenone, and it was completely abolished in AMPK dKO cells. This could mean that AMPK and PKD share the same mechanism of posttranslational regulation of MFF, and this site was simply not detected, because no direct mass spectromery analysis was performed in the recent study (Fig. 9D).

Next, we performed similar overexpression experiments of wild type Flag-hMFF or MFF non-phosphorylatable mutants together with GFP or GFP-PKD-CA in wild type HEK293T and HEK293T AMPKα1/α2 dKO cells in parallel (Fig. 10). Strikingly, upon deletion of AMPK we observed a dramatic difference in phosphorylation signal of overexpressed MFF. In HEK293T AMPKα1/α2 dKO cells overexpression of the constitutively active form of PKD (GFP-PKD-CA) resulted in a strong increase of MFF phosphorylation as indicated by all three phosphor-specific antibodies.

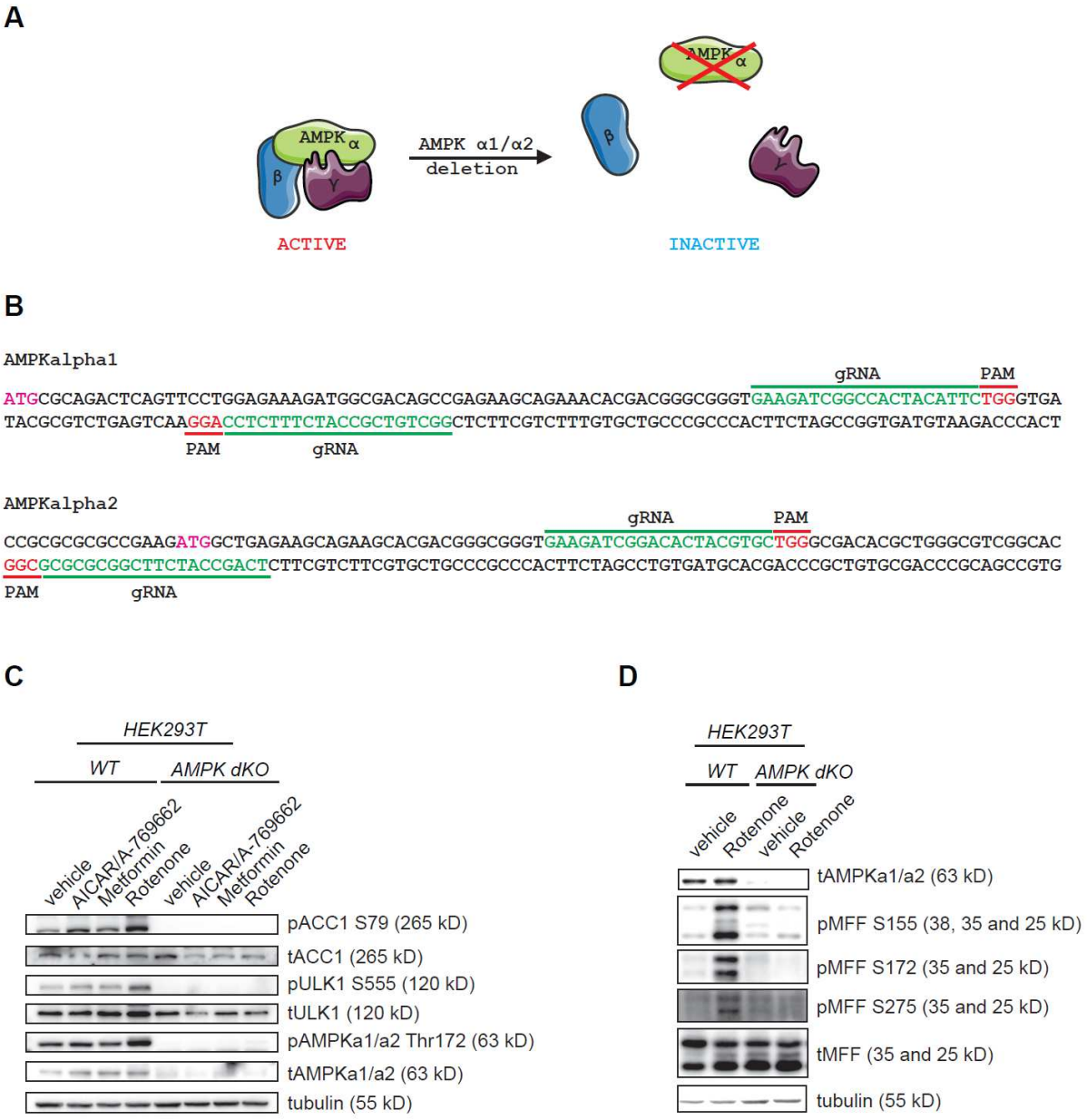

Figure 9. Generation strategy and validation of AMPK-deficient cells. (A) Explanatory illustration of the knockout strategy. (B) CRISPR/Cas9 targeting of genomic sequences of AMPK α1 and α2 genes using complementary guide RNA pairs (Strategy adapted from (Toyama et al., 2016)). (C) Immunoblotting of cell lysates from wild type (WT) and AMPK α1/α2 double knockout (AMPK dKO) HEK293T cells stimulated for 2 hours with vehicle or mixture of 2mM AICAR and 50μM A-769662 or 1μM Rotenone. Antibodies against total ACC1, phospho-ACC1 (Ser79), total ULK1, phospho-ULK1 (Ser555), total AMPK, phospho-AMPK (Thr172) and tubulin were used to detect respective proteins. (D) AMPK activity is required for energy stress-induced MFF phosphorylation. Immunoblotting of cell lysates from wild type (WT) and AMPK α1/α2 double knockout (AMPK dKO) HEK293T cells stimulated for 2 hours with vehicle or 1μM Rotenone. Antibodies against total MFF, phospho-MFF (Ser155), phospho-MFF (Ser172), phospho-MFF (Ser275), total AMPK and tubulin were used to detect respective proteins. Representative result of three independent experiments.

This result suggests that in wild type cells AMPK activity is responsible for observed high basal phosphorylation of MFF at Ser155 and Ser172, as AMPK and PKD share same sites on the common substrate (MFF). As to Ser275, the genuine PKD phosphorylation site on MFF not described for AMPK, the absence of AMPK activity potentiated phosphorylation by PKD. The remaining low basal phosphorylation of MFF could be attributed to endogenous activity of PKD kinases. Altogether, these results demonstrate that PKD1 can directly phosphorylate MFF at Ser155/Ser172/Ser275 *in vitro* and in cells independently of AMPK.

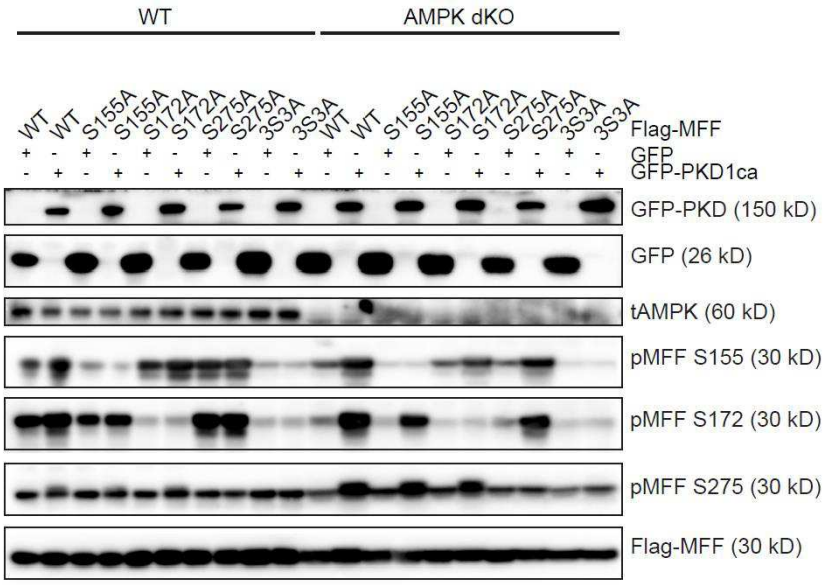

Figure 10. PKD phosphorylates MFF at Ser155 and Ser172 and Ser275 independently of AMPK. Immunoblotting of cell lysates from wild type (WT) and AMPK alpha1/alpha2 double knockout (AMPK dKO) HEK293T cells ectopically co-expressing FLAG-tagged wild type (WT) MFF or serine to alanine MFF mutants with EGFP or EGFP-tagged constitutively active (CA) PKD1. Antibodies against FLAG, phospho-MFF (Ser155), phospho-MFF (Ser172), phospho-MFF (Ser275), tubulin, AMPK alpha1/alpha2 and GFP were used to detect respective proteins. Representative result of three independent experiments.

5.3 Physiological importance of MFF phosphorylation

What is the functional consequence of MFF phosphorylation? The MFF protein was initially discovered as a factor required for DRP1-mediated mitochondrial fission (Gandre-Babbe and van der Bliek, 2008; Otera et al., 2010).

In a recent report related to mitochondrial fragmentation in response to energy stress, AMPK-mediated MFF phosphorylation at the same two sites (Ser155 and Ser172) (Toyama et al., 2016) was required for acute recruitment of DRP1 from the cytosol and subsequent mitochondrial fragmentation. Neither of the sites were located in regions required for the MFF-DRP interaction (R1, R2- repeats), yet phosphorylation was reported to increase DRP1 recruitment (Fig 11).

PKD phosphorylates MFF at one additional site (Ser275) beyond the same two sites (Ser155 and Ser172). Both sites fall within the optimal motif for PKD and AMPK, whereas the phosphorylation motif around Ser275 does not fully match the latter. Nonetheless, Ser275 still contains one typical sequence entity for basophilic kinases (PKD, AMPK), namely arginine (R) at the position (-4) even though the optimal sequence would be an arginine at (-3) in addition to a hydrophobic valine (V) at (-5). According to my previous experiments (Fig. 9D), it is also possible that AMPK may also phosphorylate Ser275. Yet, as this additional site was not reported, it was tempting to analyze whether it potentially exerts other effects.

Ser275 is in relative proximity to the coiled-coil domain, which is important for MFF dimerization. To address the effect of MFF phosphorylation on its ability to form homodimers, we co-expressed GFP-tagged wild-type MFF along with Flag-tagged wild-type MFF, non-phosphorylatable MFF S155AS172AS275A (3S3A, serines replaced with alanines) and phospho-mimetic MFF S155DS172DS275D (3S3D, serines replaced with aspartates) as well as MFF S155ES172ES275E (3S3E, serines replaced with glutamates) mutants in HEK293T cells. Subsequently, we performed immunoprecipitation experiments using Flag M2 affinity gels.

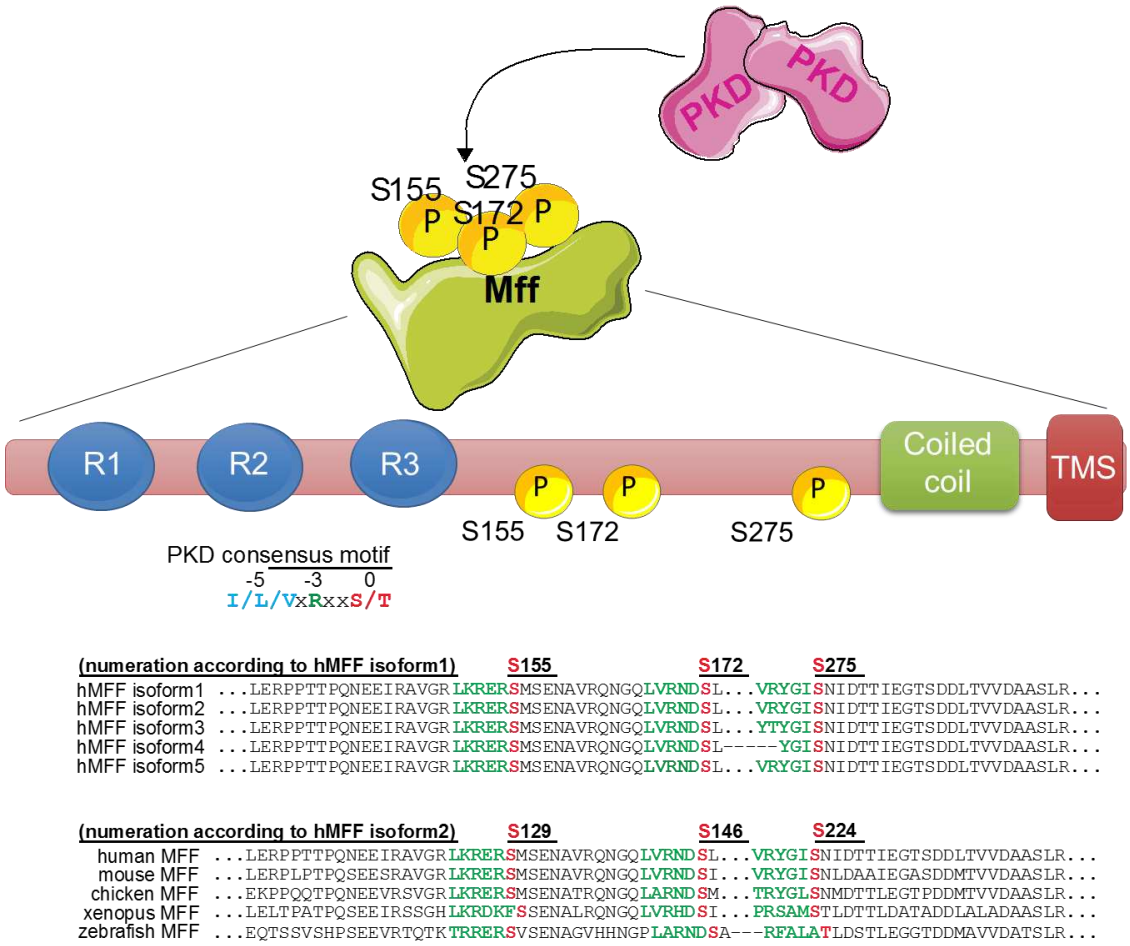

(numeration according to hMFF isoform1)	S155	S172	S275
hMFF isoform1	...LERPPTTPQNEEIRAVGRLKRERSMSENAVRQNGQLVRNDSL...VRYGISNIDTTIEGTSDDLTVVDAASLR...		
hMFF isoform2	...LERPPTTPQNEEIRAVGRLKRERSMSENAVRQNGQLVRNDSL...VRYGISNIDTTIEGTSDDLTVVDAASLR...		
hMFF isoform3	...LERPPTTPQNEEIRAVGRLKRERSMSENAVRQNGQLVRNDSL...YTYGISNIDTTIEGTSDDLTVVDAASLR...		
hMFF isoform4	...LERPPTTPQNEEIRAVGRLKRERSMSENAVRQNGQLVRNDSL-----YGISNIDTTIEGTSDDLTVVDAASLR...		
hMFF isoform5	...LERPPTTPQNEEIRAVGRLKRERSMSENAVRQNGQLVRNDSL...VRYGISNIDTTIEGTSDDLTVVDAASLR...		

(numeration according to hMFF isoform2)	S129	S146	S224
human MFF	...LERPPTTPQNEEIRAVGRLKRERSMSENAVRQNGQLVRNDSL...VRYGISNIDTTIEGTSDDLTVVDAASLR...		
mouse MFF	...LERPLPTPQSEESRAVGRLKRERSMSENAVRQNGQLVRNDSI...VRYGISNLDAAIEGASDDMTVVDAASLR...		
chicken MFF	...EKPPQQTPQNEEVRSVGRLKRERSMSENATRQNGQLARNDSM...TRYGLSNMDTTLEGTPDDMTVVDAASLR...		
xenopus MFF	...LELTPATPQSEEIRSSGHLKRDKFSSENALRQNGQLVRHDSI...PRSAMSTLDTTLDATADDLALADAASLR...		
zebrafish MFF	...EQTSSVSHPSEEVRTQTKTRRERSVSENAGVHHNGPLARNDSA---RFALATLDSTLEGGTDDMAVVDATSLR...		

Figure 11. Schematic illustration of MFF Ser155/Ser172/Ser275 triple phosphorylation by PKD. Dimeric (active) form of PKD phosphorylates MFF at Ser155 and Ser172 and Ser275, which are located in the region with no predicted domain structure. MFF functional domains are represented from amino- to carboxy-terminus. Short repeats (R1, R2, R3), which are required for DRP1 recruitment, are depicted in blue. Coiled coil domain, which is necessary for dimerization of MFF is marked in green and trans-membrane segment (TMS), which anchors MFF to OM is red. PKD phosphorylation sites in human MFF isoforms and MFF isoforms from other vertebrate species are aligned underneath the schema with general PKD consensus motif on top. PKD consensus motif within the sequence is marked in green and phosphorylation site is marked in red.

GFP-tagged wild-type MFF efficiently co-immunoprecipitated with all tested forms of MFF, whereas no interaction was detected between GFP-tagged MFF and affinity gel (empty vector control). These results indicate no significant difference in dimerization efficiency between wild type MFF and mutants (Fig. 11). Moreover, no direct interaction was detected with endogenous DRP1 in phospho-mimetic MFF mutants (3S3D, 3S3E) (data not shown). This may imply that the

observed increased recruitment of DRP1 by phospho-mimetic MFF mutants (Toyama et al., 2016) was caused by indirect effects and possible additional interactor(s).

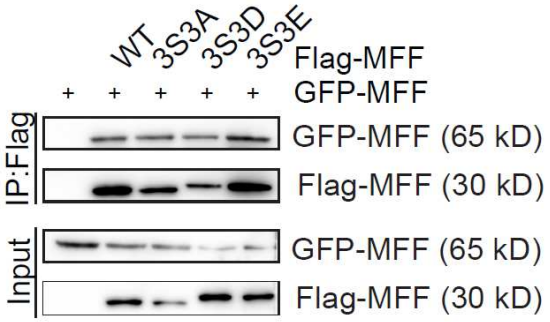

Figure 11. PKD phosphorylation of MFF does not affect its dimerization efficiency. Immunoblotting of elutions and inputs of FLAG immunoprecipitations from HEK293T cells ectopically co-expressing pcDNA-FLAG (vector control) or FLAG-tagged wild type (WT) MFF or serine to alanine MFF mutant (3S3A) or serine to aspartate (3S3D) or serine to glutamate MFF mutants with EGFP-tagged wild type MFF (GFP-MFF). Antibodies against FLAG and GFP were used to detect respective proteins. Representative result of three independent experiments.

5.4 PKD mediated phosphorylation of MFF occurs during mitosis

In the following, it was important to determine the stimuli or conditions and thus physiological relevance of PKD mediated MFF phosphorylations. AMPK was described to phosphorylate MFF in response to energy stress induced by different mitochondrial poisons such as Rotenone and Metformin (inhibits Complex we of the electron transport chain), Antimycin (Complex III inhibitor), Oligomycin (inhibits ATP synthase), which deplete intracellular ATP, as well as direct AMPK agonists (AICAR, A-769662), which directly bind AMPK. Activated AMPK phosphorylates MFF at Ser155/Ser172 and leading to increased mitochondrial DRP1 recruitment and mitochondrial fragmentation. Their data suggest that Ser155/Ser172 phosphorylation acts as the activating signal for DRP1 recruitment. The physiological context of this phosphorylation was not explored. Authors speculate that AMPK-mediated mitochondrial fragmentation should facilitate

mitophagy (Toyama et al., 2016). PKD1 was also reported to be activated on the mitochondrial surface in response to Rotenone-induced mitochondrial ROS by SFK and PKCδ (Doppler and Storz, 2007).

We could not detect MFF phosphorylation in cells lacking AMPK (AMPKα1/α2 dKO HEK 293T and AMPKα1/α2 dKO MEFs), compared to matched wild type cells, where MFF phosphorylation was robustly induced by Rotenone. It became thus apparent that not PKD, but AMPK is required for energy-stress induced MFF phosphorylation and subsequent mitochondrial fragmentation (Fig. 9D).

What are the other physiological conditions, which induce mitochondrial fragmentation? Nutrient deprivation, hypoxia, increased calcium flux have been reported to induce mitochondrial fission in different cell types. All these triggers could still be categorized as energy stress inducers and/or respectively AMPK activators. Yet, we were looking for a physiological cue that would cause a significant mitochondrial fragmentation without inducing energy stress.

One of such a condition is mitosis. During mitosis, the mitochondrial network undergoes significant fragmentation and redistribution to ensure equal partitioning of mitochondria between daughter cells (Fig 12). Yet, to our knowledge, PKD does not have any documented substrate in mitosis, and has never been described as a mitotic kinase.

We started to explore the possibility that MFF phosphorylation could contribute to mitochondrial fission specifically in mitosis. To that end, we used the human cervical adenocarcinoma cell line (HeLa), which is widely used in the mitosis field because of its ability to be readily synchronized. Additionally, we had phospho-MFF antibodies available allowing for detection of endogenous phosphorylated MFF.

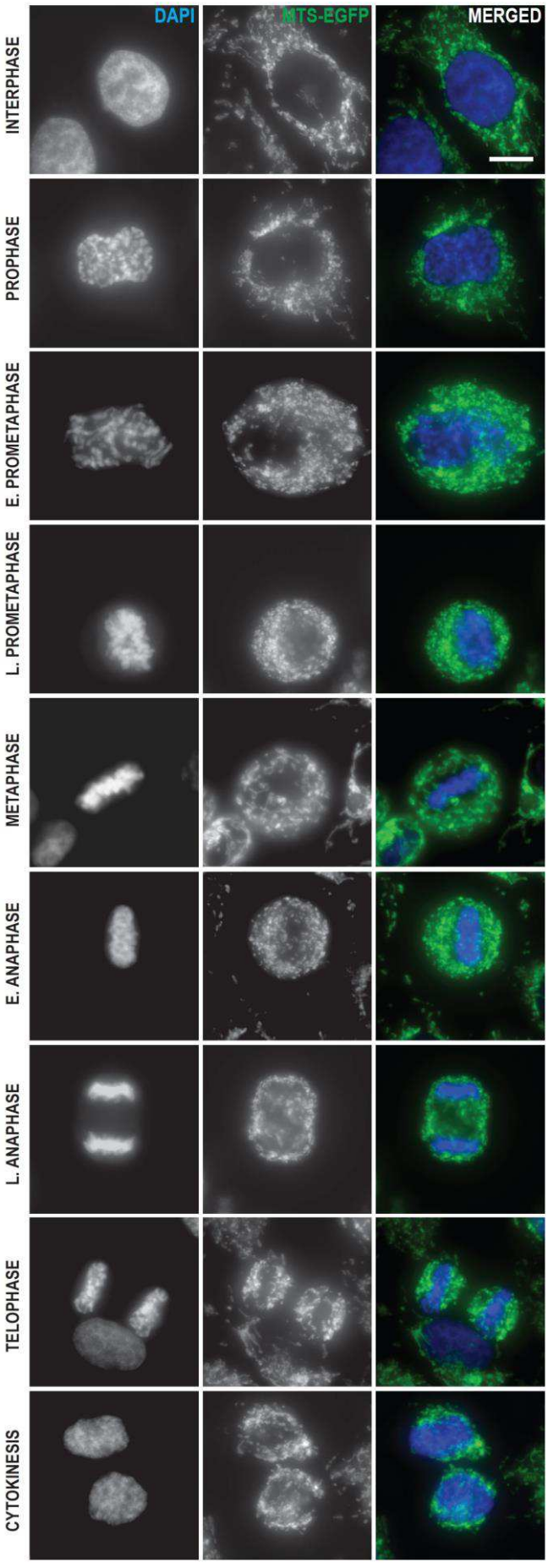
DAPI
MTS-EGFP
MERGED
INTERPHASE
PROPHASE
E. PROMETAPHASE
L. PROMETAPHASE
METAPHASE
E. ANAPHASE
L. ANAPHASE
TELOPHASE
CYTOKINESIS

Figure 12. Mitochondrial network undergoes extensive fragmentation during mitosis in HeLa cells. (A) Fluorescence microscopy images of HeLa cells in interphase and during different stages of mitosis (as indicated). HeLa cells stably express MTS-EGFP, which serves to visualize mitochondria, and chromosomes were counterstained with DAPI. Scale bar 10μm.

We synchronized HeLa cells in S-phase of the cell cycle using a double Thymidine block, which is the most physiological method of synchronization, and collected cells at different time points after their release from the block for further analysis by western blot. We expected to detect MFF phosphorylation in all stages of cell cycle with its increase in mitosis. Strikingly, MFF phosphorylation at Ser172 and Ser275 was detected only in mitosis, as it occurred exclusively with peaking cyclin B levels, and not in any other stage (Fig. 13A).

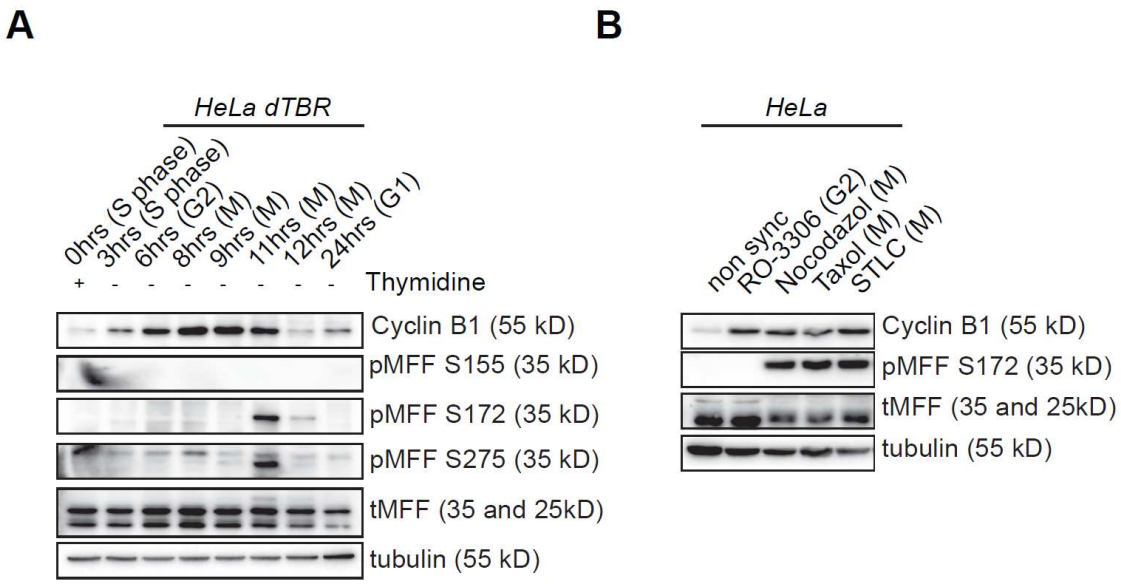

Figure 13. PKD phosphorylates MFF during mitosis. (A) Immunoblotting of cell lysates from synchronized HeLa cells obtained through a double Thymidine block. Time points after the second release are indicated along with the corresponding cell cycle stages. (B) Immunoblotting of cell lysates from non-synchronized, chemical G2- or mitosis (M) -arrested HeLa cells. Antibodies against total MFF, phospho-MFF (Ser155), phospho-MFF (Ser172), phospho-MFF (Ser275), tubulin and cyclinB1 were used to detect respective proteins. Representative result of three independent experiments.

The antibody against pSer155 MFF did not show any signal at any stage. It is possible that the pSer155 MFF antibody, which was produced in-house, does not have a strong affinity to endogenous phosphorylation of MFF in HeLa cells. Next, we corroborated these findings using different approaches. We subjected HeLa cells to chemical agents, which are routinely used to reversibly arrest cells in mitosis by interfering with assembly of the mitotic spindle: nocodazole (depolymerizes microtubules), taxol (stabilizes microtubules) and STLC (inhibitor of kinesin Eg5). To clearly dissect whether MFF phosphorylation occurs specifically in mitosis and not in late G2, which is also characterized with high cyclin B levels, we included a treatment group with the inhibitor of CDK1 (RO-3306), which reversibly arrests human cells at the G2/M border. Western blot analysis of treated cells confirmed our previous observation. Cells arrested in mitosis showed strong phosphorylation of MFF, unlike non-synchronyzed cells or cells arrested in G2/M (Fig. 13B).

Next, we asked at which stage of mitosis phosphorylation occured. To answer this question, we had to analyze MFF phosphorylation during different mitotic stages. We tested all three MFF phospho-antibodies for immunofluorescence. The commercial pSer172 MFF antibody showed consistent and specific signals, which co-localized with the mitochondrial surface, whereas pSer155 and pSer172 MFF antibodies produced in-house were not suitable for immunofluorescence experiments. Next, we synchronized HeLa cells using double thymidine block and let them to proceed to mitosis, collecting the cells at 11 hours after a thymidine release, the time-point, at which we detected MFF phosphorylation. We stained cells with antibodies against pSer172 MFF and tubulin to visualize the mitotic spindle. DNA was counterstained with DAPI. Cells were imaged and categorized into seven groups based on stages of mitotic progression - from prophase to cytokinesis, and fluorescent signal intensity of the pSer172 MFF antibody labeling was quantified (Fig. 14A, B).

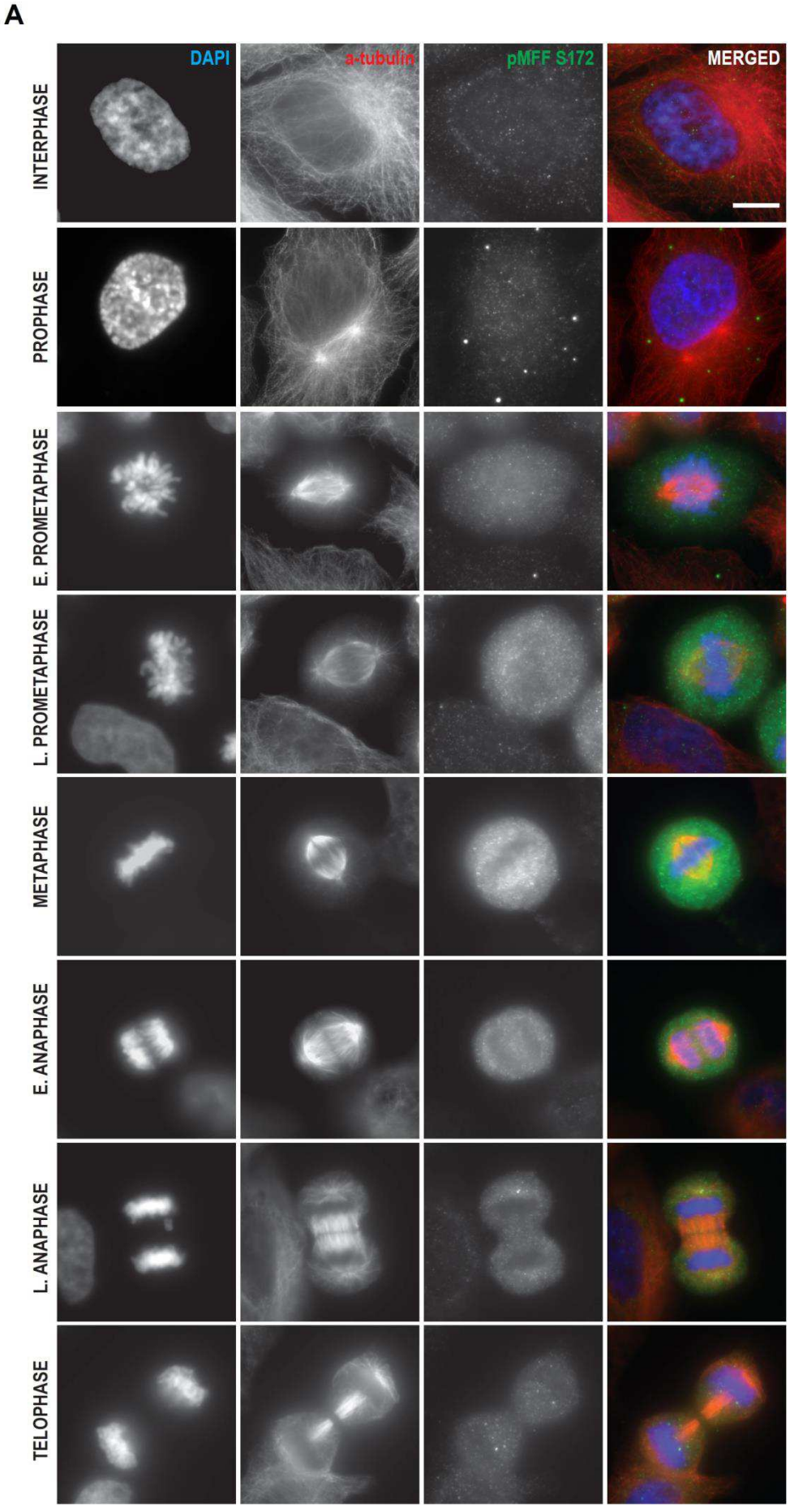
A
DAPI
a-tubulin
pMFF S172
MERGED
INTERPHASE
PROPHASE
E. PROMETAPHASE
L. PROMETAPHASE
METAPHASE
E. ANAPHASE
L. ANAPHASE
TELOPHASE

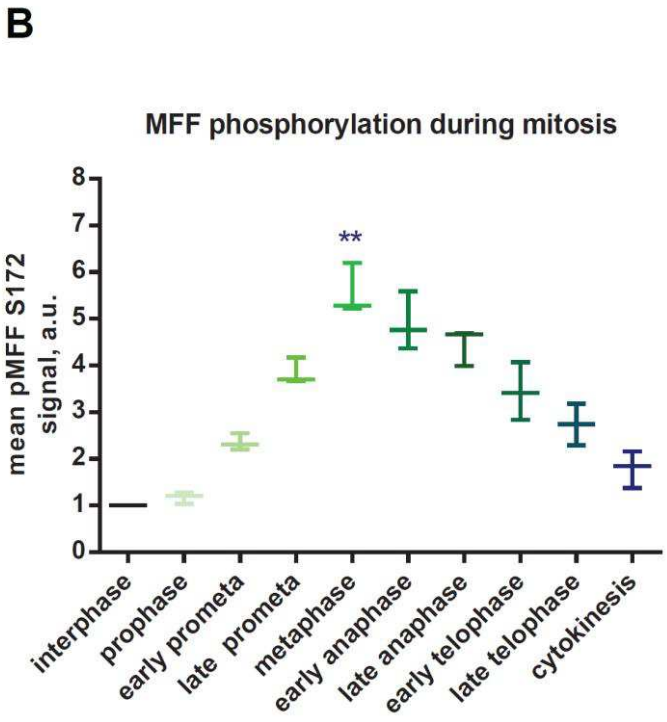

Figure 14. Mitotic MFF phosphorylation peaks at metaphase in HeLa cells. (A) Immunofluorescence images of HeLa cells synchronized double Thymidine block and collected at 11 hours after release, corresponding to the maximum of cells undergoing mitosis. Cells were stained with pSer172 MFF, chromosomes were counterstained with DAPI. Scale bar 10µm. (B) Quantification of signal intensity of pMFF Ser172 displayed in (A). For each stage signal intensity was quantified in 10 cells, 100 cells per experiment. Data are shown as mean with SD of three independent experiments. **: $p<0.01$, by one-way ANOVA.

Quantification analysis revealed that the pMFF signal gradually increased with the beginning of mitosis (prophase), peaking its maximal intensity in metaphase and then progressively decreased through mitotic exit. This observation is in the line with previous findings that mitochondrial mitotic fragmentation starts in prophase with the maximum number of cells displaying fragmented mitochondria in metaphase (Taguchi et al., 2007).

Western blot analysis indicated no changes in total protein level of MFF during cell cycle and mitosis in particular (Fig. 13A), yet it would still be important to perform a similar quantification analysis on total MFF during different mitotic stages.

It is well established that in interphasic cells, PKD kinases localize mainly to the trans-Golgi network (TGN) (Malhotra and Campelo, 2011), but can also be detected in the cytoplasm and plasma membrane (Goginashvili et al., 2015).

To investigate whether PKD kinases were activated during mitosis and to characterize their intracellular distribution during different mitotic stages, HeLa cells were synchronized in mitosis and analyzed by immunostaining with antibody against pPKD-Ser744, an established PKD activity marker. This antibody recognizes phosphorylated serine, which is located within the PKD activation loop and is common for all three PKD proteins (Yuan et al., 2006). Image analysis revealed that the phospho-PKD signal was subtle in interphasic cells, whereas it was readily detectable as bright cytoplasmic puncta already in prophase and gradually increased, as cells progressed through mitosis. Maximal signal intensity was detected during metaphase-anaphase and started to decline as cells progressed to telophase. Interestingly, during cytokinesis, the cytoplasmic phospho-PKD signal was almost as low as during the interphase, but showed strong signal in the midbody (Fig. 15). To further obtain more precise information about PKD activity during mitosis we plan to quantify the phospho-signal intensity. Altogether, these data suggest that PKDs are activated during cell division and that the peak of PKD activity coincides with maximal MFF phosphorylation.

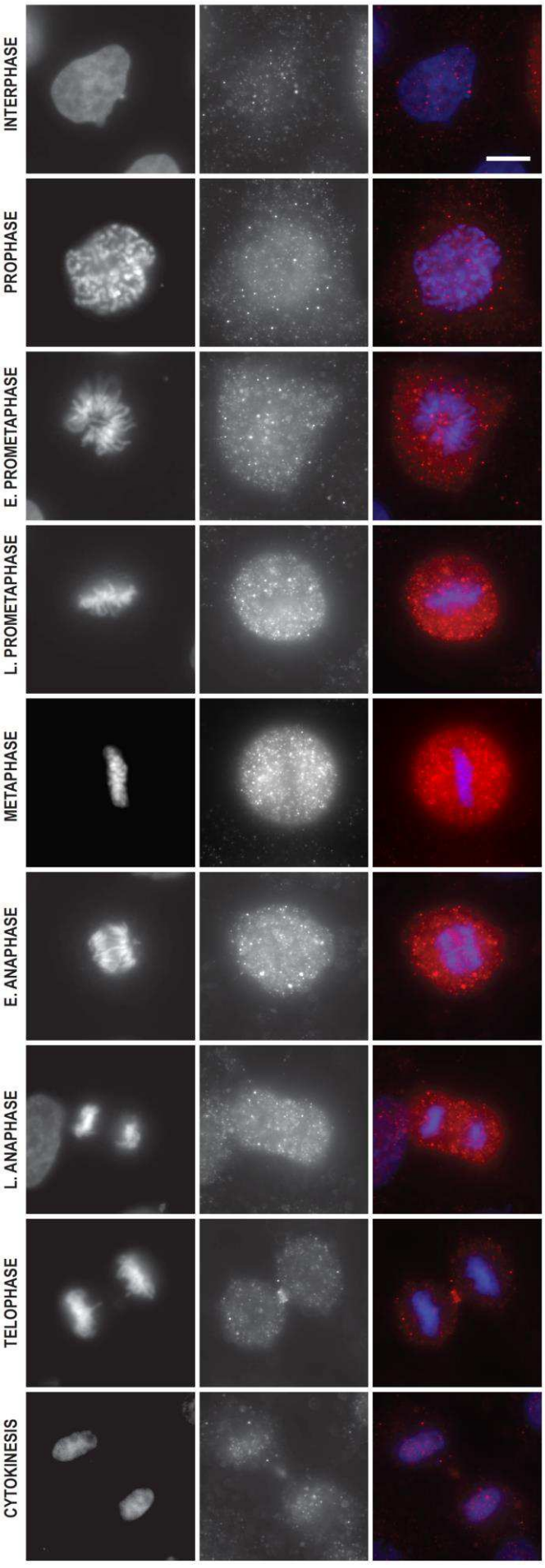
INTERPHASE
PROPHASE
E. PROMETAPHASE
L. PROMETAPHASE
METAPHASE
E. ANAPHASE
L. ANAPHASE
TELOPHASE
CYTOKINESIS

Figure 15. PKD activity is gradually increasing specifically during mitosis. (A) Immunofluorescence images of HeLa cells synchronized by double Thymidine block and collected at 11 hours after release, corresponding to maximum of cells undergoing mitosis. Cells were stained with pSer744 PKD (PKD activity marker), chromosomes were counterstained with DAPI. Different mitotic stages are indicated. Scale bar 10μm.

5.5 AMPK deletion is dispensable for mitotic MFF phosphorylation

As AMPK was previously reported to phosphorylate MFF at two out of three PKD phosphorylation sites (Ser155/Ser172), it was necessary to clarify whether AMPK is involved in observed mitotic MFF phosphorylation. To test the dependence of mitotic MFF phosphorylation on AMPK activity, we synchronized wild type and AMPKα1/α2 dKO HEK 293T cells using double thymidine block and collected them at different time points after release. Both wild type and AMPK dKO HEK 293T cells displayed a similar pattern of mitotic MFF phosphorylation, already detectable at 8 hours after release (Fig. 16A).

We also validated this result using another approach. To assess the level of mitotic MFF phosphorylation, we synchronized wild type and AMPK dKO HEK 293T cells in mitosis using nocodazole, taxol and STLC and analyzed MFF phosphorylation by western blot. No difference was detected in MFF phosphorylation levels between wild type and AMPK dKO cells (Fig. 16B).

Overall, these results indicate that AMPK activity is not required for mitotic MFF phosphorylation.

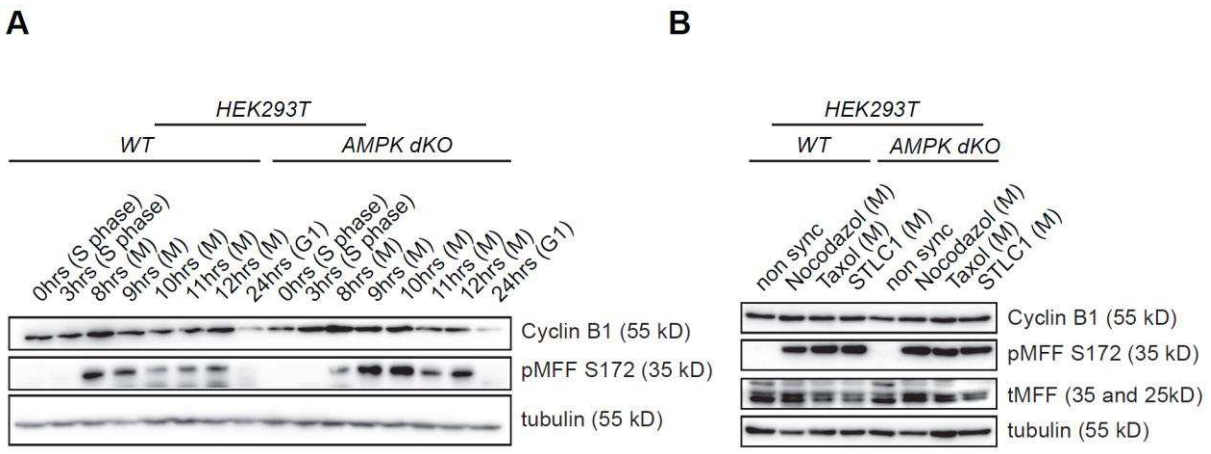

Figure 16. AMPK deletion is dispensable for mitotic MFF phosphorylation. (A) Immunoblotting of cell lysates from wild type and AMPK dKO HEK293T cells synchronized by double Thymidine block, time after second release indicated along with corresponding cell cycle stage. (B) Immunoblotting of cell lysates from non-synchronized or chemically arrested in mitosis (M) wild type and AMPK dKO HEK293T cells. Antibodies against total MFF, phospho-MFF (Ser172), tubulin and cyclinB1 were used to detect respective proteins. Representative result of three independent experiments.

5.6 PKD activity is required for mitotic MFF phosphorylation

There are three family members of PKD, so it was important to clarify which PKD kinase is responsible for MFF phosphorylation. As there is a high level of homology, a certain degree of redundancy was expected. HeLa cells, which displayed strong mitotic MFF phosphorylation, were shown to express only PKD2 and PKD3, lacking expression of PKD1. However, we performed the *in vitro* kinase assays and co-immunoprecipitation experiments by overexpressing PKD1. Thus, it is quite likely that several (if not all three) PKD kinases can phosphorylate MFF. To obtain a direct evidence for requirement of PKD for MFF-dependent mitochondrial fragmentation, we transiently depleted PKD2 and PKD3 proteins using a siRNA approach in HeLa cell line stably expressing the histone marker H2B-mCherry and mitochondria-targeted EGFP (MTS-EGFP) to directly visualize chromosomes and mitochondria (Fig. 17A).

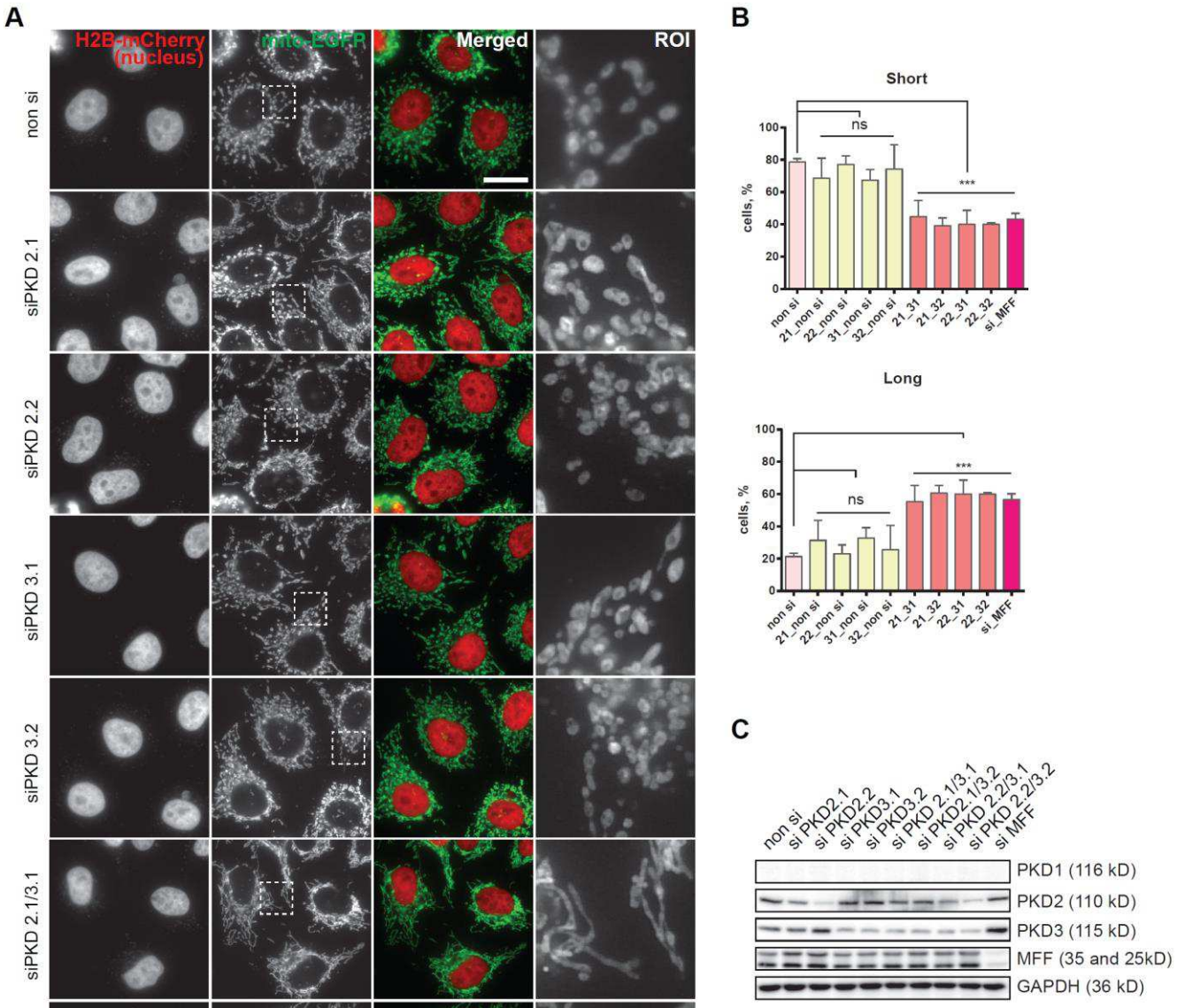
A
H2B-mCherry (nucleus)
mito-EGFP
Merged
ROI
non si
siPKD 2.1
siPKD 2.2
siPKD 3.1
siPKD 3.2
siPKD 2.1/3.1
siPKD 2.1/3.2
siPKD 2.2/3.1
siPKD 2.2/3.2
siMFF
B
Short
cells, %
ns
***
non si
21_non si
22_non si
31_non si
32_non si
21_31
21_32
22_31
22_32
si_MFF
Long
cells, %
ns
***
C
non si
si PKD2.1
si PKD2.2
si PKD3.1
si PKD3.2
si PKD 2.1/3.1
si PKD2.1/3.2
si PKD 2.2/3.1
si PKD 2.2/3.2
si MFF
PKD1 (116 kD)
PKD2 (110 kD)
PKD3 (115 kD)
MFF (35 and 25kD)
GAPDH (36 kD)

Figure 17. PKD kinases are required for mitochondrial fission in HeLa cells. (A) Fluorescence microscopy images of HeLa cells stably expressing H2B-mCherry and MTS-EGFP and marking chromosomes and mitochondria respectively. HeLa cells were treated with non-targeting si RNA (non si) or siRNAs against human PKD2 (siPKD2.1; siPKD2.2), human PKD3 (siPKD3.1; siPKD3.2) alone or in combination as indicated. (B) Mitochondrial morphology quantification of (A). Mitochondrial shape was classified as 'short' (no clear shape, less than 5µm long) or 'long' (tubular or fused, more than 5µm long) and displayed as percentage of cells having majority of their mitochondria in the respective category. For each group at least 150 cells were counted. (C) Immunoblotting of whole cell lysates from (A). Representative result of three independent experiments.

Two different siRNA were used for each PKD and knockdown efficiency was verified by western blot. Mitochondrial morphology was categorized in two groups (short/fragmented and long/fused) and quantified. Single knockdown of either PKD did not yield any significant difference in mitochondrial morphology compared to control siRNA, whereas downregulation of both PKD2 and PKD3 decreased mitochondrial fragmentation by 50%. These results indicate that both PKD2 and PKD3 kinases can contribute to phosphorylation of MFF and compensate for deficiency of either PKD. Importantly, depletion of both PKD2 and PKD3 resulted in slower cell proliferation (data not shown).

To address the requirement for PKD activity in MFF phosphorylation specifically during mitosis, we used a pharmacological inhibition approach with a new highly specific and potent inhibitor of all three PKD kinases, CRT 0066101. Inhibition of PKDs resulted in a complete abolishment of mitotic MFF phosphorylation in HeLa cells under mitotic arrest using taxol and nocodazole (Fig. 18).

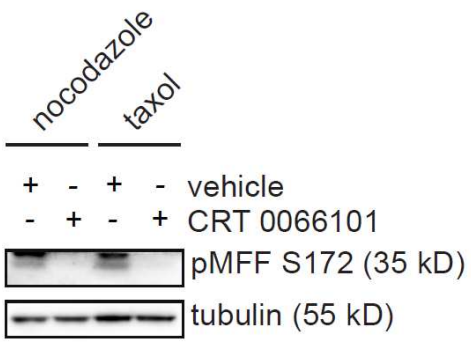

Figure 18. PKD activity is required for mitotic MFF phosphorylation (A) Immunoblotting of cell lysates from arrested in mitosis (M) using 14-hour treatment with nocodazole or taxol HeLa cells and treated with vehicle (PBS) or PKD inhibitor CRT0066101 for 4 hours. Antibodies against phospho-MFF (Ser172) and tubulin were used to detect respective proteins. Representative result of three independent experiments.

To provide genetic evidence we needed a cell line, which would lack all three members of the PKD kinase family or at least two of them. To that end, we used the CRISPR/Cas9-mediated gene editing system to generate triple PKD knockout cells (Fig. 19A). As a model system, we have chosen non-cancer mouse fibroblast NIH 3T3 cells, which express all three PKD kinases and display high basal level of mitochondrial fragmentation and very short doubling times (less than 20 hours). They also display very low AMPK activity, which we determined by initial screening of cell lines (data not shown). We did not succeed in generation of complete triple PKD knockout cells, but we managed to obtain cells carrying stop codons and in frame deletions in PKD1, PKD2 and PKD3 genes. Western blot analysis revealed that the two best clones were lacking PKD1 and PKD3 proteins, but PKD2 was still present (hereafter referred as PKD1/3 double knockout (dKO) cells) (Fig. 19B, C). This result could, for example, be explained by the requirement of PKD for cell survival.

Phenotypic analysis of mitochondrial morphology by fluorescence microscopy showed that PKD1/3 dKO cells maintain significantly elongated mitochondria (compared to parental wild type cells) as visualized by Mitotracker Red or TOM20 staining (Fig. 19 D and data not shown). Quantitative analysis of mitochondrial morphology in two separate dKO clones revealed a significant 60% reduction in mitochondrial fragmentation compared to wild type cells (Fig. 19E). They also displayed a slower cycling rate (data not shown). To assess the level of mitotic MFF phosphorylation, we synchronized wild type and PKD1/3 dKO cells in mitosis using nocodazole, taxol and STLC and analyzed MFF phosphorylation by western blot. While parental wild type NIH 3T3 cells showed robust induction in MFF phosphorylation, this phosphorylation was completely abolished in PKD1/3 dKO cells. As a negative control, we used MFF knockout MEFs (Fig. 19F).

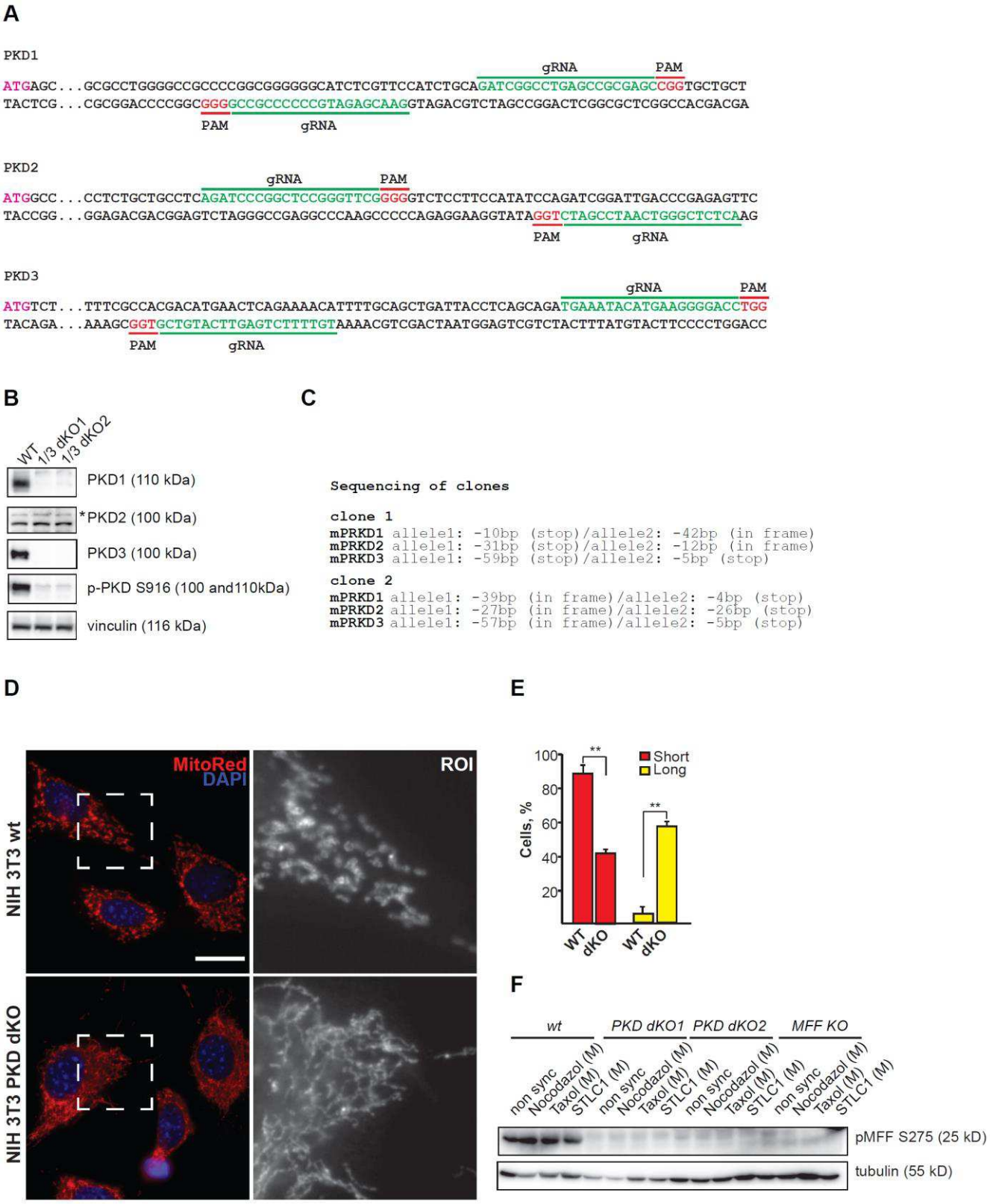

Figure 19. PKD activity is required for mitochondrial fragmentation in NIH 3T3 cells. (A) Explanatory illustration of the knockout strategy for generation of PKD-deficient cells. CRISPR/Cas9 targeting of genomic sequences of PKD 1/2/3 genes using complementary guide RNA pairs. (B) Validation of the chosen clones by western blot. Immunoblotting of cell lysates from wild type (WT) and PKD 1/3 double knockout (PKD dKO) NIH3T3 cells stimulated

for 1 hour with PMA. Antibodies against total PKD1, phospho-PKD1/2 (Ser916), total PKD2, total PKD3 and vinculin were used to detect respective proteins. (C) Validation of the chosen clones by sequencing. (D) Fluorescence microscopy images of mitochondria in WT and PKD 1/3 dKO NIH 3T3 cells. Scale bar: 20 µm. (E) Quantification of the mitochondrial morphology of cells shown in (D) by two categories: short (<5 µm), long (>5 µm). For each group at least 100 cells were counted. Data are shown as mean with SD of three independent experiments. **: $p<0.01$, by unpaired t test. (F) PKD activity is required for mitotic MFF phosphorylation. Immunoblotting of cell lysates from wild type (WT), PKD 1/3 dKO NIH 3T3 cells and MFF knockout MEFs non synchronized (non sync) or synchronized in mitosis using nocodazole, taxol or STLC for 14 hours. Antibodies against phospho-MFF (Ser275) and tubulin were used to detect respective proteins. Representative result of two independent experiments.

To further corroborate the obtained results, we also assessed PKD-dependent mitotic MFF phosphorylation in SV40-immortalized mouse embryonic fibroblasts (MEFs) carrying floxed alleles of PKD1 (PRKD1) and PKD3 (PRKD3). We isolated PKD1/3$^{fl/fl}$ MEFs from embryonic day 12 (E12) mouse embryos and transformed them with SV40-large T antigen. Cells were further transduced with Adeno-Associated viruses (AAV) encoding either EGFP-tagged Cre recombinase or EGFP alone. Cells were enriched by FACS and PKD1/PKD3 deletion efficiency was confirmed by genotyping PCR and western blot (Fig. 20A, B). To downregulate the remaining PKD2 activity, we introduced stable shRNA lentiviral constructs against mouse PKD2, which we pre-tested for their knockdown efficiency (Fig. 20C). MEFs were synchronized in mitosis using the Eg5 inhibitor STLC, which reversibly arrested cells in prometaphase of mitosis by preventing separation of the duplicated centrosomes and formation of a bipolar spindle. Treatment of MEFs for 16 hours with STLC resulted in efficient enrichment of mitotic cells. Mitotic MFF phosphorylation was readily detectable in control cells, infected with AAV-EGFP (Fig. 20D). Strikingly, deletion of PKD1 and PKD3 by AAV-Cre already led to a significant reduction in phospho-MFF signal as it was assessed by immunoblotting. Downregulation of remaining PKD2 by stable knockdown in PKD1/3 dKO MEFs resulted in almost complete abrogation of the phosphorylation signal (Fig. 20D). These results indicate that all three PKD kinases must be genetically deleted to fully abolish mitotic MFF phosphorylation.

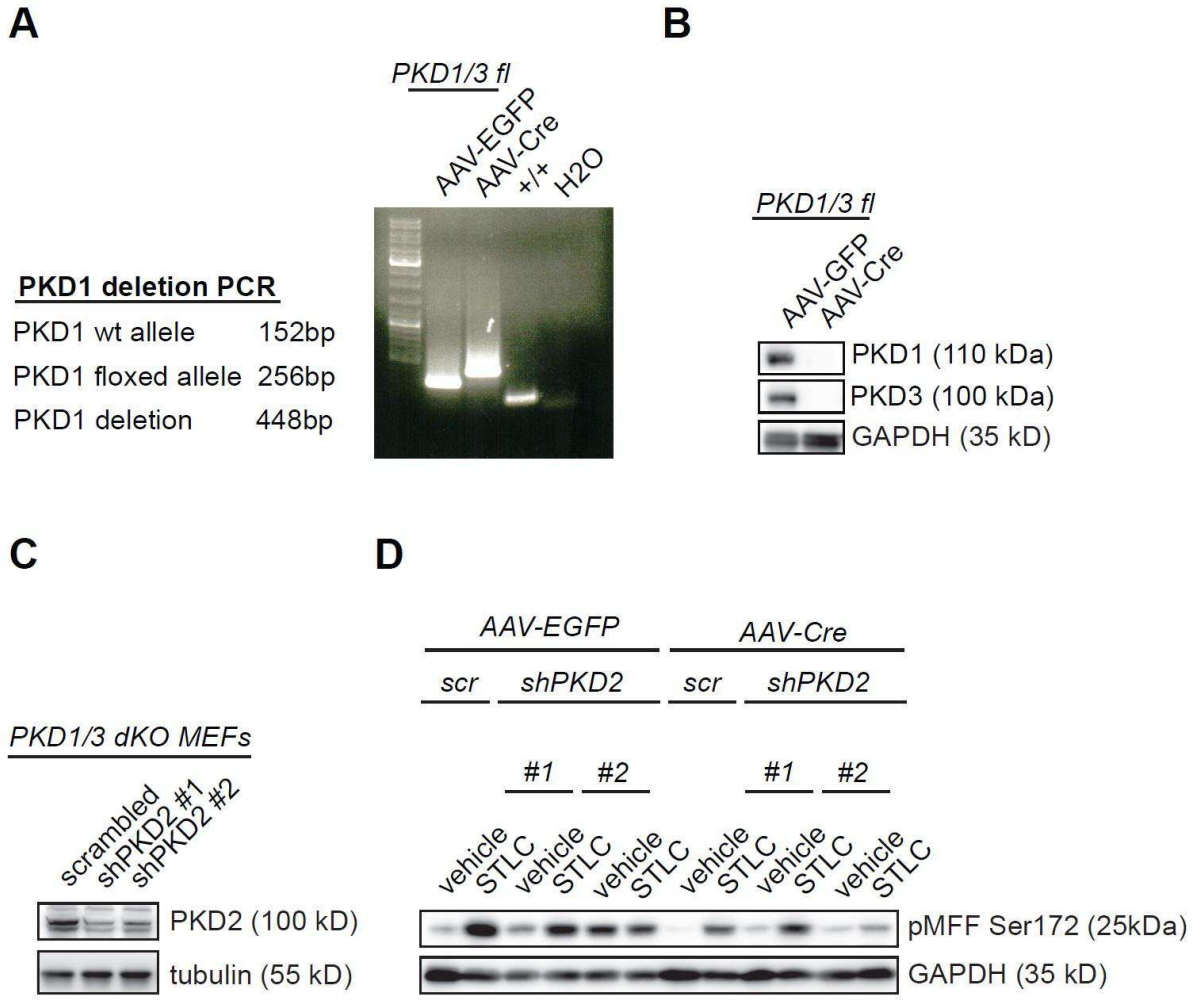

Figure 20. PKD activity is required for mitotic MFF phosphorylation (A) PKD1 and PKD3 were efficiently deleted in PKD1/3$^{fl/fl}$ MEFs when infected with AAV-Cre-EGFP, but not AAV-EGFP. Validation by genotyping PCR. (B) Immunoblotting of cell lysates from PKD1/3$^{fl/fl}$ AAV-GFP and PKD1/3$^{fl/fl}$ AAV-Cre MEFs. Antibodies against PKD1, PKD3 and GAPDH were used to detect respective proteins. (B) Immunoblotting of cell lysates from PKD1/3$^{fl/fl}$ AAV-Cre-EGFP MEFs infected with lentiviruses containing either of two non-overlapping shRNAs against PKD2 (designated as shPKD2#1 and shPKD2#2) or non-silencing shRNA (scrambled). Antibodies against PKD2 and tubulin were used to detect respective proteins. Representative result of two independent experiments. (C) Immunoblotting of cell lysates from PKD1/3$^{fl/fl}$ AAV-GFP and PKD1/3$^{fl/fl}$ AAV-Cre MEFs non-synchronized (vehicle) and synchronized in mitosis using STLC (STLC) infected with shRNAs against PKD2 (designated as shPKD2#1 and shPKD2#2). Antibodies against pMFF Ser172 and GAPDH were used to detect respective proteins. Representative result of two independent experiments.

As genetic ablation potentially results in long-term compensatory effects, it would be necessary to evaluate the physiologic impact of acute PKD inactivation on mitochondrial dynamics. To that end, we decided to take advantage of three highly potent and specific pharmacological PKD inhibitors of the second generation. As a model system, we have chosen NIH 3T3 mouse fibroblast,

as these cells display high basal level of mitochondrial fragmentation and short doubling times (less than 20 hours).

NIH 3T3 cells were treated with vehicle (control) or CRT 0066101, kb NB 142-70 and CID 755673 for 6 hours, stained for 30 minutes with MitoTracker Red and processed for fluorescence microscopy. Confocal imaging analysis revealed that pharmacological inhibition of PKD activity by three specific and structurally unrelated PKD inhibitors resulted in a consistent and significant reduction in mitochondrial fission (Fig. 21A). Interestingly, the strength of the observed phenotype strongly correlated with the potency of the PKD inhibiting compound, with the most potent and specific inhibitor (CRT 0066101) inducing the strongest phenotype (65% reduction in fragmented mitochondrial form), followed by the less potent kb NB 142-70 (50% reduction) and CID 755673 (30% reduction). Strikingly, CRT 0066101 treatment almost completely abolished mitochondrial fission, as not only the fragmented, but even the mitochondrial population of intermediate length was absent in CRT treated cells.

It was also interesting to assess whether PKD inhibition could block mitochondrial fission in response to a challenging stimulus. As such a stimulus, we have chosen Rotenone, a small molecule that inhibits Complex I of electron transport chain (NADH dehydrogenase), thus disrupting oxidative phosphorylation in mitochondria and also inducing production of mitochondrial reactive oxygen species (mROS) through hampered transfer of electrons to oxygen. Rotenone can damage mitochondrial components, inducing protein oxidation, lipid peroxidation and mtDNA damage. It is also a potent agent to stimulate mitochondrial fragmentation.

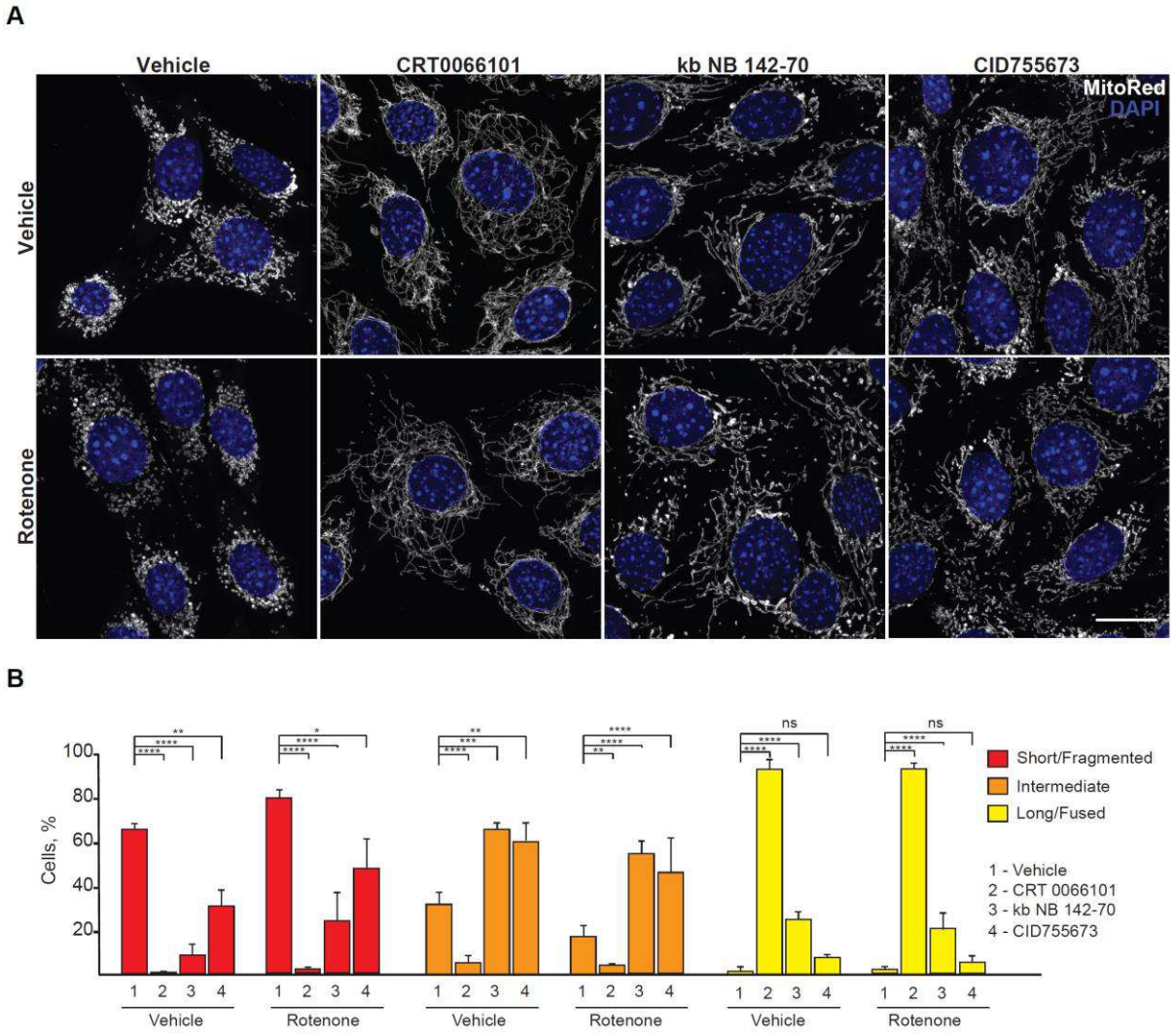

Figure 21. PKD activity is required for mitochondrial fission in mouse NIH 3T3 cells. (A) Confocal fluorescence microscopy images of NIH 3T3 cells treated with vehicle (DMSO) or one of three different PKD inhibitors (10μM CRT 0066101, 10 μM kb-NB 142-70 or 30μM CID 755673) in combination with vehicle or 1μM Rotenone. Mitochondria were stained with MitoTracker Red (pseudocolored in white) and nuclei were counterstained with DAPI. Scale bar: 20 μm. (B) Quantification of the mitochondrial morphology of cells shown in (A). Mitochondrial shape was classified as fragmented (no clear shape, less than 2μm long), intermediate (2μm - 5μm long) or long (tubular or fused, more than 5μm long) and displayed as percentage of cells having majority of their mitochondria falling in the respective category. For each group at least 300 cells were counted. Data are shown as mean with SD of three independent experiments. ****: p<0.0001, by two-way ANOVA using Dunnett's multiple comparisons test.

NIH 3T3 cells were treated with Rotenone in combination with vehicle (control) or CRT 0066101, kb NB 142-70 and CID 755673 for 6 hours, stained for 30 minutes with MitoTracker Red and processed for fluorescence microscopy. Confocal imaging analysis revealed that pharmacological inhibition of PKD activity by three different PKD inhibitors still resulted in a consistent and

significant reduction in mitochondrial fission even in response to a potent inducer of mitochondrial fragmentation (Fig. 21A). Similarly, the strength of the observed phenotype strongly correlated with the potency of the PKD inhibitor, with the most potent and specific inhibitor (CRT 0066101) inducing the strongest phenotype (77% reduction in mitochondrial fragmentation), followed by the less potent kb NB 142-70 (55% reduction) and CID 755673 (31% reduction).

If PKD inhibition can prevent mitochondrial fragmentation in response to Rotenone, can it also block mROS production? To answer this question, we decided to focus on the most specific and potent PKD inhibitor, which showed the strongest effect on mitochondrial dynamics (CRT 0066101). We treated NIH 3T3 cells with vehicle (DMSO, control) or CRT 0066101 in combination with Rotenone or vehicle (control) for 6 hours, stained for 30 minutes with DCF probe, and DCF fluorescence was quantified by flow cytometry. As expected, pharmacological inhibition of PKD activity completely abolished Rotenone-induced ROS production as evidenced from DCF-probe fluorescence. These results are in line with previous findings, which suggest that fragmented mitochondria may provide the main source of ROS (Fig. 22).

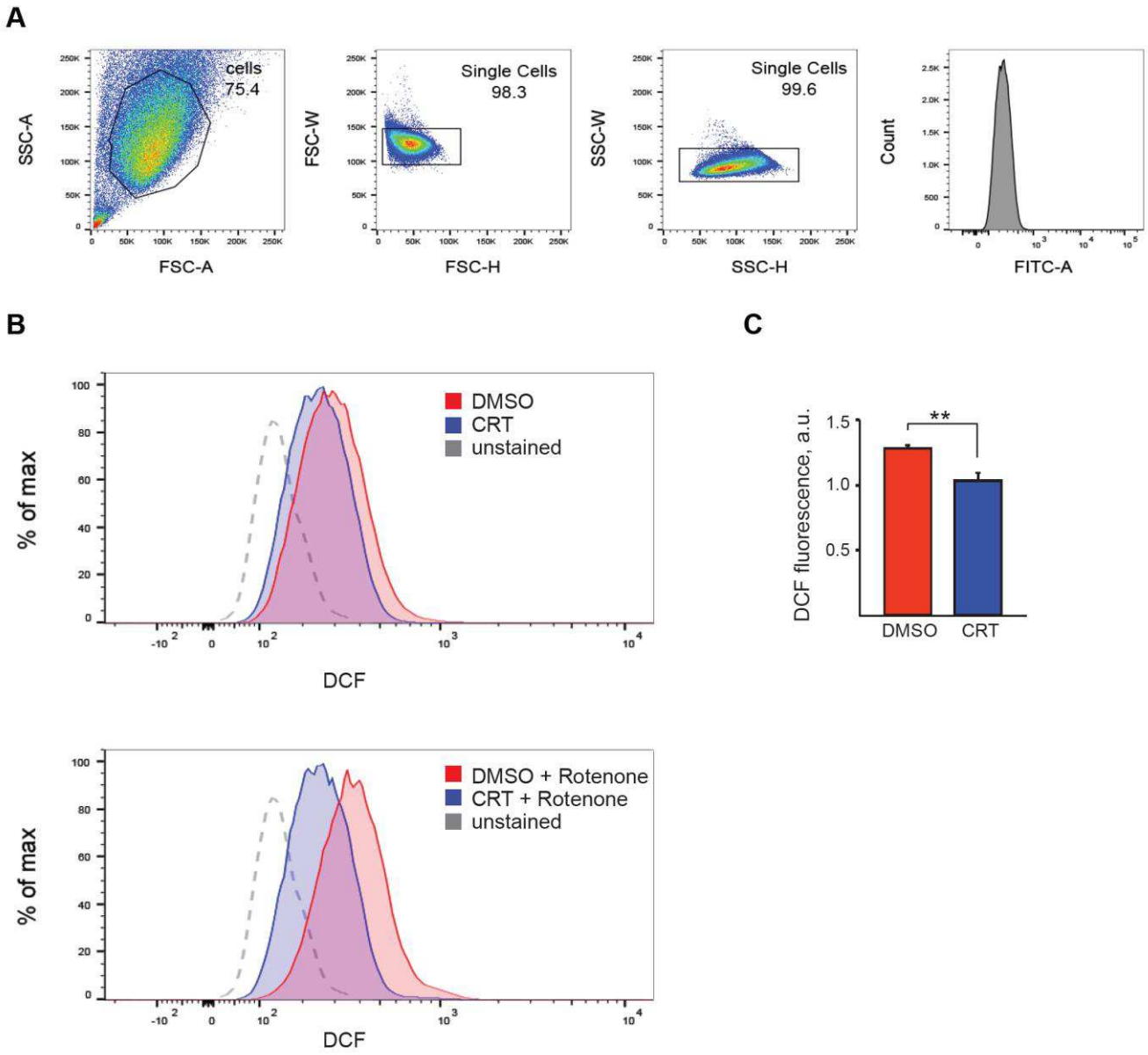

Figure 22. PKD activity is required for mROS production induced by Rotenone. (A) Gating strategy for mROS quantification experiment. NIH 3T3 cells were treated with 1μM Rotenone in combination with vehicle (DMSO) or PKD inhibitor (10μM CRT 0066101) for 6 hours. Cells were stained with 5 μM DCF probe and analyzed by flow cytometry. (B) Representative graph overlay. (C) Quantification of DCF fluorescence in response to Rotenone relative to untreated (no Rotenone, vehicle control), a.u. – arbitrary units. Data are shown as mean with SD of three independent experiments. **: $p<0.01$, using Student t-test.

To further extend our understanding of PKD inhibition effects on mitochondrial dynamics, ultrastructural analysis by TEM was employed. NIH 3T3 cells were treated with vehicle (control) or CRT 0066101 for 6 hours, fixed and processed for TEM. Ultrastructural analysis by transmission electron microscopy revealed that in CRT 0066101-treated cells mitochondria were

residing in the cytoplasm as elongated tubules or branched highly interconnected networks, unlike control vehicle-treated cells, which displayed a high degree of mitochondrial fragmentation (Fig. 24). These observations support obtained results from confocal microscopy. But to fully corroborate them, quantification analysis must be performed in the near future.

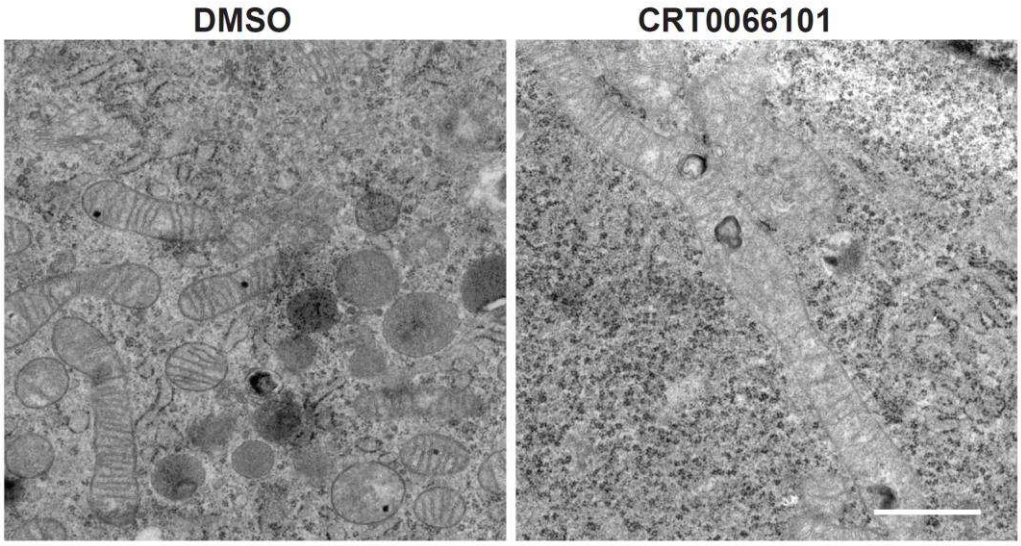

Figure 23. PKD inhibition prevents mitochondrial fission and results in strong elongation of mitochondria by unopposed fusion. (A) Electron microscopy analysis of mitochondrial morphology in NIH 3T3 cells. Representative TEM micrographs of NIH 3T3 cells treated with vehicle (DMSO) or PKD inhibitor (10μM CRT 0066101) for 6 hours. Scale bar: 1μm. Representative result of two independent experiments.

5.7 PKD-MFF mitotic axis as a potential target in anti-cancer therapy

To test the relevance of the PKD-MFF axis in the context of cancer, we focused our experiments on PANC1 cells, which are characterized by high PKD expression and activity. The PANC1 cell line is derived from a pancreatic carcinoma of ductal origin and is an established model for pancreatic cancer. We first analyzed mitochondrial morphology by immunostaining. PANC1 cells displayed high levels of basal mitochondrial fragmentation. The high rate of mitochondrial fission correlated with reported high levels of PKD activity in these cells (Guha et al., 2010; Yuan and Rozengurt, 2008). Pharmacological inhibition of PKD with CRT 0066101 resulted in a strong (40%) reduction

in the level of mitochondrial fragmentation, which was associated with increased cell death (Fig. 24 and data not shown).

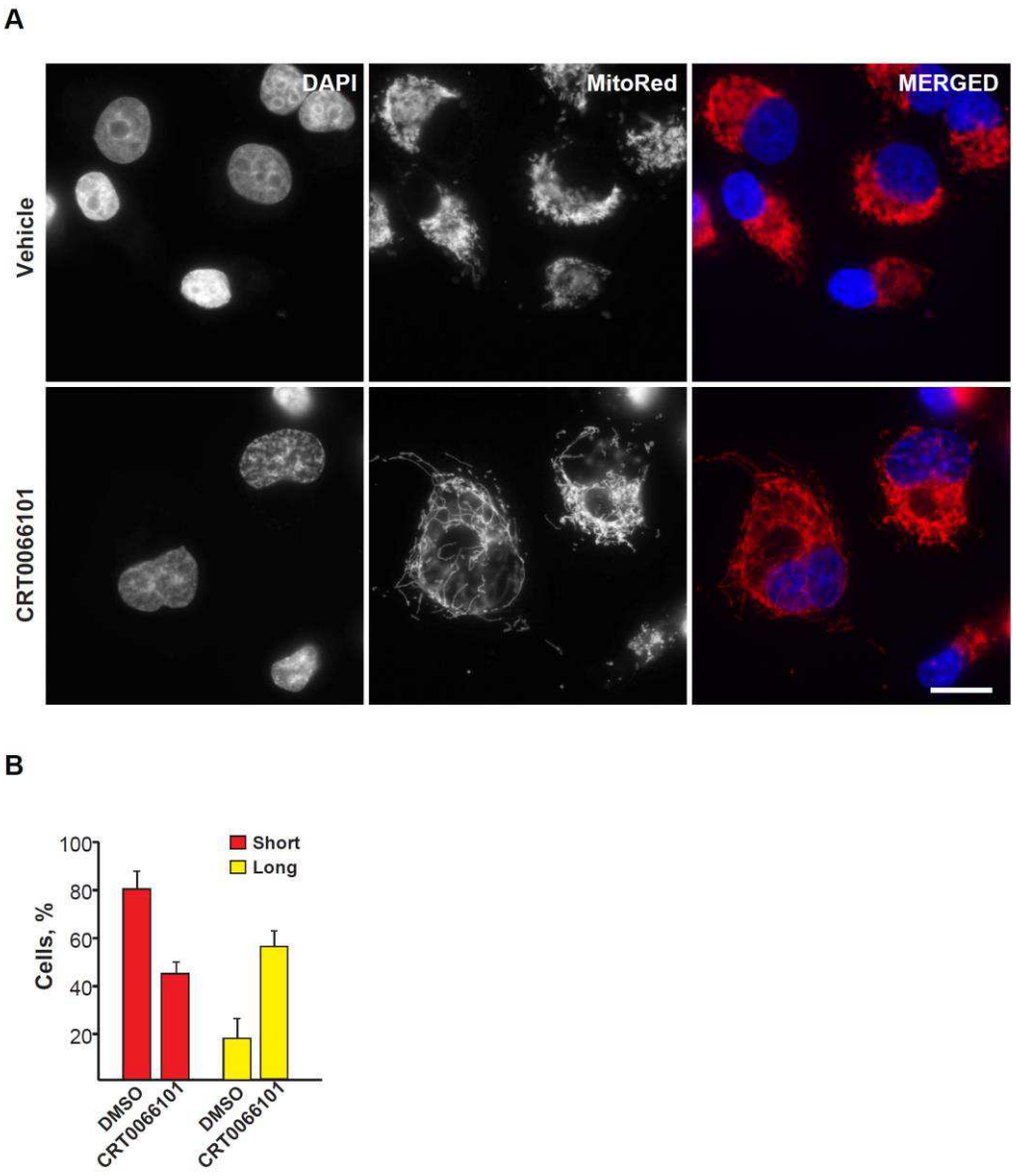

Figure 24. PKD inhibition reduces mitochondrial fission rate in pancreatic cancer PANC1 cells. (A) Fluorescence microscopy images of PANC1 cells treated with vehicle (DMSO) or PKD inhibitor (10μM CRT 0066101) for 14 hours. Mitochondria were stained with MitoTracker Red and nuclei were counterstained with DAPI. Scale bar: 20 μm. (B) Quantification of the mitochondrial morphology of cells shown in (A). Mitochondrial shape was classified as short (round or rod-like, 2-5μm long), or long (tubular or fused, more than 5μm long) and displayed as percentage of cells having majority of their mitochondria falling in the respective category. For each group at least 100 cells were counted. Data are shown as mean with SD of two independent experiments.

We plan to finish the quantification in the nearest future. Interestingly, similar results were also obtained from cervical carcinoma HeLa cells and human osteosarcoma U2OS cells (data not shown).

A recent phosphoproteome study in pancreatic cancer cells detected Ser155 and Ser 172 sites as highly enriched phosphorylation events in this type of cancer (Britton et al., 2014). As PKD phosphorylates MFF in mitosis, whereas AMPK does so in response to acute energy stress, it is likely that PKD activity is responsible for the detected basal levels of MFF phosphorylation. Thus, pharmacological inhibition of PKD and not AMPK should result in decreased levels of MFF phosphorylation. With the available phospho-MFF antibodies, we plan to test this hypothesis in the nearest future. A next question would be whether PKD inhibition would affect mitotic progression of PANC1 cells.

Overall, our work uncovered a mechanism in which PKD-mediated phosphorylation of MFF triggers mitochondrial fragmentation specifically during mitosis. This phosphorylation occurs independently of AMPK, another kinase of the CAMK group, which was recently described to phosphorylate the same site as PKD. PKD-dependent regulation of mitochondrial dynamics might be important in cancer growth and/or progression and needs further exploration.

6 Discussion

Over the last two decades, multiple studies have uncovered and strengthen the implication of mitochondrial dynamics in the pathophysiology of multiple neurodegenerative, neuromuscular and metabolic diseases. Yet the precise machinery responsible for the dynamic response of mitochondria to various stimuli remains poorly understood. Every year a new important factor is discovered, yet our understanding of molecular mechanisms that regulate activation, assembly and function of these factors is lagging behind.

In the present work, I have uncovered an unexpected role for the PKD kinases in mitochondrial dynamics. We found that all three members of the PKD kinase family were required for mitochondrial fragmentation during mitosis. Combined loss of function of PKD kinases as well as acute pharmacological inhibition of PKD activity resulted in a significant decrease in mitochondrial fission and unopposed mitochondrial fusion, as it was evidenced by dramatically elongated mitochondria in human and mouse cells, which were lacking PKD activity. PKDs exerted their effect on mitochondrial dynamics through regulation of the mitochondrial fission factor (MFF). Specifically, MFF, which acts as a main mitochondrial receptor for the large DRP1 GTPase, was found to be a direct PKD substrate. All three PKD family members could phosphorylate MFF. Such a functional redundancy resulted in a little or no effect of single PKD gene disruption and underscores the importance of this process in mitochondrial and, thus, cellular homeostasis. MFF phosphorylation was required for enhanced mobilization of DRP1-oligomers from the cytoplasmic pool. PKD activation triggered mitochondrial fragmentation specifically during mitosis. This phosphorylation occurred independently of AMPK, another kinase of the CAMK group, which was recently described to phosphorylate the same sites on MFF. PKD-dependent regulation of mitochondrial dynamics might be important in cancer growth and or progression, which needs further exploration.

6.1 Why do mitochondria have to be fragmented during mitosis?

While most of research in the mitotic field focuses on signaling events that ensure faithful chromosome segregation, far less is known about molecular mechanisms governing equal partitioning of organelles and cytoskeleton between daughter cells. Mitochondria are unique in this sense as they contain their own mitochondrial genome (Anderson et al., 1981). The mitochondrial genome exists in thousands of copies, which are packed in nucleoprotein complexes called nucleoids. Only of about 70 nm in diameter (Kukat et al., 2011), nucleoids are tethered into the inner side of the IM and appear as discrete foci, which are distributed evenly within the mitochondrial tubule (Iborra et al., 2004; Legros et al., 2004). This extraordinary regularity is maintained within any mitochondrial form ranging from fragmented to hyperfused, so every single mitochondrion contains at least one nucleoid (Capaldi et al., 2002; Margineantu et al., 2002). This non-random distribution implies the existence of an active mechanism, which regulates mtDNA partitioning within the cell. Mitochondrial dynamics as a combination of sequential fusion and division events is believed to provide such a regulation. Strikingly, mitochondrial division occurs near actively replicating nucleoids (Iborra et al., 2004; Ishihara et al., 2015; Lewis et al., 2016). And mitochondrial fusion is important for constant complementation of mitochondrial DNA, thus ensuring the stability and health of the mitochondrial genome (Chen et al., 2005). Mutations of mtDNA occur sporadically and their accumulation leads to severe pathologies in humans (such as neuromuscular dystrophy, encephalopathy). Inhibition of either fission or fusion through genetic ablation of key components in respective protein machineries results in inevitable depletion of mtDNA (Chen et al., 2005; Parone et al., 2008). Therefore it is not unusual to expect a crosstalk between nucleoid maintenance and the mitochondrial dynamics machinery.

Another crosstalk should involve the nucleus and mitochondria, as mitochondrial genome replication is not entirely autonomous; it requires regulatory proteins encoded by the nuclear

genes. Unlike nuclear DNA, mtDNA is believed to replicate continuously, occurring even in post-mitotic cells (although less efficiently). Whether nuclear and mitochondrial DNA replications are coordinated is a big controversy for several decades (Bogenhagen and Clayton, 1977; Magnusson et al., 2003). Despite the prevalent belief that mtDNA replication occurs independently of the nuclear genome, several studies detected an increase in mtDNA synthesis in S and G2 phases of the cell cycle (Antes et al., 2010; Chatre and Ricchetti, 2013; Lee et al., 2007; Martinez-Diez et al., 2006; Volpe and Eremenko, 1973). If this was the case, it would nicely explain why mitochondria are extensively fragmented during mitosis, a well-documented process during mitosis in mammalian cells. Mitochondrial fission would thus ensure not only equal distribution of mitochondria, but also control maintenance and stability of transmitted mtDNA. Failure to divide mitochondria would potentially result in unequal distribution of mitochondrial genetic material thus creating a risk when one population of cells receives very little and highly mutated mtDNA, whereas another one only "healthy" nucleiods. Therefore, we hypothesize that there could be a mitochondrial division related mitotic checkpoint, which should be fulfilled in order for the cell to progress through mitosis. In this work, we have not addressed the importance of this newly discovered PKD-MFF-DRP1 signaling axis on mitochondrial DNA transmission and copy numbers. To answer this question, we plan to test non-phosphorylatable and phosphomimetic MFF mutants in a genetic reconstitution experiment in HeLa cells lacking endogenous MFF. We will analyze effects of MFF mutants on mitochondrial dynamics in mitosis, on mitotic progression and mtDNA copy numbers.

6.2 Why MFF and no other DRP1 receptor mediate mitotic mitochondrial fragmentation?

MFF has been shown to be the prime DRP1 receptor that recruits oligomerized (tetramers) DRP1 from the cytosol to the outer mitochondrial membrane. Moreover, recent evidence suggests that mitochondrial fission sites in proximity to replicating nucleoids are marked by MFF and not FIS1, MiD49 or MiD51 (alternative DRP1 receptors). MFF knockdown resulted in decreased DRP1 colocalization to ER-marked fission sites (Lewis et al., 2016).

6.3 What is the function of these phosphorylations?

In my thesis, I show that PKD directly phosphorylates MFF at three serines (Ser155/Ser172/Ser275). AMPK was reported to phosphorylate two of these three sites (Ser155/Ser172) (Toyama et al., 2016). According to the work of Toyama et al., AMPK-mediated phosphorylations of MFF increase DRP1 recruitment to the mitochondrial surface, thus promoting fission. Moreover, phosphomimetic mutations are sufficient to induce mitochondrial division in the absence of AMPK activation. These conclusions were drawn from experiments where alanine mutants of MFF were not able to reconstitute the wild type MFF in MFF-deficient MEFs for the same level of DRP1 co-localization with the mitochondrial marker TOM20 in response to AMPK agonists. And overexpression of phosphomimetic mutants of MFF in the mouse brain resulted in more fragmented mitochondria compared to the non-phosphorylatable mutants. Although these experiments elegantly proved requirement and sufficiency of AMPK-mediated MFF phosphorylation in mitochondrial fission, it would be interesting to understand the molecular mechanism behind this activation.

PKD phosphorylates three serines (Ser155/Ser172/Ser275) located within the middle part of MFF. This region is not assigned to contain any known functional domains, repeats or to be of any predicted order. This part is also dispensable for DRP1-MFF direct interaction, which has been shown to be mediated through R1-R2 repeats within the amino-terminal region of MFF and the stalk domain of DRP1 (Frohlich et al., 2013; Otera et al., 2010). Without the solved crystal structure of MFF, it is difficult to predict what kind of impact these negative charges may have on MFF folding and function. Nevertheless, as MFF does not have any detected enzymatic activity, but rather acts as a receptor for DRP1, we tested the effect of MFF phosphorylations on MFF-DRP1 direct interaction. As in case of wild type MFF, phosphomimetic mutations did not result in any detectable interaction with DRP1 without cross-linking. This may imply that increased DRP1 recruitment may not be a sole result of changes in MFF-DRP1 binding, but rather hints towards additional interactors, which stabilize the complex or increase the incidence of MFF-DRP1 binding upon activation through MFF and possibly DRP1 phosphorylation. What could be such interactors? Cytoskeletal proteins are good candidatures in this context. It has been previously shown that mammalian mitochondria form numerous contacts with microtubules (Heggeness et al., 1978; Nangaku et al., 1994; Saxton and Hollenbeck, 2012). It has been also shown that different splice isoforms of DRP1 may preferentially bind microtubules (Strack et al., 2013). Small molecules, which interfere with microtubule polymerization/depolymerization are shown to also affect mitochondrial morphology. For example, nocodazole, which blocks microtubule polymerization, was reported to promote mitochondrial fission (Strack et al., 2013). Similarly, rotenone, which was also used in the present work as a potent inducer of mitochondrial fragmentation, was shown to inhibit assembly of microtubules and promote mitochondrial fission (Srivastava and Panda, 2007). Interestingly, in the initial siRNA screen for mitochondrial morphology defects performed in Drosophila cells, several other genes were identified along with the discovery of MFF. The list of these genes contained DRP1 as a top hit, but also three tubulin-encoding genes (*TUBA1A, TUBB8, TUBB3*) and three genes (*PAFAH1B1, MARK3, NDE1*), which encode microtubule-interacting proteins. Strikingly, this group of genes displayed a similar severe

phenotype of clumped mitochondria upon knockdown and this result was consistent in two siRNA pairs tested. Authors decided not to investigate the function of those genes, regarding them as separate genes involved in mitochondrial dynamics, briefly mentioning that those findings were consistent with the important role of microtubules in mitochondrial morphology. But what if these proteins act as a complex together with MFF and DRP1? Our own mass-spectrometry data on MFF interacting partners in HeLa cells contains several tubulin genes (e.g. *TUBA1A, TUBB, TUBB4B, TBB2A*) that are among the top potential MFF interactors and some (like *TBB2A*) were not even detected in control condition. Tubulins are also frequent contaminants of cellular preparations for mass-spectrometry analysis, so these results should still be taken with caution. To gain more insight into a potential MFF-DRP1 complex composition upon MFF phosphorylation we plan to do experiments, in which we will re-express non-phosphorylatable and phosphomimetic forms of MFF in HEK293T cells devoid of endogenous MFF and immunoprecipitated protein complexes will be analysed by mass-spectrometry. If MFF phosphorylation indeed affects abundance of certain interacting proteins, this would be a way to tackle the molecular mechanism behind PKD-mediated MFF activation.

Another attractive possibility is the involvement of certain lipid species in MFF-DRP1 interaction. *In vitro* studies showed that DRP1 bound preferentially membranes that contained cardiolipin (Bustillo-Zabalbeitia et al., 2014; Stepanyants et al., 2015). Some hints could be deduced from the known structure of DRP1. The Stalk domain is the only DRP1 domain required for DRP1-MFF binding, whereas the GTPase domain is not required, but has a positive impact. Moreover, the unstructured region called 'insert B domain' (IBD) within the DRP1 protein is located at the same position as the PH domain in highly homologous dynamin (Faelber et al., 2011; Ford et al., 2011) and the membrane binding stretch in MxA (von der Malsburg et al., 2011). IBD not only plays the inhibitory role in MFF-DRP1 interaction (Liu and Chan, 2015; Strack and Cribbs, 2012), but was also predicted as a putative membrane binding element (Mears et al., 2011). Although this prediction was not confirmed, it was also not completely disproved (Strack and Cribbs, 2012; Zhang et al., 2011). A recent study by the same group, which initially proposed lipid-interacting

function of IBD (or variable domain, VD) present some cryo-EM data on *in vitro* experiments proposing that the presence of cardiolipin in the OM may influence the helical structure, formed by DRP1 oligomers (Mears et al., 2011). Yet another study using lipidomics, microscopy and metabolomics showed that *in vivo*, increased amounts of cardiolipin correlated with tubular mitochondria and efficient oxidative phosphorylation (Guri et al., 2017). Thus, it would be interesting to know whether MFF phosphorylations could indirectly alter the lipid composition within the surrounding mitochondrial outer membrane leaflet. This line of research would need a lot of investment as lipidomics of local membranes is still a challenge.

MFF has been shown to homo-oligomerize via the coiled-coil domain, which is located at the carboxy-terminus of the protein (Gandre-Babbe and van der Bliek, 2008; Otera et al., 2010). One of the PKD phosphorylation sites on MFF is located in relative proximity to the carboxy-terminal coiled coil domain (Ser 275). Therefore, we tested whether MFF phosphorylations could affect the ability of MFF to form dimers. We co-expressed in HEK293T cells differentially tagged wild type, alanine, aspartate and glutamate mutants of MFF (GFP-tagged and Flag-tagged) and analyzed their ability to co-immunoprecipitate. We did not observe any difference in the dimerization ability of MFF mutants compared to wild-type MFF. In fact, MFF resides within approximately 200kDa complex, which does not include FIS1 or DRP1 (Gandre-Babbe and van der Bliek, 2008). It could well be that it is solely formed of MFF homo-oligomers (average molecular weight of MFF is about 30 kDa; with the longest isoform of 35 kDa and shortest of 25 kDa). We did not formally assess the ability of the mutants to form higher order oligomers, which could be evidenced by comparing MFF-oligomers obtained from phosphomimetic and non-phosphorylatable mutants using a different resolution method (Blue Native PAGE).

6.4 Why is PKD and not AMPK responsible for MFF mitotic fragmentation?

Both PKD and AMPK kinase families belong to the CAMK kinase group. They share similar basophilic substrate specificity, yet they are activated by distinct stimuli. AMPK is a well-established low energy sensor, which when activated, blocks all anabolic processes that require energy and promotes catabolic pathways necessary to replenish nutrients and ATP. AMPK is the key effector of the known tumor-suppressor kinase LKB1. LKB1 was shown to directly phosphorylate Thr172 of catalytic alpha subunit of AMPK complex, thereby stimulating its activity. Cells that lack LKB1 are highly prone to apoptosis in response to energy stress (Shaw et al., 2004). Reproduction, and mitosis in particular, are quite energy-consuming processes. In case of AMPK-mediated metabolic checkpoint, cell cycle is arrested until cellular resources (nutrients, ATP) are replenished. In this way cell makes a decision to proliferate only when there is enough energy and macromolecular building blocks to generate two daughter cells out of one parental (Gwinn et al., 2008). Such AMPK-checkpoint was shown to be present under numerous energy stress conditions such as hypoxia, starvation, mitochondrial dysfunction in response to chemical OXPHOS blockers, inhibitors of glycolysis or even direct AMPK activators (AICAR, A 769662) (Inoki et al., 2003; Shaw et al., 2004). It is believed that activation of AMPK imposes cell cycle arrest not through direct inactivation of mitotic machinery, but through inhibition of main driver of cellular growth and proliferation – the mechanistic target of rapamycin complex 1 (mTORC1). Numerous studies have proven that mitogen and nutrient signals converge on mTORC1, which controls cell proliferation and cell size (Laplante and Sabatini, 2012). The prolonged activation of AMPK results in cell cycle arrest through direct phosphorylation of TSC and Raptor, which are the main regulators of mTORC1. When mTORC1 is forced to remain activated under energy stress conditions, cells progress through cell cycle and subsequently die through apoptosis (Inoki et al.,

2003). AMPK pharmacological activators such as metformin and MT 63-78 are currently tested in clinical trials as promising anti-cancer drugs (Whitburn et al., 2017) (Zadra et al., 2014).

Unlike tumor suppressor role of AMPK, PKD kinase activity was mostly associated with hyperproliferative and aggressive cancers such as glioblastoma (Azoitei et al., 2011) and pancreatic cancer (Guha et al., 2010; Wille et al., 2014). In the heart, PKD1 was shown to control the hypertrophic growth in response to pressure overload or chronically elevated angiotensin II levels. So members of the PKD family emerge as critical regulators of proliferation and growth, but the exact molecular mechanisms and specific PKD targets remain elusive. Several PKD inhibitors are underway for clinical trials in pancreatic and colon cancer (Harikumar et al., 2010; Wei et al., 2014).

If AMPK were to phosphorylate MFF during mitosis this would likely accompany the cell cycle arrest, as the cell would activate the AMPK-regulated metabolic checkpoint and inhibit mTORC1. In some cancers, AMPK activity is important for survival under nutrient depletion. Although this compensatory activation of autophagy could be beneficial during interphase, it is unlikely to contribute specifically during mitotis. PKD is instead a very plausible candidate to drive mitotic events by regulating fragmentation of Golgi (Kienzle et al., 2013) and mitochondria (through MFF-DRP1 axis; this work), and possibly other organelles. We are just starting to elucidate the possible mitotic substrates of PKD. It is also likely that PKD may have targets that can modulate mitochondrial morphology during interphase, such candidates could be cytoskeletal proteins (e.g. tubulins, tubulin regulating enzymes, actin regulating proteins) or proteins involved in modulation of lipid composition (lipid kinases, acyl-transferases) or proteins that could sense membrane curvature (arfaptins, ARFs, Arls). The difficulty of deciphering direct PKD substrates comes from a strong compensation and redundancy within the PKD family and potential lethality of triple knockout cells.

6.5 Same substrate, same phosphorylations – different outcome? How can kinase activity/specificity determine the scenario of cellular processes?

It is not the first time that the same substrate and even the same phosphorylation sites within one substrate are assigned to different kinases. It is even the case for AMPK and PKD, as previously several proteins were independently discovered to be the targets of AMPK and PKD. For example, two members of the class IIa family of histone deacetylases (HDAC4 and HDAC5) were shown to be phosphorylated by AMPK (Chang et al., 2005; McGee et al., 2008; Mihaylova et al., 2011), whereas PKD1 was shown to phosphorylate all four class IIa HDACs (HDAC4, HDAC5, HDAC7, HDAC9) (Dequiedt et al., 2005; Matthews et al., 2010; Parra et al., 2005; Wilker et al., 2008; Xu et al., 2007). HDACs regulate transcription through deacetylation of histones and interaction with the transcription machinery, thus inhibiting expression of certain genes. One way to regulate HDACs is to control their nucleo-cytoplasmic shuttling. AMPK as PKD were shown to phosphorylate the classical 14-3-3 sites in HDACs, thereby driving them out of the nucleus. In HDAC-dependent manner, AMPK decreases glucose production by liver cells through reduction of the expression of FOXO target genes (Mihaylova et al., 2011). In case of PKD, HDAC inhibition results in the inactivation of a MEF2-mediated cardiac hypertrophy transcriptional program.

In this work, we have identified a first mitotic PKD substrate – MFF. It has been also described as an AMPK target, with the same phosphorylation sites. In this case, it is not a redundancy, but rather the opposing effects of these two families of kinases. Unlike bacterial kinases-mediated signaling cascades, which result in sequential activation/deactivation of targets, metazoan kinases form another level of complexity by regulating the regulators – when kinases can phosphorylate not only effector proteins or enzymes, but also other kinases and/or phosphatases forming a branched signaling cascade.

We believe that the phosphorylation of MFF itself does not dictate the outcome, but rather the whole signaling cascade triggered by a particular kinase. Activation of AMPK stimulates autophagy mainly through activation of ULK1 kinase (Egan et al., 2011) and inactivation of the mTORC1 kinase complex (Gwinn et al., 2008; Inoki et al., 2003). Thus, it is likely that phosphorylated MFF contributes to mitophagy through fragmentation of mitochondria, although this was not formally addressed in the AMPK study (Toyama et al., 2016). PKD induces fission of the Golgi apparatus and its vesiculation through phosphorylation of enzymes that regulate membrane lipid composition such as PI4P-kinase IIIbeta (Hausser et al., 2005), CERBP and OSRT (Olayioye and Hausser, 2012). PKD was also shown to regulate mitotic Golgi fragmentation and cell cycle progression through the MEK-Raf pathway (Kienzle et al., 2013). According to our hypothesis, PKD-mediated MFF phosphorylation is important for mitotic mitochondrial fragmentation and facilitates equal mitochondrial distribution between daughter cells.

But what if MFF phosphorylation is actually stimulating mtDNA replication? This would mean AMPK and PKD both could induce an increase in nucleoid numbers but under different physiological contexts. AMPK has been described as a positive regulator of mitochondrial biogenesis through PGC-1alpha and SIRT1 (Canto and Auwerx, 2009). There is no such evidence about PKD, and it would be an interesting option to explore.

What about the PKD-AMPK relationship? Is there a potential cross-talk? It is very likely that AMPK and PKD could regulate each other's activity. In this work, we observed that deletion of both catalytic subunits of AMPK potentiated effects of overexpression of constitutively active PKD and decreased basal MFF phosphorylation in those cells. And vice versa, PKD1 downregulation resulted in increased AMPK Thr172 phosphorylation, which is a marker of AMPK activity. There is indeed some evidence that PKD can negatively regulate AMPK. In mouse myotubes (C2C12 cells), PKD was shown to directly phosphorylate Ser491 and inactivate AMPKalpha2, thus interfering with insulin signaling in skeletal muscle (Coughlan et al., 2016). But it is also very likely that AMPK can inhibit PKD activity, as upon lack of nutrients or energy depletion AMPK induces

lipolysis and cell cycle arrest, so that cell cannot proliferate or synthesize some ceramides in the Golgi (PKD-regulated processes). Whether AMPK could inhibit PKD directly or through other regulators remains to be investigated. Our model does not exclude that AMPK and PKD could counteract each other competing for MFF phosphorylation (Fig. 25).

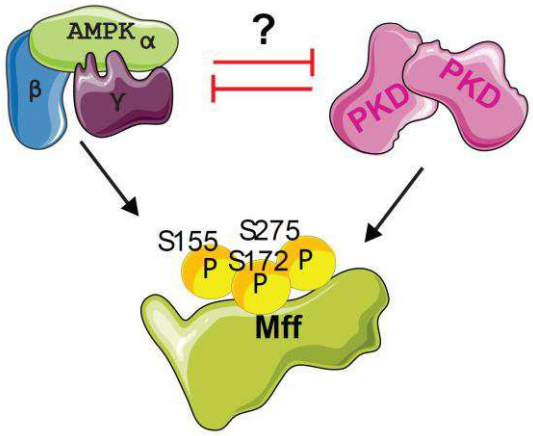

Figure 25. Possible crosstalk between AMPK and PKD kinases, which converge on MFF.

7 Conclusions

During my thesis, I discovered an unanticipated role for the PKD kinase family in mitochondrial fission. Our data demonstrated the requirement of all three PKDs for mitochondrial fragmentation. Loss of PKD activity led to blockade of mitochondrial fission and resulted in a significant elongation of mitochondria. Mechanistically, we showed that PKDs regulated mitochondrial dynamics by activating the mitochondrial fission factor (MFF) through phosphorylation of multiple sites. MFF acts as a main receptor for the large GTPase DRP1, which constricts mitochondria, and it is critical for proper mitochondrial division. All three PKD family members could phosphorylate MFF. The same phosphorylation events were previously reported to occur in response to energy stress and activation of another kinase of CAMK kinase group – AMP-dependent kinase (AMPK). These MFF phosphorylations were required for enhanced mobilization of DRP1-oligomers from the cytoplasmic pool. In contrast, PKD-mediated MFF phosphorylation and mitochondrial fragmentation occurred specifically during mitosis and did not require AMPK. As MFF phosphorylation was found to be significantly upregulated in different cancers, which was evidenced in several global phosphoproteome studies, the discovered PKD-MFF signaling axis regulating mitochondrial dynamics in mitosis could become an attractive therapeutic avenue for cancer treatment requiring further exploration.

Taken altogether, our results indicate that PKD phosphorylates MFF independently of AMPK in mammalian cells to induce mitochondrial fragmentation during mitosis. These findings are summarized in the model presented below (Fig. 26).

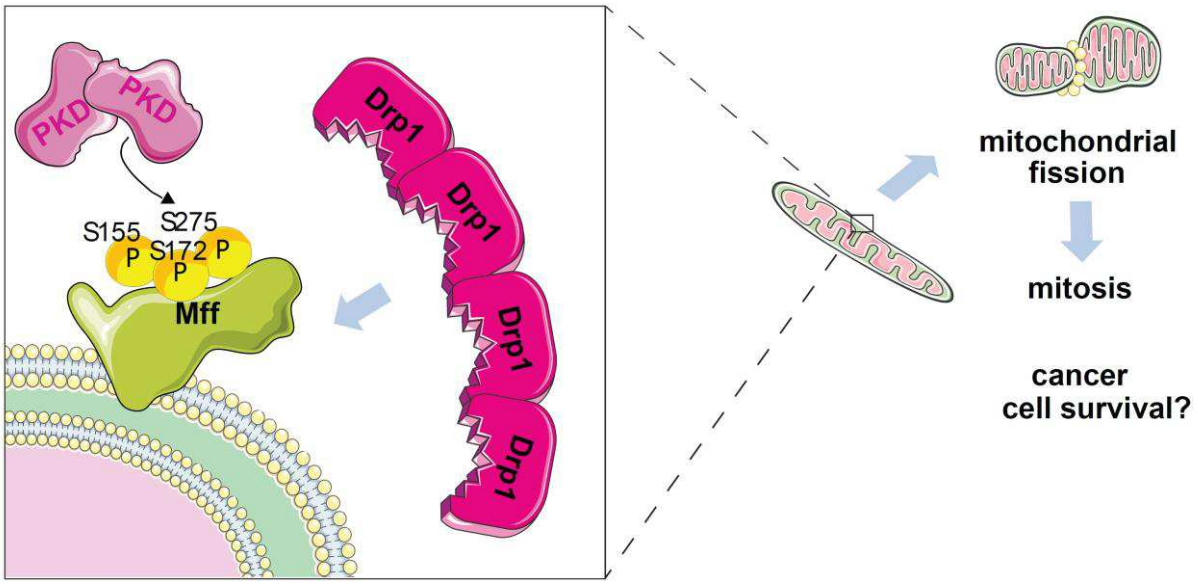

Figure 26. Model of regulation of mitotic mitochondrial fragmentation by PKD. Active PKDs phosphorylate MFF and thereby induce increased recruitment of active DRP1 tetramers from the cytoplasm to outer mitochondrial membrane. This event triggers formation of productive fission complex and subsequent mitochondrial division during mitosis. Highly proliferative cancer cells may benefit from enhanced PKD activity to ensure fast mitotic progression and survival.

8 Résumé de these

Introduction

Les mitochondries sont des organites spécialisés responsables de la production d'énergie dans tous les organismes eucaryotes. Bien que les mitochondries soient principalement considérées comme la centrale énergétique de la cellule, elles régulent également l'homéostasie du calcium, la biosynthèse des lipides, le statut oxydatif cellulaire, la division cellulaire et l'apoptose. Dans de nombreux types cellulaires chez les mammifères, elles apparaissent sous la forme de tubules interconnectés, qui partagent des copies multiples du génome mitochondrial contenu dans les nucléoïdes. Le rôle des mitochondries dans les pathologies humaines est maintenant considéré bien au-delà des défauts de la chaîne respiratoire ou des maladies neurodégénératives. Des études récentes ont clairement mis en évidence le rôle déterminant des mitochondries dans les maladies métaboliques et notamment au cours du cancer.

Le rôle des mitochondries dans le cancer fait l'objet de débats depuis des décennies. En effet, de nombreuses cellules cancéreuses ayant un métabolisme hautement glycolytique ont une respiration mitochondriale intacte, tandis que certains sous-types de cancer sont dépendant de la respiration mitochondriale. Ces contradictions ont conduit les chercheurs à regarder au-delà de la respiration mitochondriale et à se concentrer sur les autres fonctions de la mitochondrie dans le cancer. De façon intéressante, la croissance et la survie des cellules tumorales sont conditionnées par la sensibilité des mitochondries aux stress cellulaires qui joue un rôle clé dans la tumorigenèse. En effet, les cellules cancéreuses doivent proliférer dans des environnements pauvres en nutriments, hypoxiques et rendus toxiques par les traitements anticancéreux. Puisque le cancer est caractérisé par la prolifération incontrôlée de cellules anormales, l'un des principaux processus à comprendre est la façon dont les mitochondries agissent sur la progression de la mitose. Au cours de chaque division mitotique, la cellule distribue une quantité égale de matériel

génétique et d'organites entre les cellules filles. L'absence de ce processus entraîne un arrêt de la mitose, la sénescence ou l'aneuploïdie, qui sont considérés comme caractéristiques du cancer. En tant qu'unité cellulaire, les mitochondries ne sont pas formées *de novo* mais sont dérivées de celles préexistantes par un processus de fission mitochondriale (division). Le ralentissement de la division mitochondriale provoque l'allongement des mitochondries et la formation de structures en réseau fortement interconnectées. Ce ralentissement induit également des phosphorylations oxydatives défaillantes et la perte de l'ADNmt au cours de la division cellulaire.

Au cours de la mitose, les mitochondries dissocient leurs structures filamenteuses interconnectées en petites vésicules de forme ronde. La façon dont ce processus est régulé reste encore mal compris. Initialement, plusieurs facteurs ont été identifiés chez la levure. Chez les mammifères, la division mitochondriale est exécutée par deux GTPases - DRP1 ("Dynamin-related protein 1") et DYN2 ("DYNAMIN 2"). DRP1 s'assemble en complexes hélicoïdaux multimériques qui entourent la surface externe des mitochondries aux sites de division. Le recrutement de DRP1 est orchestré par le récepteur membranaire mitochondrial externe pour DRP1 appelé facteur de fission mitochondrial (MFF). L'étape de constriction finale est effectuée par DYN2 pour permettre la scission coordonnée des membranes externe et interne. Initialement, MFF a été découvert dans les cellules d'insectes en tant que facteur nécessaire à la fragmentation mitochondriale. Malgré l'existence de plusieurs autres récepteurs pour DRP1, des études sur des cellules humaines et chez la souris ont montré que MFF est nécessaire et suffisant pour cibler les complexes actifs de DRP1 sur la surface mitochondriale. Bien qu'il y ait de plus en plus d'évidences montrant la régulation de DRP1 par plusieurs kinases dans des conditions de cycle cellulaire et de stress distinctes, rien n'est connu à propos de son partenaire MFF.

Notre laboratoire étudie le rôle des protéines kinases D (PKD) dans le métabolisme. Notre équipe a identifié avec succès de nouvelles cibles de PKD1 dans la régulation des fonctions endocrines du pancréas à la fois en conditions physiologiques et physiopathologiques. Plus récemment, nous avons continué à rechercher de nouvelles cibles de cette kinase dans les macrophages au cours de

l'inflammation. Grâce à un criblage phosphoprotéomique non biaisé visant à trouver des substrats PKD dans les cellules cancéreuses humaines, nous avons identifié MFF comme une protéine candidate à travers laquelle la PKD pourrait réguler la dynamique mitochondriale.

L'objectif de cette étude était de comprendre le rôle de la phosphorylation de MFF médiée par PKD.

Résultats

Au cours du criblage phosphoprotéomique, nous avons observé que MFF était phosphorylé de manière différentielle lors de l'activation pharmacologique de PKD. Premièrement, j'ai confirmé que la phosporylation de MFF était PKD-dépendante. Pour ce faire, j'ai utilisé la protéine PKD sous une forme constitutivement active (CA) ou une forme dont l'activité kinase est inactive (kinase-Dead; (KD)). Les protéines PKD CA ou KD ont été co-exprimés avec la protéine de fusion MFF-Flag dans les cellules HEK293T. Par la suite, j'ai immunoprécipité MFF et quantifié sa phosphorylation en utilisant un anticorps dirigé contre la séquence *consensus* de *PKD phosphorylation*. L'expression de CA-PKD a entraîné une forte phosphorylation de MFF, tandis que KD-PKD était incapable d'induire une phosphorylation. Ensuite, j'ai purifié la protéine recombinante humaine MFF à partir de E. coli pour évaluer l'activité kinase *in vitro*. En utilisant le même anticorps dirigé contre la séquence *consensus* de *phosphorylation de PKD*, j'ai montré que la forme recombinante humaine de PKD1 phosphorylait MFF. J'ai ainsi confirmé que MFF est une cible directe de PKD (Fig. 1).

En collaboration avec le laboratoire du professeur Rudolf Aebersold de l'ETH à Zurich, nous avons détecté quatre sites potentiels de phosphorylation PKD-dépendants après évaluation de l'activité kinase *in vitro* (Fig. 2).

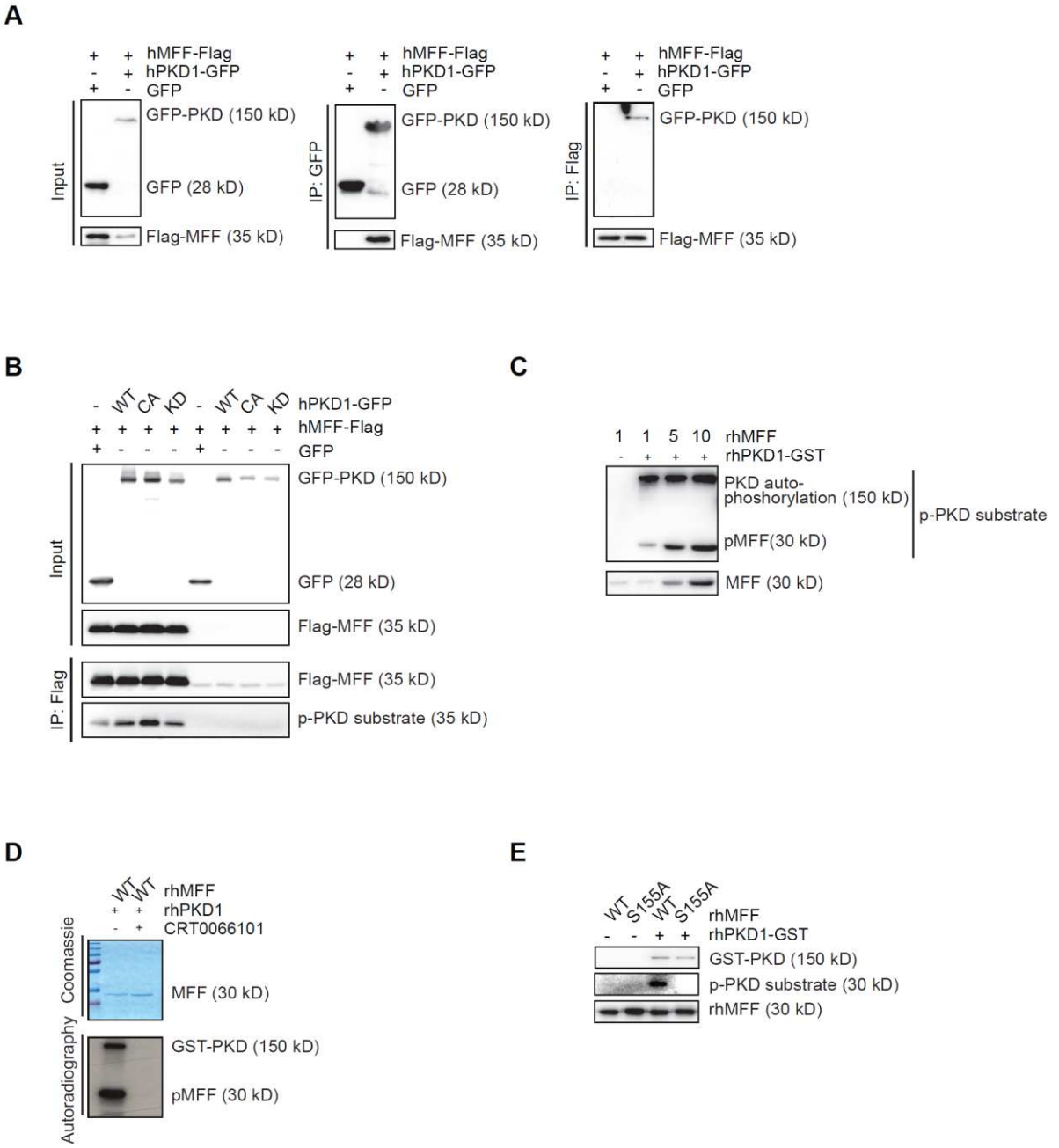

Figure 1. (A) PKD interagit avec MFF. Immunotransfert des élutions et du lysat total après co-immunoprécipitation des protéines de fusion exogènes MFF-FLAG avec PKD1-GFP et co-immunoprécipitation inverse de PKD1-GFP avec MFF-FLAG dans les cellules HEK293T. Des anticorps dirigés contre GFP et FLAG ont été utilisés pour détecter les protéines de fusion. Résultats représentatifs de trois expériences indépendantes. **(B) PKD phosphoryle MFF.** Immunotransfert des élutions et du lysat total après immunoprécipitation de FLAG dans les cellules HEK293T co-exprimant le FLAG seul (Témoin) ou MFF-FLAG avec la protéine EGFP seule ou les protéines de fusion (WT), PKD1-EGFP constitutivement actif (CA) ou la protéine PKD1-EGFP dont l'activité kinase n'est plus fonctionelle "Kinase Dead" (KD). Des anticorps dirigés contre FLAG, contre les substrats phosphophorylés de PKD et contre GFP ont été utilisés pour détecter les protéines de fusion. Résultats représentatifs de trois expériences indépendantes. **(C, D, E) PKD peut directement phosphoryler MFF. (C)** Immunotransfert après dosage de l'activité kinase in vitro. Des quantités croissantes (1, 2, 5 µg) de protéine MFF humaine recombinante (rhMFF) ont été incubées sans ou avec 50 ng de protéine

PKD1 humaine recombinante (rhPKDl) à 30 ° C pendant 30 minutes. Des anticorps dirigés contre les substrats phosphophorylés de PKD et la protéine MFF total ont été utilisés. L'astérisque (*) indique l'auto-phosphorylation de PKD1. **(D)** Lysat total et autoradiographie du dosage radioactif de l'activité kinase in vitro. La protéine humaine recombinante MFF (rhMFF) (1 µg) a été incubée avec 50 ng de protéine humaine recombinante PKD1 (rhPKD1) sans ou avec 1 µM d'inhibiteur de PKD CRT0066101 à 30 ° C pendant 30 minutes. Résultats représentatifs de trois expériences indépendantes. **(E)** Immunotransfert après dosage de l'activité kinase in vitro avec la protéine recombinante humaine MFF de type sauvage (WT) ou 1 µg de protéine mutante recombinante MFF (S155A) sans ou avec 50 ng de protéine humaine recombinante rhPKD1-GST. Des anticorps dirigés contre MFF total, le les substrats phosphophorylés de PKD et GST ont été utilisés pour détecter les protéines décrites ci-dessus.

Afin de confirmer l'importance des cinq sites potentiels de phosphorylation, nous avons effectué une mutagenèse dirigée de MFF en mutants non phosphorylables et évalué le rôle de ces sites de phosphorylation par dosage radioactif. L'utilisation d'anticorps phospho-spécifiques générés par la plateforme de production d'anticorps de l'IGBMC ont confirmé que les Sérines 155/172/275 sont directement phosphorylées par PKD (Fig. 3).

Récemment, la protéine kinase activée par l'adénosine monophosphate (AMPK) a été reportée pour induire la phosphorylation de MFF en réponse au stress énergétique (poison mitochondriales ou déplétion en ATP) sur deux des sites identifiés précédemment. Par conséquent, nous avons cherché à comprendre le lien supposé qu'il pouvait exister entre la phosphorylation de MFF par PKD et AMPK. Pour ce faire, en utilisant la technique d'édition de gène CRISPR/Cas9, j'ai généré des cellules HEK293T dans lesquelles les gènes codant pour les deux isoformes de la protéine AMPK alpha1 / alpha2 ont été inactivées. Dans ces cellules, la surexpression de PKD induisait la phosphorylation de MFF de manière indépendante vis à vis de la protéine AMPK, mais la phosphorylation dépendante du stress énergétique de MFF était complètement abolie. Ce résultat suggère que la phosphorylation de MFF implique un autre processus indépendant de AMPK (Fig. 4).

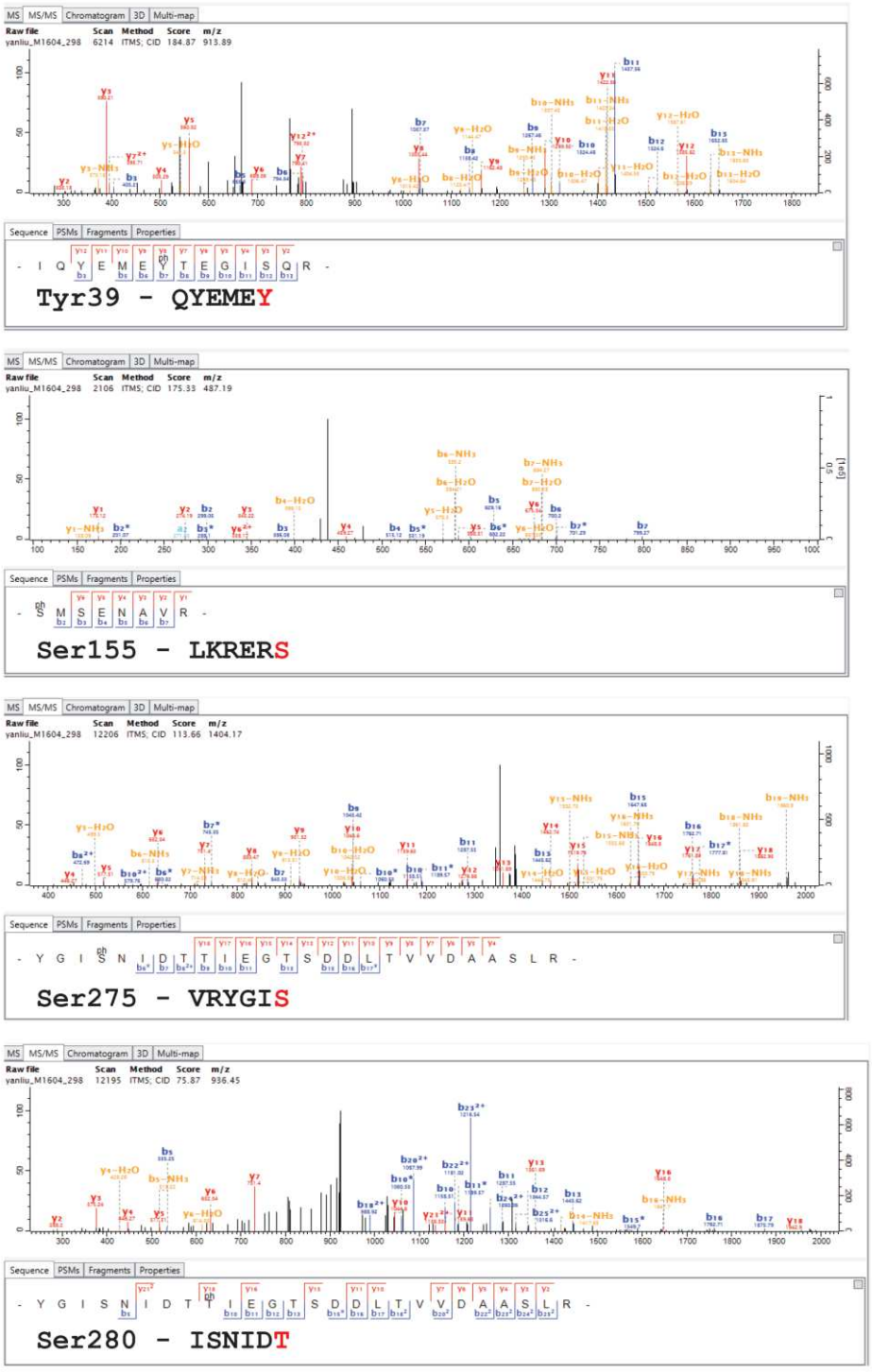

Figure 2. Spectre "MaxQuant" des sites de phosphorylation de PKD pour MFF identifié par spectrométrie de masse. Les produits du dosage de l'activité kinase in vitro (10 µg de protéine humaine recombinante MFF avec 500 ng de protéine humaine recombinante PKD1) ont été digérés avec de la trypsine et soumis à une analyse LC-MS/MS par Oribtrap XL. Les fichiers bruts ont été traités avec le logiciel MaxQuant (version 1.5.2.8). L'identification des peptides a été réalisée en utilisant le moteur de recherche Andromeda contre la base de données humaine SwissProt. Les peptides identifiés ont ensuite été visualisés par Viewer dans MaxQuant et analysés dans le logiciel Skyline. Le site de phosphorylation est marqué en rouge et sa position en acides aminés est indiquée sur toute la longueur de la protéine MFF humaine.

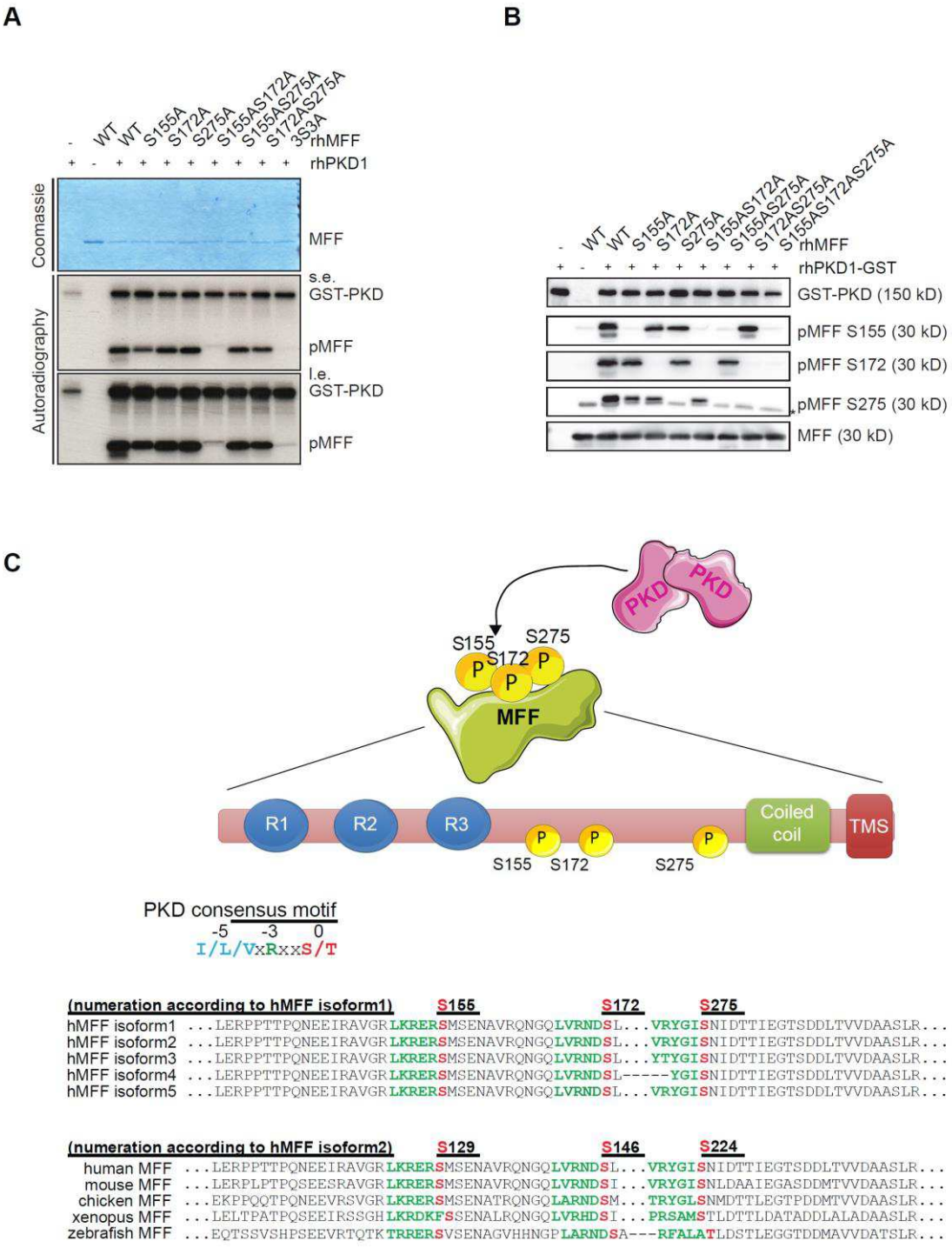

Figure 3. (A, B) PKD phosphoryle directement MFF en Ser155 / Ser172 / Ser275. (A) Lysat total et autoradiographie du dosage radioactif de l'activité kinase in vitro. La protéine humaine recombinante MFF de type sauvage (WT) ou des protéines mutantes de MFF ont été incubés sans ou avec 50 ng de protéine de fusion PKD1-GST (rhPKDl-GST) à 30 ° C pendant 30 minutes. (s.e.) indique une exposition courte, (l.e.) indique une exposition longue. **(B)** Immunotransfert après dosage de l'activité kinase in vitro. La protéine humaine recombinante MFF de type sauvage (WT) ou des protéines mutantes de MFF ont été incubées sans ou avec 50 ng de protéine de fusion PKD1-GST (rhPKDl-GST) à 30 ° C pendant 30 minutes. Des anticorps dirigés contre PKD1, la phospho-Ser155, la phospho-Ser172, la phospho-Ser275 et la protéine MFF totale ont été utilisées pour détecter les protéines décrites ci-dessus. L'astérisque (*) indique la forme non-phosphorylée de MFF reconnue par l'anticorps anti phospho-Ser275. Résultats représentatifs

de trois expériences indépendantes. **(C) Illustration schématique de la triple phosphorylation de MFF en Ser155 / Ser172 / Ser275 par PKD.** La forme dimérique et active de PKD phosphoryle MFF en Ser155, Ser172 et Ser275, qui sont situés dans la région prédites sans domaines. Les domaines fonctionnels de MFF sont représentés de l'extrémité N-terminal à l'extrémité C-terminal. Les répétitions courtes (R1, R2, R3), nécessaires pour le recrutement de DRP1, sont représentées en bleu. Le domaine sous forme de super hélice, qui est nécessaire pour la dimérisation du MFF, est marqué en vert et le segment trans-membranaire (TMS), qui ancre MFF dans la membrane externe est en rouge. Les sites de phosphorylation de PKD pour les isoformes humaines de MFF et pour celles provenant d'autres espèces de vertébrés sont alignés sous le schéma avec un motif général de consensus PKD sur le dessus. Le motif consensus PKD au sein de la séquence est marqué en vert et le site de phosphorylation est marqué en rouge.

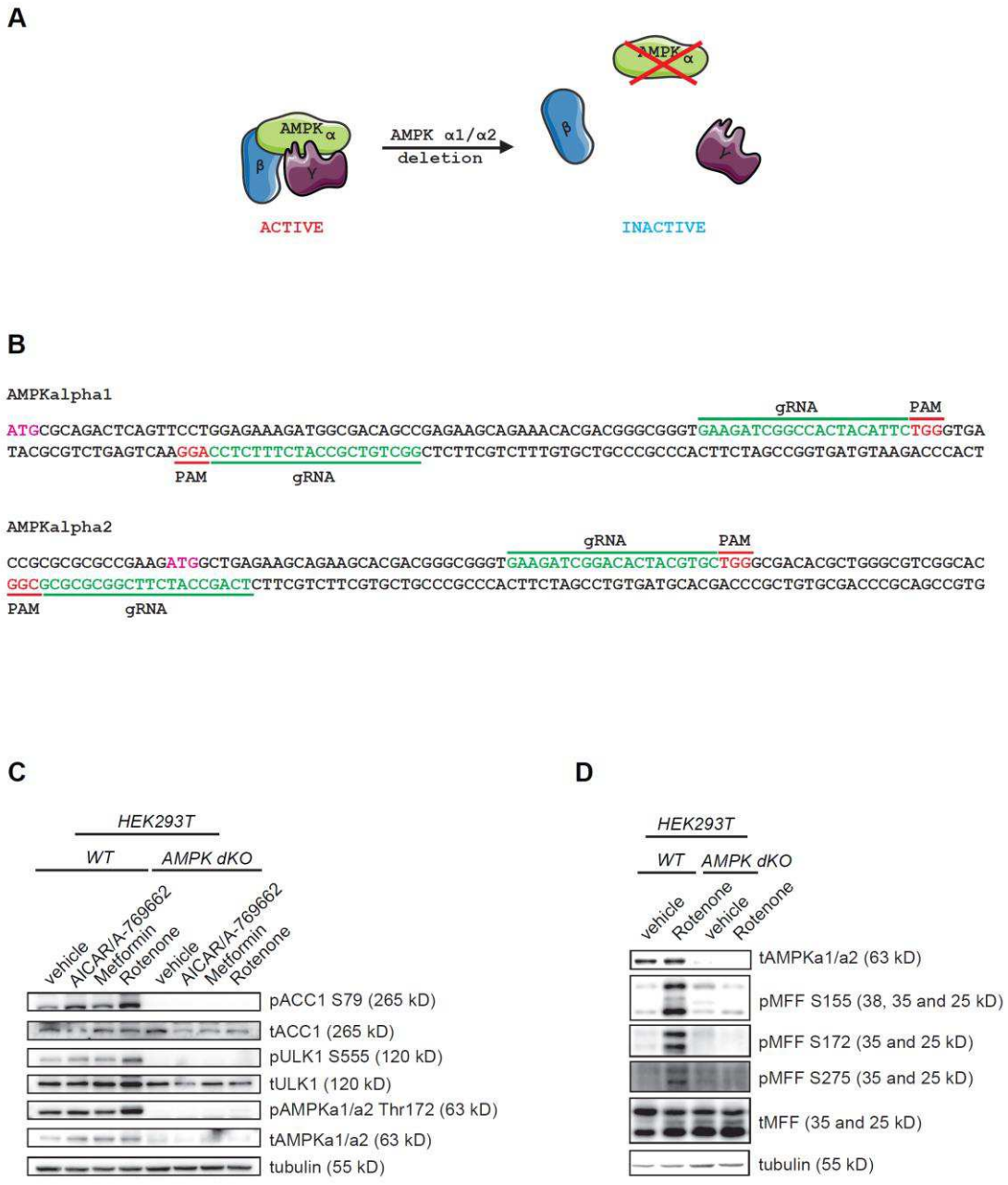

Figure 4. Stratégie de génération et validation des cellules déficientes en AMPK. (A) Illustration explicative de la stratégie utilisée pour la délétion totale de AMPK. **(B)** Stratégie CRISPR / Cas9 ciblant des séquences génomiques des

gènes AMPK α1 et α2 en utilisant des paires d'ARN guide complémentaires (Stratégie adaptée de (Toyama et al., 2016)). **(C)** Immunotransfert des lysats cellulaires provenant de cellules HEK293T de type sauvage (WT) ou dans lesquelles les gènes α1/α2 codant pour l'AMPK ont été inactivés (AMPK dKO). Les cellules ont été préalablement stimulées pendant 2 heures avec le véhicule ou un mélange de 2 mM de AICAR et 50 µM de A-769662 ou 1 µM de roténone. Des anticorps dirigés contre la protéine ACC1 totale, phospho-ACC1 (Ser79), la protéine ULK1 totale, phospho-ULK1 (Ser555), la protéine AMPK totale, phospho-AMPK (Thr172) et la tubuline ont été utilisés pour détecter les protéines. **(D)** L'activité de l'AMPK est requise pour la phosphorylation du MFF induite par le stress énergétique. Immunotransfert des lysats cellulaires provenant de cellules HEK293T de type sauvage (WT) ou dans lesquels les gènes α1/α2 codant pour l'AMPK ont été inactivés (AMPK dKO) stimulées pendant 2 heures avec le véhicule ou 1µM roténone. Des anticorps dirigés contre la protéine MFF total, phospho-MFF (Ser155), phospho-MFF (Ser172), phospho-MFF (Ser275), la protéine AMPK totale et la tubuline ont été utilisés pour détecter les protéines décrites ci-dessus. Résultats représentatifs de trois expériences indépendantes.

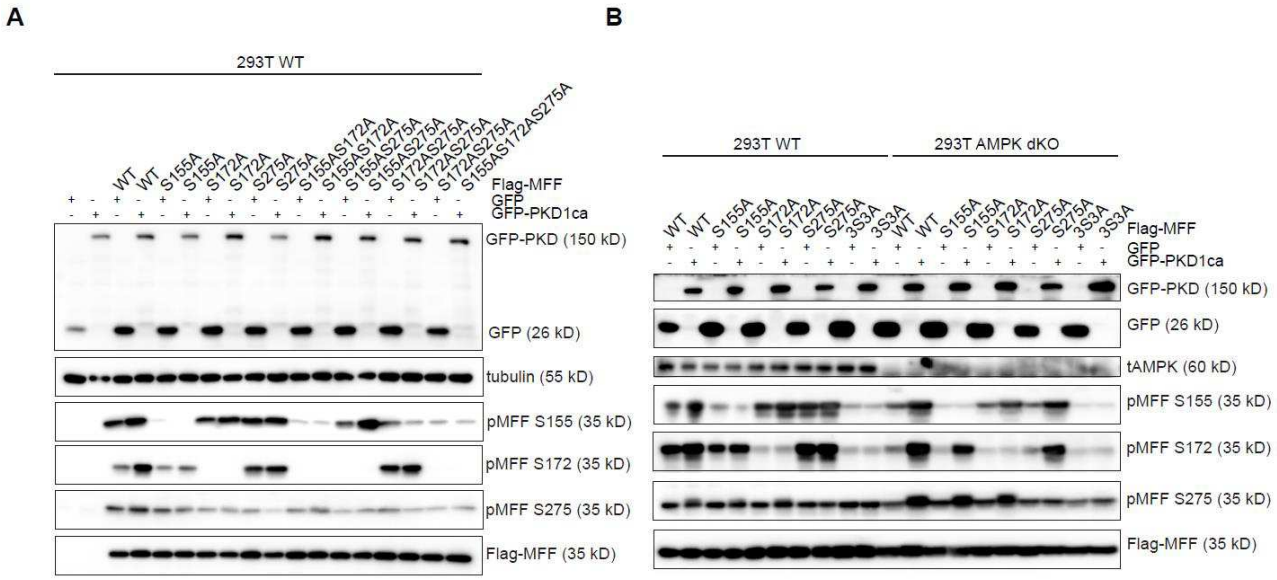

Figure 5. (A) PKD phosphoryle la protéine MFF en Ser155 / Ser172 / Ser275 dans les cellules. Immunotransfert des lysats cellulaires provenant de cellules HEK293T co-exprimant pcDNA-FLAG (vecteur témoin) ou la protéine de fusion MFF- FLAG (WT) ou les mutants MFF-EGFP ou la protéine PKD1-EGFP constitutivement active (CA). Des anticorps dirigés contre FLAG, phospho-MFF (Ser155), phospho-MFF (Ser172), phospho-MFF (Ser275), la tubuline et GFP ont été utilisés pour détecter les protéines. Résultats représentatifs de trois expériences indépendantes**. (B) PKD phosphoryle MFF en Ser155, Ser172 et Ser275 de manière AMPK-indépendante.** Immunotransfert des lysats cellulaires provenant des cellules HEK293T de type sauvage (WT) ou dans lesquelles les gènes α1/α2 codant pour l'AMPK ont été inactivés (AMPK dKO) co-exprimant MFF-FLAG ou des mutants MFF-EGFP ou la protéine PKD1-EGFP constitutivement active (CA). Des anticorps dirigés contre FLAG, phospho-MFF (Ser155), phospho-MFF (Ser172), phospho-MFF (Ser275), la tubuline, l'AMPK α 1 / α 2 et GFP ont été utilisés détecter les protéines. Résultats représentatifs de trois expériences indépendantes.

Comme l'AMPK régule la fission mitochondriale via MFF en réponse aux poisons mitochondriaux, j'ai émis l'hypothèse que cette phosphorylation pouvait se produire pendant la mitose. Ainsi, j'ai utilisé une lignée de cellules cancéreuses, les cellules HeLa, qui peuvent être facilement synchronisé dans différentes étapes du cycle cellulaire. Pour ce faire, j'ai induit l'arrêt de la mitose en utilisant plusieurs agents pharmacologiques et j'ai synchronisé les cellules avec deux blocages successifs avec de la thymidine concentrée. Ainsi, j'ai découvert pour la première fois que la phosphorylation de MFF par PKD se produit pendant la mitose (Fig. 6, 7, 8).

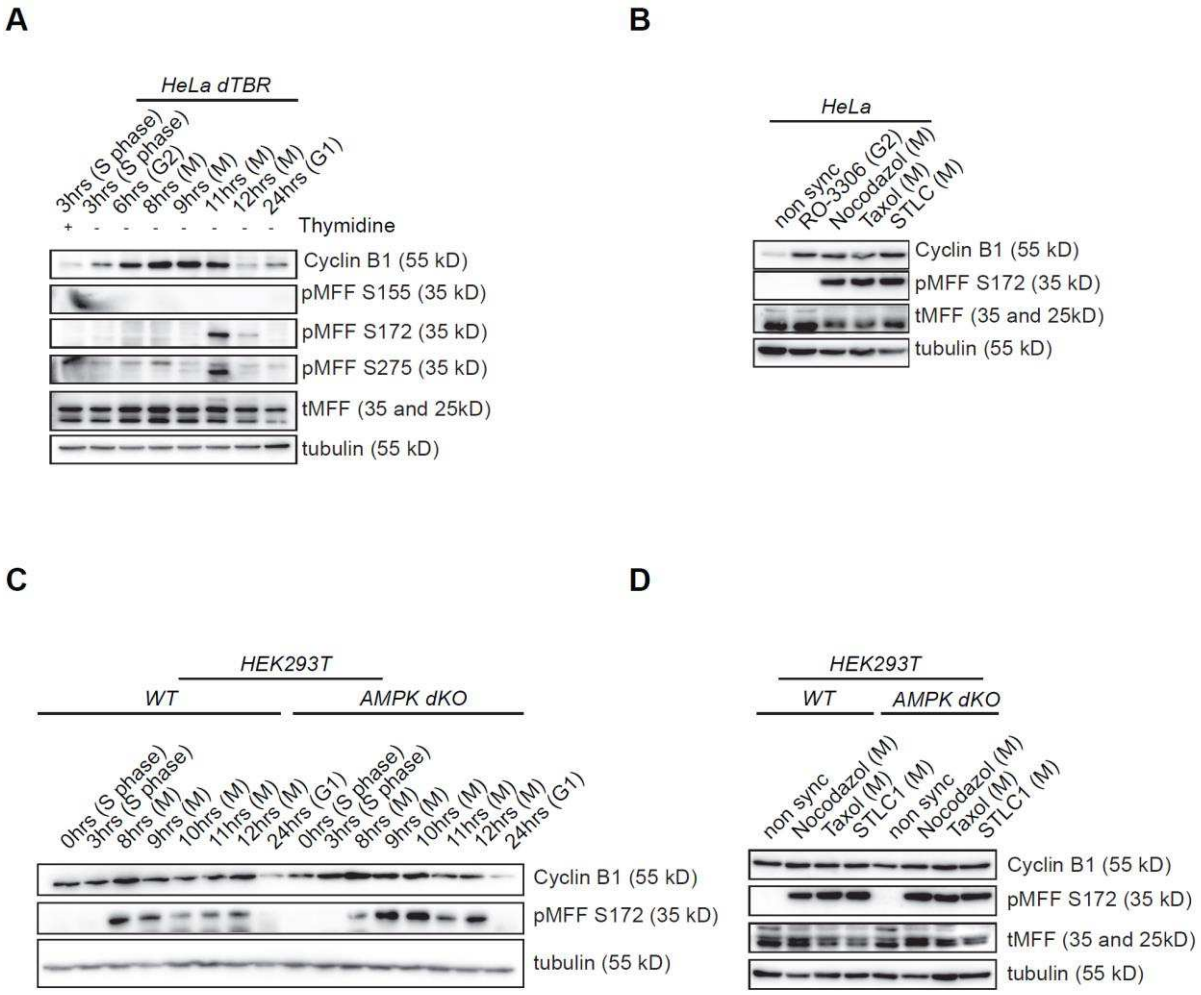

Figure 6. (A, B) PKD phosphoryle le MFF pendant la mitose. (A) Immunotransfert des lysats cellulaires provenant de cellules HeLA synchronisées par un double blocage thymidine, le temps après synchronisation est indiqué avec le stade correspondant du cycle cellulaire. **(B)** Immunotransfert des lysats provenant de cellules non synchronisées ou arrêtés chimiquement au stade G2 ou en mitose (M) au cours du cycle cellulaire. Des anticorps dirigés contre la protéine MFF totale, phospho-MFF (Ser155), phospho-MFF (Ser172), le phospho-MFF (Ser275), la tubuline et la cycline B1 ont été utilisés pour détecter les protéines. Résultats représentatifs de trois expériences indépendantes. **(C, D) La délétion d'AMPK n'affecte pas la phosphorylation mitotique de MFF. (C)** Immunotransfert de lysats cellulaires provenant de

cellules HEK293T de type sauvage et AMPK dKO synchronisées par double bloc de thymidine, le temps après la deuxième libération indiqué avec le stade du cycle cellulaire correspondant. **(D)** Immunotransfert de lysats cellulaires provenant de cellules HEK293 T de type sauvage ou dans lesquelles les gènes α1/α2 codant pour l'AMPK ont été inactivés (AMPK dKO). Les cellules ne sont pas synchronisées ou chimiquement arrêtées en mitose (M). Des anticorps dirigés contre la protéine MFF totale, le phospho-MFF (Ser172), la tubuline et la cycline B1 ont été utilisés pour détecter les protéines mentionnées ci-dessus. Résultats représentatifs de trois expériences indépendantes.

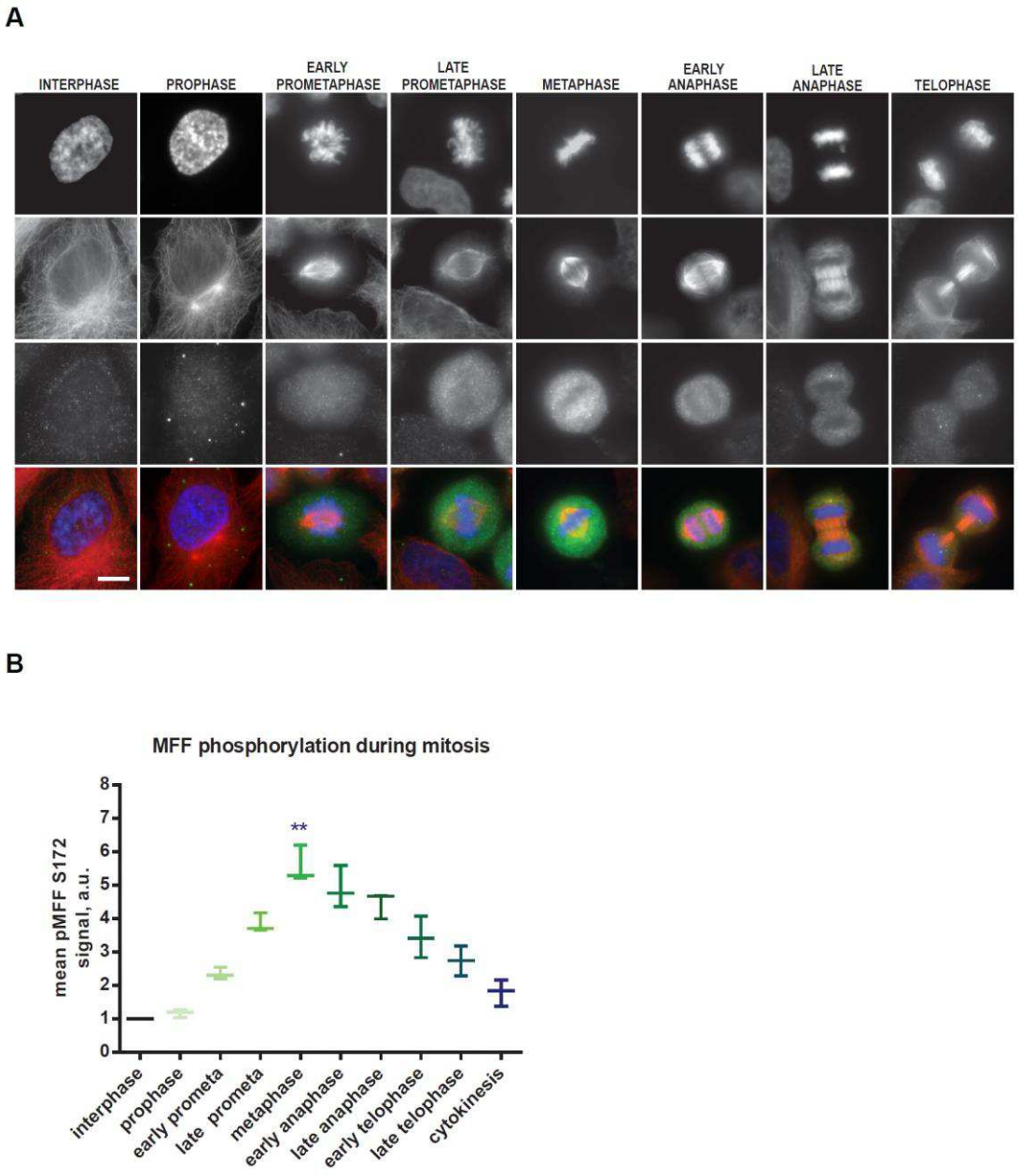

Figure 7. (A, B) La phosphorylation mitotique de MFF atteint un pic durant la métaphase des cellules HeLa. (A) Les images d'immunofluorescence des cellules HeLa synchronisées par un double blocage thymidine et recueilli 11 heures après synchronisation, temps correspondant au maximum de cellules en mitose. Les cellules ont été marquées avec un anticorps anti-pSer172 MFF, les chromosomes ont été marqués avec du DAPI. Barre d'échelle 10µm. **(B)** Quantification de l'intensité du signal de Ser172 pMFF. Pour chaque étape, l'intensité du signal a été quantifiée dans 10

cellules, 100 cellules par expérience. Les données représentent les moyennes ± SD de trois expériences indépendantes. **: p <0,01, par ANOVA à un facteur.

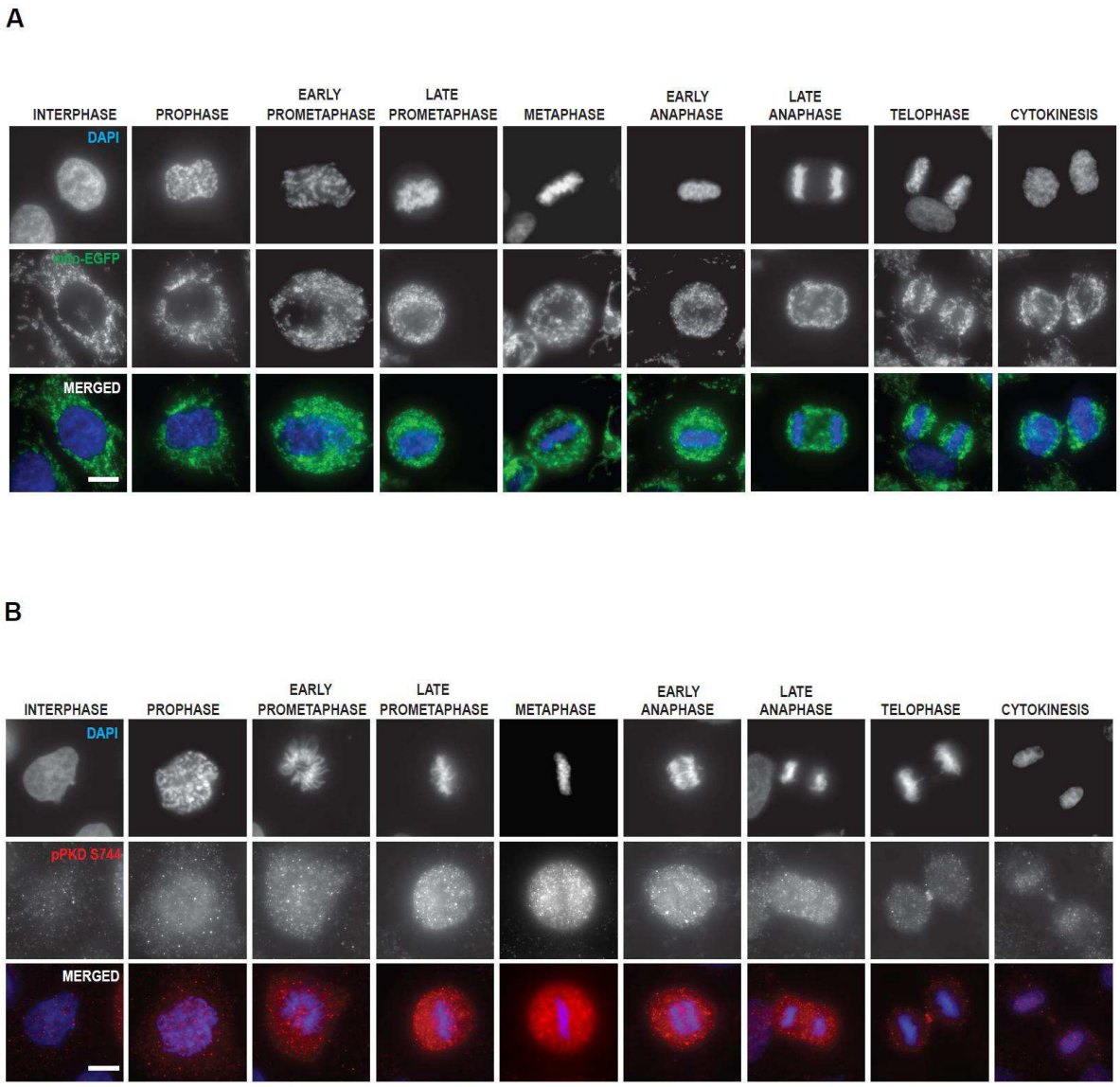

Figure 8. (A) Le réseau mitochondrial subit une fragmentation étendue pendant la mitose dans les cellules HeLa. Images en microscopie à fluorescence des cellules HeLa en interphase et pendant les différentes étapes de la mitose (comme indiqué). Les cellules HeLa expriment de manière stable la protéine de fusion MTS-EGFP, qui permet de visualiser les mitochondries, et les chromosomes sont marqués avec DAPI. Barre d'échelle 10µm. **(B) l'activité PKD est progressivement et spécifiquement augmentée au cours de la mitose.** Images d'immunofluorescence de cellules HeLa synchronisées par un double blocage thymidine et recueillies après 11 heures, ce qui correspond correspondant au maximum de cellules en mitose. Les cellules ont été marquées avec un anticorps anti-pSer744 PKD (marqueur d'activité PKD), les chromosomes ont été marqués avec DAPI. Différents stades mitotiques sont indiqués. Barre d'échelle 10µm.

Pour fournir des preuves génétiques, j'ai utilisé la technique d'édition de gène CRISPR/Cas9 pour invalider les trois membres de la famille des protéines kinase PKD dans les fibroblastes de souris (cellules NIH 3T3). L'analyse de la morphologie mitochondriale par microscopie à fluorescence a montré une diminution de 60% de la fragmentation mitochondriale dans les cellules déficientes pour PKD par rapport aux cellules témoins de type sauvage.

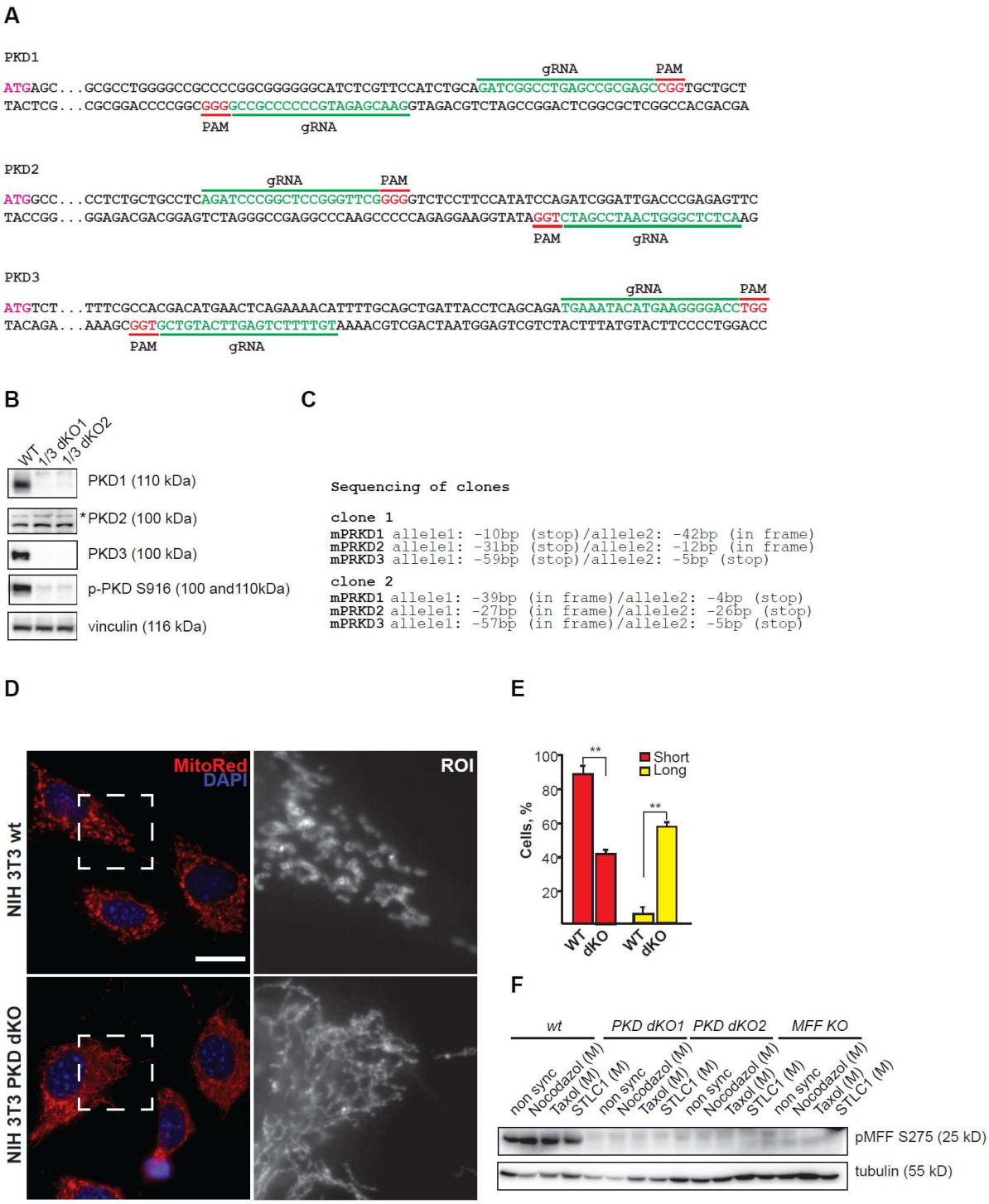

Figure 9. L'activité PKD est requise pour la fragmentation mitochondriale dans les cellules NIH 3T3. (A) Illustration explicative de la stratégie pour générer des cellules PKD-déficientes. Stratégie CRISPR / Cas9 ciblant des séquences génomiques des gènes PKD 1/2/3 en utilisant des paires d'ARN guide complémentaires. **(B)** Validation des clones choisis par western blot. Immunotransfert des lysats cellulaires provenant des cellules NIH 3T3 de type sauvage (WT) et PKD 1/3 double délétion (PKD dKO) stimulées pendant 1 heure avec du PMA. Des anticorps dirigés contre la protéine PKD1 totale, phospho-PKD1 / 2 (Ser916), la protéine PKD2 totale, la protéine PKD3 totale et la vinculine ont été utilisés pour détecter les protéines**. (C)** Validation des clones choisis par séquençage. **(D)** Images de microscopie à fluorescence des mitochondries dans les cellules WT et PKD 1/3 dKO NIH 3T3. Barre d'échelle: 20 µm. **(E)** Quantification de la morphologie mitochondriale des cellules montrées en (D) en deux catégories: courtes (<5 µm), longues (> 5 µm). Pour chaque groupe, au moins 100 cellules ont été comptées. Les données sont représentées comme la moyenne ± SD de trois expériences indépendantes. **: p <0,01, par test t non apparié. **(F)** L'activité de PKD est requise pour la phosphorylation mitotique de MFF. Immunotransfert des lysats cellulaires provenant de cellules NIH 3T3 de type sauvage (WT), PKD 1/3 dKO et de fibroblastes embryoniques murins (MEFs) dont le gène codant pour MFF a été délèté. Les MEFS n'ont pas été synchronisés ou synchronisés en mitose en utilisant le nocodazole, le taxol ou le STLC pendant 14 heures. Des anticorps dirigés contre phospho-MFF (Ser275) et la tubuline ont été utilisés pour détecter les protéines respectives. Résultats représentatifs de deux expériences indépendantes.

Ensuite, j'ai examiné l'impact physiologique de l'inactivation de PKD sur la dynamique mitochondriale. Pour ce faire j'ai utilisé trois inhibiteurs, structurellement indépendants, de l'activité de PKD dans les cellules humaines et murines. L'inhibition pharmacologiques de PKD a entraîné une réduction significative de la fission mitochondriale, mise en évidence par microscopie confocale (Fig. 10).

Pour tester la pertinence de l'axe PKD-MFF dans le contexte du cancer, j'ai décidé de réaliser mes expériences sur les cellules cancéreuses pancréatiques PANC1. La lignée cellulaire PANC1 est dérivée d'un carcinome pancréatique d'origine canalaire et est un modèle établi pour le cancer du pancréas. Ces cellules sont caractérisées par une expression et une activité élevées de PKD. J'ai d'abord analysé la morphologie mitochondriale par immunomarquage. Les cellules PANC1 présentaient des niveaux élevés de fragmentation mitochondriale basale. Le taux de fission mitochondriale élevé est fortement corrélé avec le niveau accru d'activité PKD dans ces cellules. L'inhibition pharmacologique de la PKD a entraîné une réduction drastique de la fragmentation mitochondriale, associée à une mort cellulaire plus grande (Fig. 11).

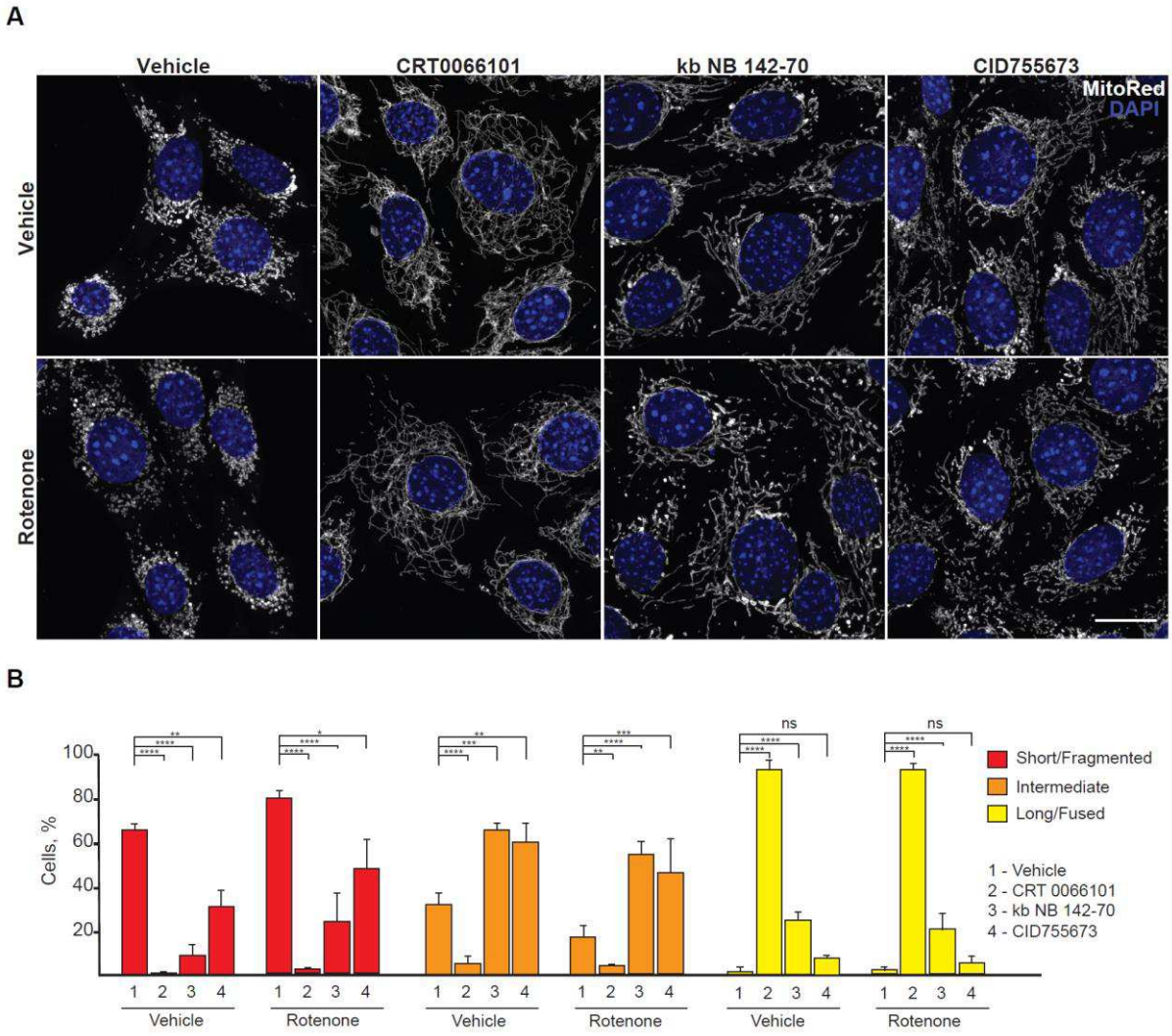

Figure 10. L'activité PKD est requise pour la fission mitochondriale dans les cellules NIH 3T3 de souris. (A) Images de microscopie confocale à fluorescence de cellules NIH 3T3 traitées avec le véhicule (DMSO) ou l'un des trois inhibiteurs de PKD différents (10µM CRT 0066101, 10 µM kb-NB 142-70 ou 30µM CID 755673) en combinaison avec le véhicule ou 1µM roténone. Les mitochondries ont été marquées avec du "MitoTracker Red" (pseudocoloré en blanc) et les noyaux ont été marqués avec du DAPI. Barre d'échelle: 20 µm. **(B)** Quantification de la morphologie mitochondriale des cellules présentées en (A). La forme mitochondriale a été classée comme fragmentée (pas de forme claire, moins de 2µm de long), intermédiaire (2µm - 5µm de long) ou longue (tubulaire ou fusionnée, plus de 5µm) et exprimée en pourcentage de cellules selon la catégorie respective des mitochondries. Pour chaque groupe, au moins 300 cellules ont été comptées. Les données sont représentées comme la moyenne ± SD de trois expériences indépendantes. ****: p <0,0001, par ANOVA à deux voies en utilisant le test de comparaison multiple de Dunnett.

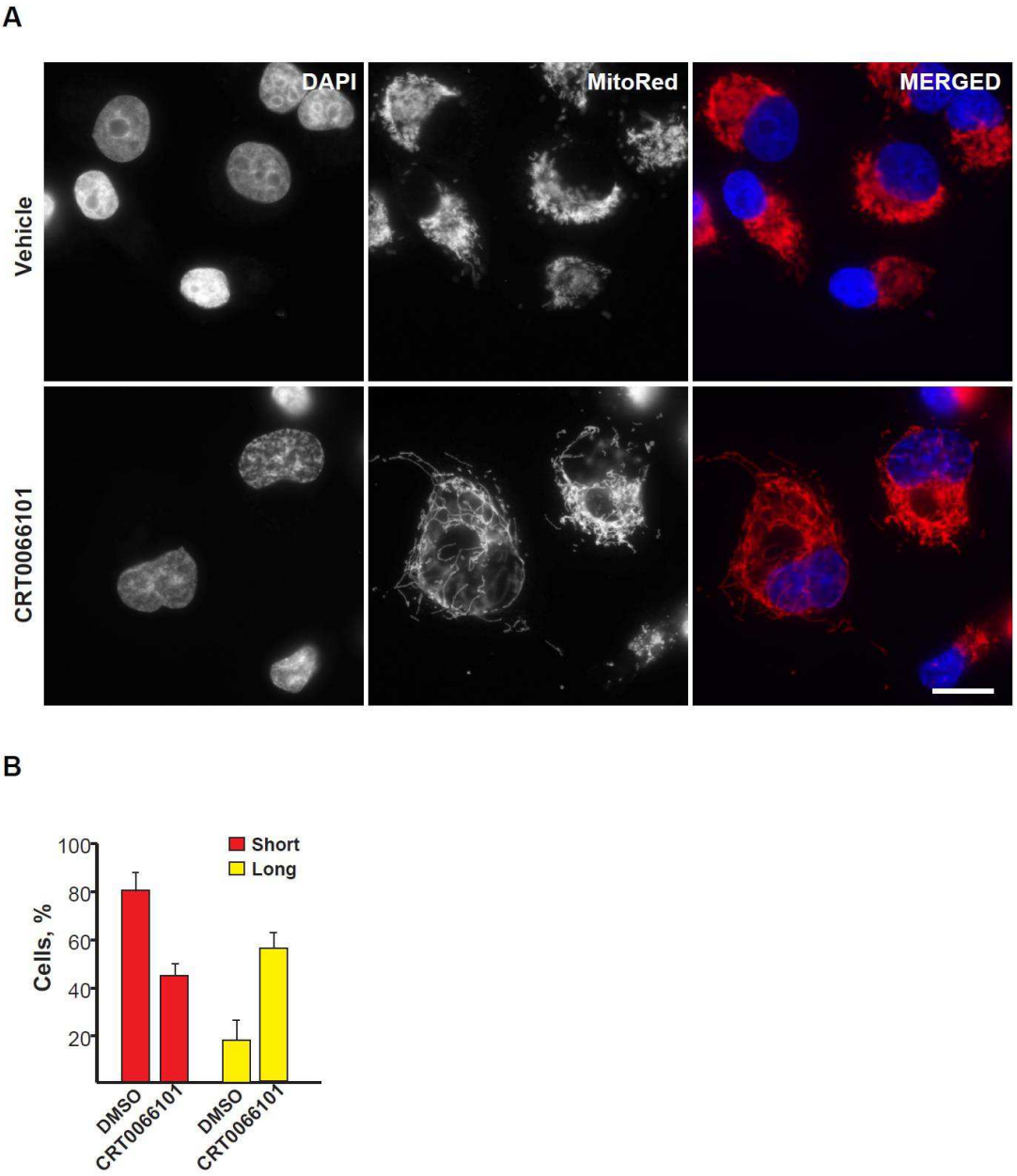

Figure 11. L'inhibition de PKD réduit le taux de fission mitochondriale dans les cellules cancéreuses pancréatiques PANC1. (A) Images de microscopie à fluorescence de cellules PANC1 traitées avec un véhicule (DMSO) ou un inhibiteur de PKD (10 µM CRT 0066101) pendant 14 heures. Les mitochondries ont été marqueées avec du "MitoTracker Red" et les noyaux ont été marquées avec du DAPI. Barre d'échelle: 20 µm. **(B)** Quantification de la morphologie mitochondriale des cellules présentées en (A). La forme mitochondriale a été classée comme courte (ronde ou en forme de tige, 2-5µm de long), ou long (tubulaire ou fusionné, plus de 5µm de long) et exprimée en pourcentage de cellules selon la catégorie respective des mitochondries. Pour chaque groupe, au moins 100 cellules ont été comptées. Les données sont représentées comme la moyenne ± SD de deux expériences indépendantes.

Conclusions

Dans l'ensemble, mon travail a permis de révéler un mécanisme dans lequel la phosphorylation du MFF médiée par PKD déclenche la fragmentation mitochondriale spécifiquement au cours la mitose. À ce jour, il s'agit du premier substrat de PKD à être phosphorylé au cours de la mitose, établissant un nouveau rôle pour PKD en tant que kinase mitotique. La dépendance de ce processus à la protéine PKD pourrait expliquer l'augmentation de l'expression des protéines de PKD dans le cancer. Elle pourrait aussi fournir une justification pour l'inhibition de PKD dans certains types de cancer caractérisés par une fragmentation mitochondriale élevée et un cycle cellulaire rapide. Ainsi, la régulation PKD-dépendante de la dynamique mitochondriale pourrait être importante dans la croissance et / ou dans la progression du cancer.

References

Acharya, U., Mallabiabarrena, A., Acharya, J.K., and Malhotra, V. (1998). Signaling via mitogen-activated protein kinase kinase (MEK1) is required for Golgi fragmentation during mitosis. Cell *92*, 183-192.

Aicart-Ramos, C., He, S.D., Land, M., and Rubin, C.S. (2016). A Novel Conserved Domain Mediates Dimerization of Protein Kinase D (PKD) Isoforms: DIMERIZATION IS ESSENTIAL FOR PKD-DEPENDENT REGULATION OF SECRETION AND INNATE IMMUNITY. J Biol Chem *291*, 23516-23531.

Alexander, C., Votruba, M., Pesch, U.E., Thiselton, D.L., Mayer, S., Moore, A., Rodriguez, M., Kellner, U., Leo-Kottler, B., Auburger, G.*, et al.* (2000). OPA1, encoding a dynamin-related GTPase, is mutated in autosomal dominant optic atrophy linked to chromosome 3q28. Nature genetics *26*, 211-215.

Alphey, L., Jimenez, J., and Glover, D. (1998). A Drosophila homologue of oxysterol binding protein (OSBP)--implications for the role of OSBP. Biochim Biophys Acta *1395*, 159-164.

Altan-Bonnet, N., Phair, R.D., Polishchuk, R.S., Weigert, R., and Lippincott-Schwartz, J. (2003). A role for Arf1 in mitotic Golgi disassembly, chromosome segregation, and cytokinesis. Proc Natl Acad Sci U S A *100*, 13314-13319.

Anderson, S., Bankier, A.T., Barrell, B.G., de Bruijn, M.H., Coulson, A.R., Drouin, J., Eperon, I.C., Nierlich, D.P., Roe, B.A., Sanger, F.*, et al.* (1981). Sequence and organization of the human mitochondrial genome. Nature *290*, 457-465.

Andrews, R.M., Kubacka, I., Chinnery, P.F., Lightowlers, R.N., Turnbull, D.M., and Howell, N. (1999). Reanalysis and revision of the Cambridge reference sequence for human mitochondrial DNA. Nature genetics *23*, 147.

Antes, A., Tappin, I., Chung, S., Lim, R., Lu, B., Parrott, A.M., Hill, H.Z., Suzuki, C.K., and Lee, C.G. (2010). Differential regulation of full-length genome and a single-stranded 7S DNA along the cell cycle in human mitochondria. Nucleic acids research *38*, 6466-6476.

Asencio, C., Davidson, I.F., Santarella-Mellwig, R., Ly-Hartig, T.B., Mall, M., Wallenfang, M.R., Mattaj, I.W., and Gorjanacz, M. (2012). Coordination of kinase and phosphatase activities by Lem4 enables nuclear envelope reassembly during mitosis. Cell *150*, 122-135.

Attardi, G., Chomyn, A., Montoya, J., and Ojala, D. (1982). Identification and mapping of human mitochondrial genes. Birth defects original article series *18*, 85-98.

Azoitei, N., Kleger, A., Schoo, N., Thal, D.R., Brunner, C., Pusapati, G.V., Filatova, A., Genze, F., Moller, P., Acker, T.*, et al.* (2011). Protein kinase D2 is a novel regulator of glioblastoma growth and tumor formation. Neuro-oncology *13*, 710-724.

Backer, J.S. (1995). New alleles of mgm1: a gene encoding a protein with a GTP-binding domain related to dynamin. Current genetics *28*, 499-501.

Bai, C., Sen, P., Hofmann, K., Ma, L., Goebl, M., Harper, J.W., and Elledge, S.J. (1996). SKP1 connects cell cycle regulators to the ubiquitin proteolysis machinery through a novel motif, the F-box. Cell *86*, 263-274.

Ball, E.H., and Singer, S.J. (1982). Mitochondria are associated with microtubules and not with intermediate filaments in cultured fibroblasts. Proc Natl Acad Sci U S A *79*, 123-126.

Baron, C.L., and Malhotra, V. (2002). Role of diacylglycerol in PKD recruitment to the TGN and protein transport to the plasma membrane. Science *295*, 325-328.

Barr, A.R., and Gergely, F. (2007). Aurora-A: the maker and breaker of spindle poles. J Cell Sci *120*, 2987-2996.

Barr, F.A., Puype, M., Vandekerckhove, J., and Warren, G. (1997). GRASP65, a protein involved in the stacking of Golgi cisternae. Cell *91*, 253-262.

Barr, F.A., and Short, B. (2003). Golgins in the structure and dynamics of the Golgi apparatus. Current opinion in cell biology *15*, 405-413.

Beg, Z.H., Allmann, D.W., and Gibson, D.M. (1973). Modulation of 3-hydroxy-3-methylglutaryl coenzyme A reductase activity with cAMP and wth protein fractions of rat liver cytosol. Biochem Biophys Res Commun *54*, 1362-1369.
Bitoun, M., Bevilacqua, J.A., Eymard, B., Prudhon, B., Fardeau, M., Guicheney, P., and Romero, N.B. (2009). A new centronuclear myopathy phenotype due to a novel dynamin 2 mutation. Neurology *72*, 93-95.
Bitoun, M., Bevilacqua, J.A., Prudhon, B., Maugenre, S., Taratuto, A.L., Monges, S., Lubieniecki, F., Cances, C., Uro-Coste, E., Mayer, M.*, et al.* (2007). Dynamin 2 mutations cause sporadic centronuclear myopathy with neonatal onset. Annals of neurology *62*, 666-670.
Bitoun, M., Maugenre, S., Jeannet, P.Y., Lacene, E., Ferrer, X., Laforet, P., Martin, J.J., Laporte, J., Lochmuller, H., Beggs, A.H.*, et al.* (2005). Mutations in dynamin 2 cause dominant centronuclear myopathy. Nature genetics *37*, 1207-1209.
Bjorklund, M.A., Vaahtomeri, K., Peltonen, K., Viollet, B., Makela, T.P., Band, A.M., and Laiho, M. (2010). Non-CDK-bound p27 (p27(NCDK)) is a marker for cell stress and is regulated through the Akt/PKB and AMPK-kinase pathways. Experimental cell research *316*, 762-774.
Bleazard, W., McCaffery, J.M., King, E.J., Bale, S., Mozdy, A., Tieu, Q., Nunnari, J., and Shaw, J.M. (1999). The dynamin-related GTPase Dnm1 regulates mitochondrial fission in yeast. Nat Cell Biol *1*, 298-304.
Bogenhagen, D., and Clayton, D.A. (1977). Mouse L cell mitochondrial DNA molecules are selected randomly for replication throughout the cell cycle. Cell *11*, 719-727.
Bossard, C., Bresson, D., Polishchuk, R.S., and Malhotra, V. (2007). Dimeric PKD regulates membrane fission to form transport carriers at the TGN. J Cell Biol *179*, 1123-1131.
Brindley, D.N., Pilquil, C., Sariahmetoglu, M., and Reue, K. (2009). Phosphatidate degradation: phosphatidate phosphatases (lipins) and lipid phosphate phosphatases. Biochim Biophys Acta *1791*, 956-961.
Britton, D., Zen, Y., Quaglia, A., Selzer, S., Mitra, V., Lobetaner, C., Jung, S., Bohm, G., Schmid, P., Prefot, P.*, et al.* (2014). Quantification of pancreatic cancer proteome and phosphorylome: indicates molecular events likely contributing to cancer and activity of drug targets. PLoS One *9*, e90948.
Brown, G.G., Gadaleta, G., Pepe, G., Saccone, C., and Sbisa, E. (1986). Structural conservation and variation in the D-loop-containing region of vertebrate mitochondrial DNA. J Mol Biol *192*, 503-511.
Bruinsma, W., Macurek, L., Freire, R., Lindqvist, A., and Medema, R.H. (2014). Bora and Aurora-A continue to activate Plk1 in mitosis. J Cell Sci *127*, 801-811.
Bui, H.T., Karren, M.A., Bhar, D., and Shaw, J.M. (2012). A novel motif in the yeast mitochondrial dynamin Dnm1 is essential for adaptor binding and membrane recruitment. J Cell Biol *199*, 613-622.
Bustillo-Zabalbeitia, I., Montessuit, S., Raemy, E., Basanez, G., Terrones, O., and Martinou, J.C. (2014). Specific interaction with cardiolipin triggers functional activation of Dynamin-Related Protein 1. PLoS One *9*, e102738.
Canto, C., and Auwerx, J. (2009). PGC-1alpha, SIRT1 and AMPK, an energy sensing network that controls energy expenditure. Current opinion in lipidology *20*, 98-105.
Capaldi, R.A., Aggeler, R., Gilkerson, R., Hanson, G., Knowles, M., Marcus, A., Margineantu, D., Marusich, M., Murray, J., Oglesbee, D.*, et al.* (2002). A replicating module as the unit of mitochondrial structure and functioning. Biochim Biophys Acta *1555*, 192-195.
Carlson, C.A., and Kim, K.H. (1973). Regulation of hepatic acetyl coenzyme A carboxylase by phosphorylation and dephosphorylation. J Biol Chem *248*, 378-380.
Chacinska, A. (2017). Cell biology: Sort and destroy. Nature *543*, 324-325.
Chang, S., Bezprozvannaya, S., Li, S., and Olson, E.N. (2005). An expression screen reveals modulators of class II histone deacetylase phosphorylation. Proc Natl Acad Sci U S A *102*, 8120-8125.
Chappie, J.S., Acharya, S., Liu, Y.W., Leonard, M., Pucadyil, T.J., and Schmid, S.L. (2009). An intramolecular signaling element that modulates dynamin function in vitro and in vivo. Mol Biol Cell *20*, 3561-3571.

Chappie, J.S., Mears, J.A., Fang, S., Leonard, M., Schmid, S.L., Milligan, R.A., Hinshaw, J.E., and Dyda, F. (2011). A pseudoatomic model of the dynamin polymer identifies a hydrolysis-dependent powerstroke. Cell *147*, 209-222.
Chatre, L., and Ricchetti, M. (2013). Prevalent coordination of mitochondrial DNA transcription and initiation of replication with the cell cycle. Nucleic acids research *41*, 3068-3078.
Chen, H., and Chan, D.C. (2010). Physiological functions of mitochondrial fusion. Annals of the New York Academy of Sciences *1201*, 21-25.
Chen, H., Chomyn, A., and Chan, D.C. (2005). Disruption of fusion results in mitochondrial heterogeneity and dysfunction. J Biol Chem *280*, 26185-26192.
Chen, H., Detmer, S.A., Ewald, A.J., Griffin, E.E., Fraser, S.E., and Chan, D.C. (2003). Mitofusins Mfn1 and Mfn2 coordinately regulate mitochondrial fusion and are essential for embryonic development. J Cell Biol *160*, 189-200.
Chen, H., McCaffery, J.M., and Chan, D.C. (2007). Mitochondrial fusion protects against neurodegeneration in the cerebellum. Cell *130*, 548-562.
Chen, H., Ren, S., Clish, C., Jain, M., Mootha, V., McCaffery, J.M., and Chan, D.C. (2015). Titration of mitochondrial fusion rescues Mff-deficient cardiomyopathy. J Cell Biol *211*, 795-805.
Chen, J., Deng, F., Li, J., and Wang, Q.J. (2008). Selective binding of phorbol esters and diacylglycerol by individual C1 domains of the PKD family. Biochem J *411*, 333-342.
Chen, L., Liu, T., Tran, A., Lu, X., Tomilov, A.A., Davies, V., Cortopassi, G., Chiamvimonvat, N., Bers, D.M., Votruba, M.*, et al.* (2012). OPA1 mutation and late-onset cardiomyopathy: mitochondrial dysfunction and mtDNA instability. J Am Heart Assoc *1*, e003012.
Chung, J.Y., Steen, J.A., and Schwarz, T.L. (2016). Phosphorylation-Induced Motor Shedding Is Required at Mitosis for Proper Distribution and Passive Inheritance of Mitochondria. Cell reports *16*, 2142-2155.
Corton, J.M., Gillespie, J.G., Hawley, S.A., and Hardie, D.G. (1995). 5-aminoimidazole-4-carboxamide ribonucleoside. A specific method for activating AMP-activated protein kinase in intact cells? European journal of biochemistry *229*, 558-565.
Coughlan, K.A., Valentine, R.J., Sudit, B.S., Allen, K., Dagon, Y., Kahn, B.B., Ruderman, N.B., and Saha, A.K. (2016). PKD1 Inhibits AMPKalpha2 through Phosphorylation of Serine 491 and Impairs Insulin Signaling in Skeletal Muscle Cells. J Biol Chem *291*, 5664-5675.
Cowell, C.F., Yan, I.K., Eiseler, T., Leightner, A.C., Doppler, H., and Storz, P. (2009). Loss of cell-cell contacts induces NF-kappaB via RhoA-mediated activation of protein kinase D1. J Cell Biochem *106*, 714-728.
Davies, V.J., Hollins, A.J., Piechota, M.J., Yip, W., Davies, J.R., White, K.E., Nicols, P.P., Boulton, M.E., and Votruba, M. (2007). Opa1 deficiency in a mouse model of autosomal dominant optic atrophy impairs mitochondrial morphology, optic nerve structure and visual function. Human molecular genetics *16*, 1307-1318.
Delettre, C., Lenaers, G., Griffoin, J.M., Gigarel, N., Lorenzo, C., Belenguer, P., Pelloquin, L., Grosgeorge, J., Turc-Carel, C., Perret, E.*, et al.* (2000). Nuclear gene OPA1, encoding a mitochondrial dynamin-related protein, is mutated in dominant optic atrophy. Nature genetics *26*, 207-210.
Dequiedt, F., Van Lint, J., Lecomte, E., Van Duppen, V., Seufferlein, T., Vandenheede, J.R., Wattiez, R., and Kettmann, R. (2005). Phosphorylation of histone deacetylase 7 by protein kinase D mediates T cell receptor-induced Nur77 expression and apoptosis. J Exp Med *201*, 793-804.
Doda, J.N., Wright, C.T., and Clayton, D.A. (1981). Elongation of displacement-loop strands in human and mouse mitochondrial DNA is arrested near specific template sequences. Proc Natl Acad Sci U S A *78*, 6116-6120.
Doppler, H., and Storz, P. (2007). A novel tyrosine phosphorylation site in protein kinase D contributes to oxidative stress-mediated activation. J Biol Chem *282*, 31873-31881.
Doppler, H., Storz, P., Li, J., Comb, M.J., and Toker, A. (2005). A phosphorylation state-specific antibody recognizes Hsp27, a novel substrate of protein kinase D. J Biol Chem *280*, 15013-15019.
Ducommun, S., Deak, M., Sumpton, D., Ford, R.J., Nunez Galindo, A., Kussmann, M., Viollet, B., Steinberg, G.R., Foretz, M., Dayon, L.*, et al.* (2015). Motif affinity and mass spectrometry proteomic approach for the discovery of cellular AMPK targets: identification of mitochondrial fission factor as a new AMPK substrate. Cell Signal *27*, 978-988.

Dykens, J.A., Jamieson, J., Marroquin, L., Nadanaciva, S., Billis, P.A., and Will, Y. (2008). Biguanide-induced mitochondrial dysfunction yields increased lactate production and cytotoxicity of aerobically-poised HepG2 cells and human hepatocytes in vitro. Toxicology and applied pharmacology *233*, 203-210.
Egan, D., Kim, J., Shaw, R.J., and Guan, K.L. (2011). The autophagy initiating kinase ULK1 is regulated via opposing phosphorylation by AMPK and mTOR. Autophagy *7*, 643-644.
Ekena, K., and Stevens, T.H. (1995). The Saccharomyces cerevisiae MVP1 gene interacts with VPS1 and is required for vacuolar protein sorting. Mol Cell Biol *15*, 1671-1678.
Ellenberg, J., Siggia, E.D., Moreira, J.E., Smith, C.L., Presley, J.F., Worman, H.J., and Lippincott-Schwartz, J. (1997). Nuclear membrane dynamics and reassembly in living cells: targeting of an inner nuclear membrane protein in interphase and mitosis. J Cell Biol *138*, 1193-1206.
Emanuele, M.J., Lan, W., Jwa, M., Miller, S.A., Chan, C.S., and Stukenberg, P.T. (2008). Aurora B kinase and protein phosphatase 1 have opposing roles in modulating kinetochore assembly. J Cell Biol *181*, 241-254.
Faelber, K., Posor, Y., Gao, S., Held, M., Roske, Y., Schulze, D., Haucke, V., Noe, F., and Daumke, O. (2011). Crystal structure of nucleotide-free dynamin. Nature *477*, 556-560.
Fahrner, J.A., Liu, R., Perry, M.S., Klein, J., and Chan, D.C. (2016). A novel de novo dominant negative mutation in DNM1L impairs mitochondrial fission and presents as childhood epileptic encephalopathy. Am J Med Genet A *170*, 2002-2011.
Fan, S., Liu, B., Sun, L., Lv, X.B., Lin, Z., Chen, W., Chen, W., Tang, Q., Wang, Y., Su, Y.*, et al.* (2015). Mitochondrial fission determines cisplatin sensitivity in tongue squamous cell carcinoma through the BRCA1-miR-593-5p-MFF axis. Oncotarget *6*, 14885-14904.
Feinstein, T.N., and Linstedt, A.D. (2007). Mitogen-activated protein kinase kinase 1-dependent Golgi unlinking occurs in G2 phase and promotes the G2/M cell cycle transition. Mol Biol Cell *18*, 594-604.
Feng, H., Ren, M., Chen, L., and Rubin, C.S. (2007). Properties, regulation, and in vivo functions of a novel protein kinase D: Caenorhabditis elegans DKF-2 links diacylglycerol second messenger to the regulation of stress responses and life span. J Biol Chem *282*, 31273-31288.
Ferguson, S.M., and De Camilli, P. (2012). Dynamin, a membrane-remodelling GTPase. Nature reviews Molecular cell biology *13*, 75-88.
Fielitz, J., Kim, M.S., Shelton, J.M., Qi, X., Hill, J.A., Richardson, J.A., Bassel-Duby, R., and Olson, E.N. (2008). Requirement of protein kinase D1 for pathological cardiac remodeling. Proc Natl Acad Sci U S A *105*, 3059-3063.
Fischle, W., Tseng, B.S., Dormann, H.L., Ueberheide, B.M., Garcia, B.A., Shabanowitz, J., Hunt, D.F., Funabiki, H., and Allis, C.D. (2005). Regulation of HP1-chromatin binding by histone H3 methylation and phosphorylation. Nature *438*, 1116-1122.
Ford, M.G., Jenni, S., and Nunnari, J. (2011). The crystal structure of dynamin. Nature *477*, 561-566.
Fransson, A., Ruusala, A., and Aspenstrom, P. (2003). Atypical Rho GTPases have roles in mitochondrial homeostasis and apoptosis. J Biol Chem *278*, 6495-6502.
Fransson, S., Ruusala, A., and Aspenstrom, P. (2006). The atypical Rho GTPases Miro-1 and Miro-2 have essential roles in mitochondrial trafficking. Biochem Biophys Res Commun *344*, 500-510.
Franz-Wachtel, M., Eisler, S.A., Krug, K., Wahl, S., Carpy, A., Nordheim, A., Pfizenmaier, K., Hausser, A., and Macek, B. (2012). Global detection of protein kinase D-dependent phosphorylation events in nocodazole-treated human cells. Mol Cell Proteomics *11*, 160-170.
Friedman, J.R., Lackner, L.L., West, M., DiBenedetto, J.R., Nunnari, J., and Voeltz, G.K. (2011). ER tubules mark sites of mitochondrial division. Science *334*, 358-362.
Frohlich, C., Grabiger, S., Schwefel, D., Faelber, K., Rosenbaum, E., Mears, J., Rocks, O., and Daumke, O. (2013). Structural insights into oligomerization and mitochondrial remodelling of dynamin 1-like protein. EMBO J *32*, 1280-1292.
Fuchs, Y.F., Eisler, S.A., Link, G., Schlicker, O., Bunt, G., Pfizenmaier, K., and Hausser, A. (2009). A Golgi PKD activity reporter reveals a crucial role of PKD in nocodazole-induced Golgi dispersal. Traffic *10*, 858-867.

Fugmann, T., Hausser, A., Schoffler, P., Schmid, S., Pfizenmaier, K., and Olayioye, M.A. (2007). Regulation of secretory transport by protein kinase D-mediated phosphorylation of the ceramide transfer protein. J Cell Biol *178*, 15-22.
Gandre-Babbe, S., and van der Bliek, A.M. (2008). The novel tail-anchored membrane protein Mff controls mitochondrial and peroxisomal fission in mammalian cells. Mol Biol Cell *19*, 2402-2412.
Gehart, H., Goginashvili, A., Beck, R., Morvan, J., Erbs, E., Formentini, I., De Matteis, M.A., Schwab, Y., Wieland, F.T., and Ricci, R. (2012). The BAR domain protein Arfaptin-1 controls secretory granule biogenesis at the trans-Golgi network. Dev Cell *23*, 756-768.
Gelens, L., Qian, J., Bollen, M., and Saurin, A.T. (2018). The Importance of Kinase-Phosphatase Integration: Lessons from Mitosis. Trends Cell Biol *28*, 6-21.
Glater, E.E., Megeath, L.J., Stowers, R.S., and Schwarz, T.L. (2006). Axonal transport of mitochondria requires milton to recruit kinesin heavy chain and is light chain independent. J Cell Biol *173*, 545-557.
Glover, D.M., Leibowitz, M.H., McLean, D.A., and Parry, H. (1995). Mutations in aurora prevent centrosome separation leading to the formation of monopolar spindles. Cell *81*, 95-105.
Goginashvili, A., Zhang, Z., Erbs, E., Spiegelhalter, C., Kessler, P., Mihlan, M., Pasquier, A., Krupina, K., Schieber, N., Cinque, L.*, et al.* (2015). Insulin granules. Insulin secretory granules control autophagy in pancreatic beta cells. Science *347*, 878-882.
Goni, F.M., and Alonso, A. (1999). Structure and functional properties of diacylglycerols in membranes. Prog Lipid Res *38*, 1-48.
Goransson, O., McBride, A., Hawley, S.A., Ross, F.A., Shpiro, N., Foretz, M., Viollet, B., Hardie, D.G., and Sakamoto, K. (2007). Mechanism of action of A-769662, a valuable tool for activation of AMP-activated protein kinase. J Biol Chem *282*, 32549-32560.
Gorsich, S.W., and Shaw, J.M. (2004). Importance of mitochondrial dynamics during meiosis and sporulation. Mol Biol Cell *15*, 4369-4381.
Graham, T.R., and Burd, C.G. (2011). Coordination of Golgi functions by phosphatidylinositol 4-kinases. Trends Cell Biol *21*, 113-121.
Gray, M.W., Burger, G., and Lang, B.F. (1999). Mitochondrial evolution. Science *283*, 1476-1481.
Grigoriev, I., Gouveia, S.M., van der Vaart, B., Demmers, J., Smyth, J.T., Honnappa, S., Splinter, D., Steinmetz, M.O., Putney, J.W., Jr., Hoogenraad, C.C.*, et al.* (2008). STIM1 is a MT-plus-end-tracking protein involved in remodeling of the ER. Current biology : CB *18*, 177-182.
Guha, S., Tanasanvimon, S., Sinnett-Smith, J., and Rozengurt, E. (2010). Role of protein kinase D signaling in pancreatic cancer. Biochemical pharmacology *80*, 1946-1954.
Guizzunti, G., and Seemann, J. (2016). Mitotic Golgi disassembly is required for bipolar spindle formation and mitotic progression. Proc Natl Acad Sci U S A *113*, E6590-E6599.
Guri, Y., Colombi, M., Dazert, E., Hindupur, S.K., Roszik, J., Moes, S., Jenoe, P., Heim, M.H., Riezman, I., Riezman, H.*, et al.* (2017). mTORC2 Promotes Tumorigenesis via Lipid Synthesis. Cancer cell *32*, 807-823 e812.
Gwinn, D.M., Shackelford, D.B., Egan, D.F., Mihaylova, M.M., Mery, A., Vasquez, D.S., Turk, B.E., and Shaw, R.J. (2008). AMPK phosphorylation of raptor mediates a metabolic checkpoint. Mol Cell *30*, 214-226.
Hammond, A.T., and Glick, B.S. (2000). Dynamics of transitional endoplasmic reticulum sites in vertebrate cells. Mol Biol Cell *11*, 3013-3030.
Hanada, K., Kumagai, K., Tomishige, N., and Yamaji, T. (2009). CERT-mediated trafficking of ceramide. Biochim Biophys Acta *1791*, 684-691.
Hanai, A., Ohgi, M., Yagi, C., Ueda, T., Shin, H.W., and Nakayama, K. (2016). Class I Arfs (Arf1 and Arf3) and Arf6 are localized to the Flemming body and play important roles in cytokinesis. Journal of biochemistry *159*, 201-208.
Hannak, E., Kirkham, M., Hyman, A.A., and Oegema, K. (2001). Aurora-A kinase is required for centrosome maturation in Caenorhabditis elegans. J Cell Biol *155*, 1109-1116.
Harding, A., Giles, N., Burgess, A., Hancock, J.F., and Gabrielli, B.G. (2003). Mechanism of mitosis-specific activation of MEK1. J Biol Chem *278*, 16747-16754.
Harikumar, K.B., Kunnumakkara, A.B., Ochi, N., Tong, Z., Deorukhkar, A., Sung, B., Kelland, L., Jamieson, S., Sutherland, R., Raynham, T.*, et al.* (2010). A novel small-molecule inhibitor of protein

kinase D blocks pancreatic cancer growth in vitro and in vivo. Molecular cancer therapeutics *9*, 1136-1146.
Hausser, A., Storz, P., Martens, S., Link, G., Toker, A., and Pfizenmaier, K. (2005). Protein kinase D regulates vesicular transport by phosphorylating and activating phosphatidylinositol-4 kinase IIIbeta at the Golgi complex. Nat Cell Biol *7*, 880-886.
Hawley, S.A., Boudeau, J., Reid, J.L., Mustard, K.J., Udd, L., Makela, T.P., Alessi, D.R., and Hardie, D.G. (2003). Complexes between the LKB1 tumor suppressor, STRAD alpha/beta and MO25 alpha/beta are upstream kinases in the AMP-activated protein kinase cascade. Journal of biology *2*, 28.
Hawley, S.A., Pan, D.A., Mustard, K.J., Ross, L., Bain, J., Edelman, A.M., Frenguelli, B.G., and Hardie, D.G. (2005). Calmodulin-dependent protein kinase kinase-beta is an alternative upstream kinase for AMP-activated protein kinase. Cell metabolism *2*, 9-19.
Heggeness, M.H., Simon, M., and Singer, S.J. (1978). Association of mitochondria with microtubules in cultured cells. Proc Natl Acad Sci U S A *75*, 3863-3866.
Herzog, F., Primorac, I., Dube, P., Lenart, P., Sander, B., Mechtler, K., Stark, H., and Peters, J.M. (2009). Structure of the anaphase-promoting complex/cyclosome interacting with a mitotic checkpoint complex. Science *323*, 1477-1481.
Iborra, F.J., Kimura, H., and Cook, P.R. (2004). The functional organization of mitochondrial genomes in human cells. BMC biology *2*, 9.
Iglesias, T., and Rozengurt, E. (1998). Protein kinase D activation by mutations within its pleckstrin homology domain. J Biol Chem *273*, 410-416.
Inoki, K., Zhu, T., and Guan, K.L. (2003). TSC2 mediates cellular energy response to control cell growth and survival. Cell *115*, 577-590.
Ishihara, N., Nomura, M., Jofuku, A., Kato, H., Suzuki, S.O., Masuda, K., Otera, H., Nakanishi, Y., Nonaka, I., Goto, Y.*, et al.* (2009). Mitochondrial fission factor Drp1 is essential for embryonic development and synapse formation in mice. Nat Cell Biol *11*, 958-966.
Ishihara, T., Ban-Ishihara, R., Maeda, M., Matsunaga, Y., Ichimura, A., Kyogoku, S., Aoki, H., Katada, S., Nakada, K., Nomura, M.*, et al.* (2015). Dynamics of mitochondrial DNA nucleoids regulated by mitochondrial fission is essential for maintenance of homogeneously active mitochondria during neonatal heart development. Mol Cell Biol *35*, 211-223.
Ittner, A., Block, H., Reichel, C.A., Varjosalo, M., Gehart, H., Sumara, G., Gstaiger, M., Krombach, F., Zarbock, A., and Ricci, R. (2012). Regulation of PTEN activity by p38delta-PKD1 signaling in neutrophils confers inflammatory responses in the lung. J Exp Med *209*, 2229-2246.
Izawa, D., and Pines, J. (2015). The mitotic checkpoint complex binds a second CDC20 to inhibit active APC/C. Nature *517*, 631-634.
Jaggi, M., Rao, P.S., Smith, D.J., Wheelock, M.J., Johnson, K.R., Hemstreet, G.P., and Balaji, K.C. (2005). E-cadherin phosphorylation by protein kinase D1/protein kinase C{mu} is associated with altered cellular aggregation and motility in prostate cancer. Cancer Res *65*, 483-492.
Jat, P.S., Cepko, C.L., Mulligan, R.C., and Sharp, P.A. (1986). Recombinant retroviruses encoding simian virus 40 large T antigen and polyomavirus large and middle T antigens. Mol Cell Biol *6*, 1204-1217.
Jensen, E.D., Gopalakrishnan, R., and Westendorf, J.J. (2009). Bone morphogenic protein 2 activates protein kinase D to regulate histone deacetylase 7 localization and repression of Runx2. J Biol Chem *284*, 2225-2234.
Jesch, S.A., Mehta, A.J., Velliste, M., Murphy, R.F., and Linstedt, A.D. (2001). Mitotic Golgi is in a dynamic equilibrium between clustered and free vesicles independent of the ER. Traffic *2*, 873-884.
Jhun, B.S., J, O.U., Adaniya, S.M., Mancini, T.J., Cao, J.L., King, M.E., Landi, A.K., Ma, H., Shin, M., Yang, D.*, et al.* (2018). Protein kinase D activation induces mitochondrial fragmentation and dysfunction in cardiomyocytes. The Journal of physiology.
Jones, R.G., Plas, D.R., Kubek, S., Buzzai, M., Mu, J., Xu, Y., Birnbaum, M.J., and Thompson, C.B. (2005). AMP-activated protein kinase induces a p53-dependent metabolic checkpoint. Mol Cell *18*, 283-293.

Jongsma, M.L., Berlin, I., and Neefjes, J. (2015). On the move: organelle dynamics during mitosis. Trends Cell Biol *25*, 112-124.
Kanfer, G., Courtheoux, T., Peterka, M., Meier, S., Soste, M., Melnik, A., Reis, K., Aspenstrom, P., Peter, M., Picotti, P.*, et al.* (2015). Mitotic redistribution of the mitochondrial network by Miro and Cenp-F. Nature communications *6*, 8015.
Kano, F., Takenaka, K., Yamamoto, A., Nagayama, K., Nishida, E., and Murata, M. (2000). MEK and Cdc2 kinase are sequentially required for Golgi disassembly in MDCK cells by the mitotic Xenopus extracts. J Cell Biol *149*, 357-368.
Kashatus, D.F., Lim, K.H., Brady, D.C., Pershing, N.L., Cox, A.D., and Counter, C.M. (2011). RALA and RALBP1 regulate mitochondrial fission at mitosis. Nat Cell Biol *13*, 1108-1115.
Kemper, C., Habib, S.J., Engl, G., Heckmeyer, P., Dimmer, K.S., and Rapaport, D. (2008). Integration of tail-anchored proteins into the mitochondrial outer membrane does not require any known import components. J Cell Sci *121*, 1990-1998.
Kettenbach, A.N., Schweppe, D.K., Faherty, B.K., Pechenick, D., Pletnev, A.A., and Gerber, S.A. (2011). Quantitative phosphoproteomics identifies substrates and functional modules of Aurora and Polo-like kinase activities in mitotic cells. Sci Signal *4*, rs5.
Kienzle, C., Eisler, S.A., Villeneuve, J., Brummer, T., Olayioye, M.A., and Hausser, A. (2013). PKD controls mitotic Golgi complex fragmentation through a Raf-MEK1 pathway. Mol Biol Cell *24*, 222-233.
Kim, J., Kundu, M., Viollet, B., and Guan, K.L. (2011). AMPK and mTOR regulate autophagy through direct phosphorylation of Ulk1. Nat Cell Biol *13*, 132-141.
King, N.P., Lee, T.M., Sawaya, M.R., Cascio, D., and Yeates, T.O. (2008). Structures and functional implications of an AMP-binding cystathionine beta-synthase domain protein from a hyperthermophilic archaeon. J Mol Biol *380*, 181-192.
King, R.W., Peters, J.M., Tugendreich, S., Rolfe, M., Hieter, P., and Kirschner, M.W. (1995). A 20S complex containing CDC27 and CDC16 catalyzes the mitosis-specific conjugation of ubiquitin to cyclin B. Cell *81*, 279-288.
Koch, J., Feichtinger, R.G., Freisinger, P., Pies, M., Schrodl, F., Iuso, A., Sperl, W., Mayr, J.A., Prokisch, H., and Haack, T.B. (2016). Disturbed mitochondrial and peroxisomal dynamics due to loss of MFF causes Leigh-like encephalopathy, optic atrophy and peripheral neuropathy. J Med Genet *53*, 270-278.
Krumpe, K., Frumkin, I., Herzig, Y., Rimon, N., Ozbalci, C., Brugger, B., Rapaport, D., and Schuldiner, M. (2012). Ergosterol content specifies targeting of tail-anchored proteins to mitochondrial outer membranes. Mol Biol Cell *23*, 3927-3935.
Kudo, N., Kumagai, K., Matsubara, R., Kobayashi, S., Hanada, K., Wakatsuki, S., and Kato, R. (2010). Crystal structures of the CERT START domain with inhibitors provide insights into the mechanism of ceramide transfer. J Mol Biol *396*, 245-251.
Kukat, C., Wurm, C.A., Spahr, H., Falkenberg, M., Larsson, N.G., and Jakobs, S. (2011). Super-resolution microscopy reveals that mammalian mitochondrial nucleoids have a uniform size and frequently contain a single copy of mtDNA. Proc Natl Acad Sci U S A *108*, 13534-13539.
Labrousse, A.M., Zappaterra, M.D., Rube, D.A., and van der Bliek, A.M. (1999). C. elegans dynamin-related protein DRP-1 controls severing of the mitochondrial outer membrane. Mol Cell *4*, 815-826.
Lakin, N.D., and Jackson, S.P. (1999). Regulation of p53 in response to DNA damage. Oncogene *18*, 7644-7655.
Lane, J.D., and Allan, V.J. (1999). Microtubule-based endoplasmic reticulum motility in Xenopus laevis: activation of membrane-associated kinesin during development. Mol Biol Cell *10*, 1909-1922.
Lane, N., and Martin, W. (2010). The energetics of genome complexity. Nature *467*, 929-934.
Laplante, M., and Sabatini, D.M. (2012). mTOR signaling in growth control and disease. Cell *149*, 274-293.
Lee, J.E., Westrate, L.M., Wu, H., Page, C., and Voeltz, G.K. (2016). Multiple dynamin family members collaborate to drive mitochondrial division. Nature *540*, 139-143.

Lee, S., Kim, S., Sun, X., Lee, J.H., and Cho, H. (2007). Cell cycle-dependent mitochondrial biogenesis and dynamics in mammalian cells. Biochem Biophys Res Commun *357*, 111-117.
Legros, F., Malka, F., Frachon, P., Lombes, A., and Rojo, M. (2004). Organization and dynamics of human mitochondrial DNA. J Cell Sci *117*, 2653-2662.
Letellier, T., Heinrich, R., Malgat, M., and Mazat, J.P. (1994). The kinetic basis of threshold effects observed in mitochondrial diseases: a systemic approach. Biochem J *302 (Pt 1)*, 171-174.
Lewis, M.R., and Lewis, W.H. (1914). Mitochondria in Tissue Culture. Science *39*, 330-333.
Lewis, S.C., Uchiyama, L.F., and Nunnari, J. (2016). ER-mitochondria contacts couple mtDNA synthesis with mitochondrial division in human cells. Science *353*, aaf5549.
Liang, J., Shao, S.H., Xu, Z.X., Hennessy, B., Ding, Z., Larrea, M., Kondo, S., Dumont, D.J., Gutterman, J.U., Walker, C.L.*, et al.* (2007). The energy sensing LKB1-AMPK pathway regulates p27(kip1) phosphorylation mediating the decision to enter autophagy or apoptosis. Nat Cell Biol *9*, 218-224.
Liljedahl, M., Maeda, Y., Colanzi, A., Ayala, I., Van Lint, J., and Malhotra, V. (2001). Protein kinase D regulates the fission of cell surface destined transport carriers from the trans-Golgi network. Cell *104*, 409-420.
Lim, K.H., Brady, D.C., Kashatus, D.F., Ancrile, B.B., Der, C.J., Cox, A.D., and Counter, C.M. (2010). Aurora-A phosphorylates, activates, and relocalizes the small GTPase RalA. Mol Cell Biol *30*, 508-523.
Lin, C.Y., Madsen, M.L., Yarm, F.R., Jang, Y.J., Liu, X., and Erikson, R.L. (2000). Peripheral Golgi protein GRASP65 is a target of mitotic polo-like kinase (Plk) and Cdc2. Proc Natl Acad Sci U S A *97*, 12589-12594.
Liu, D., Vader, G., Vromans, M.J., Lampson, M.A., and Lens, S.M. (2009). Sensing chromosome bi-orientation by spatial separation of aurora B kinase from kinetochore substrates. Science *323*, 1350-1353.
Liu, R., and Chan, D.C. (2015). The mitochondrial fission receptor Mff selectively recruits oligomerized Drp1. Mol Biol Cell *26*, 4466-4477.
Loson, O.C., Song, Z., Chen, H., and Chan, D.C. (2013). Fis1, Mff, MiD49, and MiD51 mediate Drp1 recruitment in mitochondrial fission. Mol Biol Cell *24*, 659-667.
Lowe, M., Rabouille, C., Nakamura, N., Watson, R., Jackman, M., Jamsa, E., Rahman, D., Pappin, D.J., and Warren, G. (1998). Cdc2 kinase directly phosphorylates the cis-Golgi matrix protein GM130 and is required for Golgi fragmentation in mitosis. Cell *94*, 783-793.
Lu, L., Ladinsky, M.S., and Kirchhausen, T. (2009). Cisternal organization of the endoplasmic reticulum during mitosis. Mol Biol Cell *20*, 3471-3480.
Lukas, C., Sorensen, C.S., Kramer, E., Santoni-Rugiu, E., Lindeneg, C., Peters, J.M., Bartek, J., and Lukas, J. (1999). Accumulation of cyclin B1 requires E2F and cyclin-A-dependent rearrangement of the anaphase-promoting complex. Nature *401*, 815-818.
Macaskill, A.F., Rinholm, J.E., Twelvetrees, A.E., Arancibia-Carcamo, I.L., Muir, J., Fransson, A., Aspenstrom, P., Attwell, D., and Kittler, J.T. (2009). Miro1 is a calcium sensor for glutamate receptor-dependent localization of mitochondria at synapses. Neuron *61*, 541-555.
Magnusson, J., Orth, M., Lestienne, P., and Taanman, J.W. (2003). Replication of mitochondrial DNA occurs throughout the mitochondria of cultured human cells. Experimental cell research *289*, 133-142.
Malhotra, V., and Campelo, F. (2011). PKD regulates membrane fission to generate TGN to cell surface transport carriers. Cold Spring Harb Perspect Biol *3*.
Margineantu, D.H., Gregory Cox, W., Sundell, L., Sherwood, S.W., Beechem, J.M., and Capaldi, R.A. (2002). Cell cycle dependent morphology changes and associated mitochondrial DNA redistribution in mitochondria of human cell lines. Mitochondrion *1*, 425-435.
Martinez-Diez, M., Santamaria, G., Ortega, A.D., and Cuezva, J.M. (2006). Biogenesis and dynamics of mitochondria during the cell cycle: significance of 3'UTRs. PLoS One *1*, e107.
Matthews, S.A., Navarro, M.N., Sinclair, L.V., Emslie, E., Feijoo-Carnero, C., and Cantrell, D.A. (2010). Unique functions for protein kinase D1 and protein kinase D2 in mammalian cells. Biochem J *432*, 153-163.

McGee, S.L., van Denderen, B.J., Howlett, K.F., Mollica, J., Schertzer, J.D., Kemp, B.E., and Hargreaves, M. (2008). AMP-activated protein kinase regulates GLUT4 transcription by phosphorylating histone deacetylase 5. Diabetes *57*, 860-867.
Mears, J.A., Lackner, L.L., Fang, S., Ingerman, E., Nunnari, J., and Hinshaw, J.E. (2011). Conformational changes in Dnm1 support a contractile mechanism for mitochondrial fission. Nature structural & molecular biology *18*, 20-26.
Meeusen, S., DeVay, R., Block, J., Cassidy-Stone, A., Wayson, S., McCaffery, J.M., and Nunnari, J. (2006). Mitochondrial inner-membrane fusion and crista maintenance requires the dynamin-related GTPase Mgm1. Cell *127*, 383-395.
Menendez-Benito, V., van Deventer, S.J., Jimenez-Garcia, V., Roy-Luzarraga, M., van Leeuwen, F., and Neefjes, J. (2013). Spatiotemporal analysis of organelle and macromolecular complex inheritance. Proc Natl Acad Sci U S A *110*, 175-180.
Merklinger, E., Gofman, Y., Kedrov, A., Driessen, A.J., Ben-Tal, N., Shai, Y., and Rapaport, D. (2012). Membrane integration of a mitochondrial signal-anchored protein does not require additional proteinaceous factors. Biochem J *442*, 381-389.
Mertins, P., Mani, D.R., Ruggles, K.V., Gillette, M.A., Clauser, K.R., Wang, P., Wang, X., Qiao, J.W., Cao, S., Petralia, F.*, et al.* (2016). Proteogenomics connects somatic mutations to signalling in breast cancer. Nature *534*, 55-62.
Mihaylova, M.M., Vasquez, D.S., Ravnskjaer, K., Denechaud, P.D., Yu, R.T., Alvarez, J.G., Downes, M., Evans, R.M., Montminy, M., and Shaw, R.J. (2011). Class IIa histone deacetylases are hormone-activated regulators of FOXO and mammalian glucose homeostasis. Cell *145*, 607-621.
Mishra, P., and Chan, D.C. (2014). Mitochondrial dynamics and inheritance during cell division, development and disease. Nature reviews Molecular cell biology *15*, 634-646.
Mokranjac, D., and Neupert, W. (2007). Protein import into isolated mitochondria. Methods in molecular biology *372*, 277-286.
Mori, D., Yano, Y., Toyo-oka, K., Yoshida, N., Yamada, M., Muramatsu, M., Zhang, D., Saya, H., Toyoshima, Y.Y., Kinoshita, K.*, et al.* (2007). NDEL1 phosphorylation by Aurora-A kinase is essential for centrosomal maturation, separation, and TACC3 recruitment. Mol Cell Biol *27*, 352-367.
Musacchio, A. (2011). Spindle assembly checkpoint: the third decade. Philosophical transactions of the Royal Society of London Series B, Biological sciences *366*, 3595-3604.
Musacchio, A. (2015). The Molecular Biology of Spindle Assembly Checkpoint Signaling Dynamics. Current biology : CB *25*, R1002-1018.
Nangaku, M., Sato-Yoshitake, R., Okada, Y., Noda, Y., Takemura, R., Yamazaki, H., and Hirokawa, N. (1994). KIF1B, a novel microtubule plus end-directed monomeric motor protein for transport of mitochondria. Cell *79*, 1209-1220.
Navarro, M.N., Feijoo-Carnero, C., Arandilla, A.G., Trost, M., and Cantrell, D.A. (2014). Protein kinase D2 is a digital amplifier of T cell receptor-stimulated diacylglycerol signaling in naive CD8(+) T cells. Sci Signal *7*, ra99.
Neupert, W., and Herrmann, J.M. (2007). Translocation of proteins into mitochondria. Annual review of biochemistry *76*, 723-749.
Nhek, S., Ngo, M., Yang, X., Ng, M.M., Field, S.J., Asara, J.M., Ridgway, N.D., and Toker, A. (2010). Regulation of oxysterol-binding protein Golgi localization through protein kinase D-mediated phosphorylation. Mol Biol Cell *21*, 2327-2337.
Nothwehr, S.F., Conibear, E., and Stevens, T.H. (1995). Golgi and vacuolar membrane proteins reach the vacuole in vps1 mutant yeast cells via the plasma membrane. J Cell Biol *129*, 35-46.
Oakhill, J.S., Chen, Z.P., Scott, J.W., Steel, R., Castelli, L.A., Ling, N., Macaulay, S.L., and Kemp, B.E. (2010). beta-Subunit myristoylation is the gatekeeper for initiating metabolic stress sensing by AMP-activated protein kinase (AMPK). Proc Natl Acad Sci U S A *107*, 19237-19241.
Oakhill, J.S., Steel, R., Chen, Z.P., Scott, J.W., Ling, N., Tam, S., and Kemp, B.E. (2011). AMPK is a direct adenylate charge-regulated protein kinase. Science *332*, 1433-1435.
Okamoto, K., and Shaw, J.M. (2005). Mitochondrial morphology and dynamics in yeast and multicellular eukaryotes. Annual review of genetics *39*, 503-536.

Okuno, D., Iino, R., and Noji, H. (2011). Rotation and structure of FoF1-ATP synthase. Journal of biochemistry *149*, 655-664.
Olayioye, M.A., and Hausser, A. (2012). Integration of non-vesicular and vesicular transport processes at the Golgi complex by the PKD-CERT network. Biochim Biophys Acta *1821*, 1096-1103.
Olichon, A., Emorine, L.J., Descoins, E., Pelloquin, L., Brichese, L., Gas, N., Guillou, E., Delettre, C., Valette, A., Hamel, C.P.*, et al.* (2002). The human dynamin-related protein OPA1 is anchored to the mitochondrial inner membrane facing the inter-membrane space. FEBS Lett *523*, 171-176.
Olsen, J.V., Vermeulen, M., Santamaria, A., Kumar, C., Miller, M.L., Jensen, L.J., Gnad, F., Cox, J., Jensen, T.S., Nigg, E.A.*, et al.* (2010). Quantitative phosphoproteomics reveals widespread full phosphorylation site occupancy during mitosis. Sci Signal *3*, ra3.
Osellame, L.D., Singh, A.P., Stroud, D.A., Palmer, C.S., Stojanovski, D., Ramachandran, R., and Ryan, M.T. (2016). Cooperative and independent roles of the Drp1 adaptors Mff, MiD49 and MiD51 in mitochondrial fission. J Cell Sci *129*, 2170-2181.
Otera, H., Wang, C., Cleland, M.M., Setoguchi, K., Yokota, S., Youle, R.J., and Mihara, K. (2010). Mff is an essential factor for mitochondrial recruitment of Drp1 during mitochondrial fission in mammalian cells. J Cell Biol *191*, 1141-1158.
Otsuga, D., Keegan, B.R., Brisch, E., Thatcher, J.W., Hermann, G.J., Bleazard, W., and Shaw, J.M. (1998). The dynamin-related GTPase, Dnm1p, controls mitochondrial morphology in yeast. J Cell Biol *143*, 333-349.
Owen, M.R., Doran, E., and Halestrap, A.P. (2000). Evidence that metformin exerts its anti-diabetic effects through inhibition of complex 1 of the mitochondrial respiratory chain. Biochem J *348 Pt 3*, 607-614.
Palmer, C.S., Elgass, K.D., Parton, R.G., Osellame, L.D., Stojanovski, D., and Ryan, M.T. (2013). Adaptor proteins MiD49 and MiD51 can act independently of Mff and Fis1 in Drp1 recruitment and are specific for mitochondrial fission. J Biol Chem *288*, 27584-27593.
Pang, T., Xiong, B., Li, J.Y., Qiu, B.Y., Jin, G.Z., Shen, J.K., and Li, J. (2007). Conserved alpha-helix acts as autoinhibitory sequence in AMP-activated protein kinase alpha subunits. J Biol Chem *282*, 495-506.
Papazyan, R., Doche, M., Waldron, R.T., Rozengurt, E., Moyer, M.P., and Rey, O. (2008). Protein kinase D isozymes activation and localization during mitosis. Experimental cell research *314*, 3057-3068.
Parone, P.A., Da Cruz, S., Tondera, D., Mattenberger, Y., James, D.I., Maechler, P., Barja, F., and Martinou, J.C. (2008). Preventing mitochondrial fission impairs mitochondrial function and leads to loss of mitochondrial DNA. PLoS One *3*, e3257.
Parra, M., Kasler, H., McKinsey, T.A., Olson, E.N., and Verdin, E. (2005). Protein kinase D1 phosphorylates HDAC7 and induces its nuclear export after T-cell receptor activation. J Biol Chem *280*, 13762-13770.
Paweletz, N. (1967). [On the function of the "Flemming body" during division of animal cells]. Die Naturwissenschaften *54*, 533-535.
Pereira, F., Soares, P., Carneiro, J., Pereira, L., Richards, M.B., Samuels, D.C., and Amorim, A. (2008). Evidence for variable selective pressures at a large secondary structure of the human mitochondrial DNA control region. Molecular biology and evolution *25*, 2759-2770.
Poteryaev, D., Squirrell, J.M., Campbell, J.M., White, J.G., and Spang, A. (2005). Involvement of the actin cytoskeleton and homotypic membrane fusion in ER dynamics in Caenorhabditis elegans. Mol Biol Cell *16*, 2139-2153.
Praefcke, G.J., and McMahon, H.T. (2004). The dynamin superfamily: universal membrane tubulation and fission molecules? Nature reviews Molecular cell biology *5*, 133-147.
Preisinger, C., Korner, R., Wind, M., Lehmann, W.D., Kopajtich, R., and Barr, F.A. (2005). Plk1 docking to GRASP65 phosphorylated by Cdk1 suggests a mechanism for Golgi checkpoint signalling. EMBO J *24*, 753-765.
Puhka, M., Joensuu, M., Vihinen, H., Belevich, I., and Jokitalo, E. (2012). Progressive sheet-to-tubule transformation is a general mechanism for endoplasmic reticulum partitioning in dividing mammalian cells. Mol Biol Cell *23*, 2424-2432.

Puhka, M., Vihinen, H., Joensuu, M., and Jokitalo, E. (2007). Endoplasmic reticulum remains continuous and undergoes sheet-to-tubule transformation during cell division in mammalian cells. J Cell Biol *179*, 895-909.
Pusapati, G.V., Krndija, D., Armacki, M., von Wichert, G., von Blume, J., Malhotra, V., Adler, G., and Seufferlein, T. (2010). Role of the second cysteine-rich domain and Pro275 in protein kinase D2 interaction with ADP-ribosylation factor 1, trans-Golgi network recruitment, and protein transport. Mol Biol Cell *21*, 1011-1022.
Rahn, J.J., Stackley, K.D., and Chan, S.S. (2013). Opa1 is required for proper mitochondrial metabolism in early development. PLoS One *8*, e59218.
Ran, F.A., Hsu, P.D., Wright, J., Agarwala, V., Scott, D.A., and Zhang, F. (2013). Genome engineering using the CRISPR-Cas9 system. Nat Protoc *8*, 2281-2308.
Ren, M., Feng, H., Fu, Y., Land, M., and Rubin, C.S. (2009). Protein kinase D is an essential regulator of C. elegans innate immunity. Immunity *30*, 521-532.
Rey, O., and Rozengurt, E. (2001). Protein kinase D interacts with Golgi via its cysteine-rich domain. Biochem Biophys Res Commun *287*, 21-26.
Rossignol, R., Faustin, B., Rocher, C., Malgat, M., Mazat, J.P., and Letellier, T. (2003). Mitochondrial threshold effects. Biochem J *370*, 751-762.
Roth, M.G. (2008). Molecular mechanisms of PLD function in membrane traffic. Traffic *9*, 1233-1239.
Rudolph, M.J., Amodeo, G.A., Iram, S.H., Hong, S.P., Pirino, G., Carlson, M., and Tong, L. (2007). Structure of the Bateman2 domain of yeast Snf4: dimeric association and relevance for AMP binding. Structure *15*, 65-74.
Russo, G.J., Louie, K., Wellington, A., Macleod, G.T., Hu, F., Panchumarthi, S., and Zinsmaier, K.E. (2009). Drosophila Miro is required for both anterograde and retrograde axonal mitochondrial transport. The Journal of neuroscience : the official journal of the Society for Neuroscience *29*, 5443-5455.
Saldivar, J.C., Cortez, D., and Cimprich, K.A. (2017). The essential kinase ATR: ensuring faithful duplication of a challenging genome. Nature reviews Molecular cell biology *18*, 622-636.
Saxton, W.M., and Hollenbeck, P.J. (2012). The axonal transport of mitochondria. J Cell Sci *125*, 2095-2104.
Scott, J.W., Hawley, S.A., Green, K.A., Anis, M., Stewart, G., Scullion, G.A., Norman, D.G., and Hardie, D.G. (2004). CBS domains form energy-sensing modules whose binding of adenosine ligands is disrupted by disease mutations. The Journal of clinical investigation *113*, 274-284.
Shaw, R.J., Kosmatka, M., Bardeesy, N., Hurley, R.L., Witters, L.A., DePinho, R.A., and Cantley, L.C. (2004). The tumor suppressor LKB1 kinase directly activates AMP-activated kinase and regulates apoptosis in response to energy stress. Proc Natl Acad Sci U S A *101*, 3329-3335.
Shaw, R.J., Lamia, K.A., Vasquez, D., Koo, S.H., Bardeesy, N., Depinho, R.A., Montminy, M., and Cantley, L.C. (2005). The kinase LKB1 mediates glucose homeostasis in liver and therapeutic effects of metformin. Science *310*, 1642-1646.
Sheng, Z.H., and Cai, Q. (2012). Mitochondrial transport in neurons: impact on synaptic homeostasis and neurodegeneration. Nature reviews Neuroscience *13*, 77-93.
Sherr, C.J. (1993). Mammalian G1 cyclins. Cell *73*, 1059-1065.
Shima, D.T., Haldar, K., Pepperkok, R., Watson, R., and Warren, G. (1997). Partitioning of the Golgi apparatus during mitosis in living HeLa cells. J Cell Biol *137*, 1211-1228.
Smirnova, E., Griparic, L., Shurland, D.L., and van der Bliek, A.M. (2001). Dynamin-related protein Drp1 is required for mitochondrial division in mammalian cells. Mol Biol Cell *12*, 2245-2256.
Smirnova, E., Shurland, D.L., Ryazantsev, S.N., and van der Bliek, A.M. (1998). A human dynamin-related protein controls the distribution of mitochondria. J Cell Biol *143*, 351-358.
Song, K., Backs, J., McAnally, J., Qi, X., Gerard, R.D., Richardson, J.A., Hill, J.A., Bassel-Duby, R., and Olson, E.N. (2006). The transcriptional coactivator CAMTA2 stimulates cardiac growth by opposing class II histone deacetylases. Cell *125*, 453-466.
Song, Z., Ghochani, M., McCaffery, J.M., Frey, T.G., and Chan, D.C. (2009). Mitofusins and OPA1 mediate sequential steps in mitochondrial membrane fusion. Mol Biol Cell *20*, 3525-3532.

Spelbrink, J.N., Li, F.Y., Tiranti, V., Nikali, K., Yuan, Q.P., Tariq, M., Wanrooij, S., Garrido, N., Comi, G., Morandi, L.*, et al.* (2001). Human mitochondrial DNA deletions associated with mutations in the gene encoding Twinkle, a phage T7 gene 4-like protein localized in mitochondria. Nature genetics *28*, 223-231.
Spitaler, M., Emslie, E., Wood, C.D., and Cantrell, D. (2006). Diacylglycerol and protein kinase D localization during T lymphocyte activation. Immunity *24*, 535-546.
Srivastava, P., and Panda, D. (2007). Rotenone inhibits mammalian cell proliferation by inhibiting microtubule assembly through tubulin binding. The FEBS journal *274*, 4788-4801.
Stepanyants, N., Macdonald, P.J., Francy, C.A., Mears, J.A., Qi, X., and Ramachandran, R. (2015). Cardiolipin's propensity for phase transition and its reorganization by dynamin-related protein 1 form a basis for mitochondrial membrane fission. Mol Biol Cell *26*, 3104-3116.
Storz, P., Doppler, H., Johannes, F.J., and Toker, A. (2003). Tyrosine phosphorylation of protein kinase D in the pleckstrin homology domain leads to activation. J Biol Chem *278*, 17969-17976.
Storz, P., Doppler, H., and Toker, A. (2005). Protein kinase D mediates mitochondrion-to-nucleus signaling and detoxification from mitochondrial reactive oxygen species. Mol Cell Biol *25*, 8520-8530.
Stowers, R.S., Megeath, L.J., Gorska-Andrzejak, J., Meinertzhagen, I.A., and Schwarz, T.L. (2002). Axonal transport of mitochondria to synapses depends on milton, a novel Drosophila protein. Neuron *36*, 1063-1077.
Strack, S., and Cribbs, J.T. (2012). Allosteric modulation of Drp1 mechanoenzyme assembly and mitochondrial fission by the variable domain. J Biol Chem *287*, 10990-11001.
Strack, S., Wilson, T.J., and Cribbs, J.T. (2013). Cyclin-dependent kinases regulate splice-specific targeting of dynamin-related protein 1 to microtubules. J Cell Biol *201*, 1037-1051.
Subathra, M., Qureshi, A., and Luberto, C. (2011). Sphingomyelin synthases regulate protein trafficking and secretion. PLoS One *6*, e23644.
Sumara, G., Formentini, I., Collins, S., Sumara, I., Windak, R., Bodenmiller, B., Ramracheya, R., Caille, D., Jiang, H., Platt, K.A.*, et al.* (2009). Regulation of PKD by the MAPK p38delta in insulin secretion and glucose homeostasis. Cell *136*, 235-248.
Sumara, I., Gimenez-Abian, J.F., Gerlich, D., Hirota, T., Kraft, C., de la Torre, C., Ellenberg, J., and Peters, J.M. (2004). Roles of polo-like kinase 1 in the assembly of functional mitotic spindles. Current biology : CB *14*, 1712-1722.
Sunkel, C.E., and Glover, D.M. (1988). polo, a mitotic mutant of Drosophila displaying abnormal spindle poles. J Cell Sci *89 (Pt 1)*, 25-38.
Sutterlin, C., Hsu, P., Mallabiabarrena, A., and Malhotra, V. (2002). Fragmentation and dispersal of the pericentriolar Golgi complex is required for entry into mitosis in mammalian cells. Cell *109*, 359-369.
Sutterlin, C., Lin, C.Y., Feng, Y., Ferris, D.K., Erikson, R.L., and Malhotra, V. (2001). Polo-like kinase is required for the fragmentation of pericentriolar Golgi stacks during mitosis. Proc Natl Acad Sci U S A *98*, 9128-9132.
Suzuki, A., Okamoto, S., Lee, S., Saito, K., Shiuchi, T., and Minokoshi, Y. (2007). Leptin stimulates fatty acid oxidation and peroxisome proliferator-activated receptor alpha gene expression in mouse C2C12 myoblasts by changing the subcellular localization of the alpha2 form of AMP-activated protein kinase. Mol Cell Biol *27*, 4317-4327.
Suzuki, M., Jeong, S.Y., Karbowski, M., Youle, R.J., and Tjandra, N. (2003). The solution structure of human mitochondria fission protein Fis1 reveals a novel TPR-like helix bundle. J Mol Biol *334*, 445-458.
Taguchi, N., Ishihara, N., Jofuku, A., Oka, T., and Mihara, K. (2007). Mitotic phosphorylation of dynamin-related GTPase Drp1 participates in mitochondrial fission. J Biol Chem *282*, 11521-11529.
Tanaka, T., Cosma, M.P., Wirth, K., and Nasmyth, K. (1999). Identification of cohesin association sites at centromeres and along chromosome arms. Cell *98*, 847-858.
Tanaka, T.U., Rachidi, N., Janke, C., Pereira, G., Galova, M., Schiebel, E., Stark, M.J., and Nasmyth, K. (2002). Evidence that the Ipl1-Sli15 (Aurora kinase-INCENP) complex promotes chromosome bi-orientation by altering kinetochore-spindle pole connections. Cell *108*, 317-329.

Tanaka, Y., Kanai, Y., Okada, Y., Nonaka, S., Takeda, S., Harada, A., and Hirokawa, N. (1998). Targeted disruption of mouse conventional kinesin heavy chain, kif5B, results in abnormal perinuclear clustering of mitochondria. Cell *93*, 1147-1158.
Thyberg, J., and Moskalewski, S. (1992). Reorganization of the Golgi complex in association with mitosis: redistribution of mannosidase II to the endoplasmic reticulum and effects of brefeldin A. Journal of submicroscopic cytology and pathology *24*, 495-508.
Toji, S., Yabuta, N., Hosomi, T., Nishihara, S., Kobayashi, T., Suzuki, S., Tamai, K., and Nojima, H. (2004). The centrosomal protein Lats2 is a phosphorylation target of Aurora-A kinase. Genes to cells : devoted to molecular & cellular mechanisms *9*, 383-397.
Toyama, E.Q., Herzig, S., Courchet, J., Lewis, T.L., Jr., Loson, O.C., Hellberg, K., Young, N.P., Chen, H., Polleux, F., Chan, D.C.*, et al.* (2016). Metabolism. AMP-activated protein kinase mediates mitochondrial fission in response to energy stress. Science *351*, 275-281.
Uhlmann, F., Lottspeich, F., and Nasmyth, K. (1999). Sister-chromatid separation at anaphase onset is promoted by cleavage of the cohesin subunit Scc1. Nature *400*, 37-42.
Vagnarelli, P., Ribeiro, S., Sennels, L., Sanchez-Pulido, L., de Lima Alves, F., Verheyen, T., Kelly, D.A., Ponting, C.P., Rappsilber, J., and Earnshaw, W.C. (2011). Repo-Man coordinates chromosomal reorganization with nuclear envelope reassembly during mitotic exit. Dev Cell *21*, 328-342.
van der Bliek, A.M. (1999). Functional diversity in the dynamin family. Trends Cell Biol *9*, 96-102.
Viana, R., Towler, M.C., Pan, D.A., Carling, D., Viollet, B., Hardie, D.G., and Sanz, P. (2007). A conserved sequence immediately N-terminal to the Bateman domains in AMP-activated protein kinase gamma subunits is required for the interaction with the beta subunits. J Biol Chem *282*, 16117-16125.
Villani, M., Subathra, M., Im, Y.B., Choi, Y., Signorelli, P., Del Poeta, M., and Luberto, C. (2008). Sphingomyelin synthases regulate production of diacylglycerol at the Golgi. Biochem J *414*, 31-41.
Villeneuve, J., Scarpa, M., Ortega-Bellido, M., and Malhotra, V. (2013). MEK1 inactivates Myt1 to regulate Golgi membrane fragmentation and mitotic entry in mammalian cells. EMBO J *32*, 72-85.
Volpe, P., and Eremenko, T. (1973). Nuclear and cytoplasmic DNA synthesis during the mitotic cycle of HeLa cells. European journal of biochemistry *32*, 227-232.
von der Malsburg, A., Abutbul-Ionita, I., Haller, O., Kochs, G., and Danino, D. (2011). Stalk domain of the dynamin-like MxA GTPase protein mediates membrane binding and liposome tubulation via the unstructured L4 loop. J Biol Chem *286*, 37858-37865.
Waizenegger, I.C., Hauf, S., Meinke, A., and Peters, J.M. (2000). Two distinct pathways remove mammalian cohesin from chromosome arms in prophase and from centromeres in anaphase. Cell *103*, 399-410.
Wang, Q.J. (2006). PKD at the crossroads of DAG and PKC signaling. Trends Pharmacol Sci *27*, 317-323.
Wang, Y., Seemann, J., Pypaert, M., Shorter, J., and Warren, G. (2003). A direct role for GRASP65 as a mitotically regulated Golgi stacking factor. EMBO J *22*, 3279-3290.
Wasilewski, M., Chojnacka, K., and Chacinska, A. (2017). Protein trafficking at the crossroads to mitochondria. Biochim Biophys Acta *1864*, 125-137.
Waterham, H.R., Koster, J., van Roermund, C.W., Mooyer, P.A., Wanders, R.J., and Leonard, J.V. (2007). A lethal defect of mitochondrial and peroxisomal fission. N Engl J Med *356*, 1736-1741.
Wei, J.H., Zhang, Z.C., Wynn, R.M., and Seemann, J. (2015). GM130 Regulates Golgi-Derived Spindle Assembly by Activating TPX2 and Capturing Microtubules. Cell *162*, 287-299.
Wei, N., Chu, E., Wipf, P., and Schmitz, J.C. (2014). Protein kinase d as a potential chemotherapeutic target for colorectal cancer. Molecular cancer therapeutics *13*, 1130-1141.
Welburn, J.P., Vleugel, M., Liu, D., Yates, J.R., 3rd, Lampson, M.A., Fukagawa, T., and Cheeseman, I.M. (2010). Aurora B phosphorylates spatially distinct targets to differentially regulate the kinetochore-microtubule interface. Mol Cell *38*, 383-392.
Wenger, J., Klinglmayr, E., Frohlich, C., Eibl, C., Gimeno, A., Hessenberger, M., Puehringer, S., Daumke, O., and Goettig, P. (2013). Functional mapping of human dynamin-1-like GTPase domain based on x-ray structure analyses. PLoS One *8*, e71835.
Whitburn, J., Edwards, C.M., and Sooriakumaran, P. (2017). Metformin and Prostate Cancer: a New Role for an Old Drug. Current urology reports *18*, 46.

Wilker, P.R., Kohyama, M., Sandau, M.M., Albring, J.C., Nakagawa, O., Schwarz, J.J., and Murphy, K.M. (2008). Transcription factor Mef2c is required for B cell proliferation and survival after antigen receptor stimulation. Nature immunology *9*, 603-612.
Wille, C., Kohler, C., Armacki, M., Jamali, A., Gossele, U., Pfizenmaier, K., Seufferlein, T., and Eiseler, T. (2014). Protein kinase D2 induces invasion of pancreatic cancer cells by regulating matrix metalloproteinases. Mol Biol Cell *25*, 324-336.
Wozniak, M.J., Bola, B., Brownhill, K., Yang, Y.C., Levakova, V., and Allan, V.J. (2009). Role of kinesin-1 and cytoplasmic dynein in endoplasmic reticulum movement in VERO cells. J Cell Sci *122*, 1979-1989.
Wurzenberger, C., and Gerlich, D.W. (2011). Phosphatases: providing safe passage through mitotic exit. Nature reviews Molecular cell biology *12*, 469-482.
Xiang, S.Y., Ouyang, K., Yung, B.S., Miyamoto, S., Smrcka, A.V., Chen, J., and Heller Brown, J. (2013). PLCepsilon, PKD1, and SSH1L transduce RhoA signaling to protect mitochondria from oxidative stress in the heart. Sci Signal *6*, ra108.
Xiang, Y., Seemann, J., Bisel, B., Punthambaker, S., and Wang, Y. (2007). Active ADP-ribosylation factor-1 (ARF1) is required for mitotic Golgi fragmentation. J Biol Chem *282*, 21829-21837.
Xiao, B., Heath, R., Saiu, P., Leiper, F.C., Leone, P., Jing, C., Walker, P.A., Haire, L., Eccleston, J.F., Davis, C.T.*, et al.* (2007). Structural basis for AMP binding to mammalian AMP-activated protein kinase. Nature *449*, 496-500.
Xiao, B., Sanders, M.J., Underwood, E., Heath, R., Mayer, F.V., Carmena, D., Jing, C., Walker, P.A., Eccleston, J.F., Haire, L.F.*, et al.* (2011). Structure of mammalian AMPK and its regulation by ADP. Nature *472*, 230-233.
Xu, X., Gera, N., Li, H., Yun, M., Zhang, L., Wang, Y., Wang, Q.J., and Jin, T. (2015). GPCR-mediated PLCbetagamma/PKCbeta/PKD signaling pathway regulates the cofilin phosphatase slingshot 2 in neutrophil chemotaxis. Mol Biol Cell *26*, 874-886.
Xu, X., Ha, C.H., Wong, C., Wang, W., Hausser, A., Pfizenmaier, K., Olson, E.N., McKinsey, T.A., and Jin, Z.G. (2007). Angiotensin II stimulates protein kinase D-dependent histone deacetylase 5 phosphorylation and nuclear export leading to vascular smooth muscle cell hypertrophy. Arterioscler Thromb Vasc Biol *27*, 2355-2362.
Yang, L., Guan, T., and Gerace, L. (1997). Integral membrane proteins of the nuclear envelope are dispersed throughout the endoplasmic reticulum during mitosis. J Cell Biol *137*, 1199-1210.
Ye, Q., Callebaut, I., Pezhman, A., Courvalin, J.C., and Worman, H.J. (1997). Domain-specific interactions of human HP1-type chromodomain proteins and inner nuclear membrane protein LBR. J Biol Chem *272*, 14983-14989.
Yi, T., Zhai, B., Yu, Y., Kiyotsugu, Y., Raschle, T., Etzkorn, M., Seo, H.C., Nagiec, M., Luna, R.E., Reinherz, E.L.*, et al.* (2014). Quantitative phosphoproteomic analysis reveals system-wide signaling pathways downstream of SDF-1/CXCR4 in breast cancer stem cells. Proc Natl Acad Sci U S A *111*, E2182-2190.
Yuan, J., Rey, O., and Rozengurt, E. (2006). Activation of protein kinase D3 by signaling through Rac and the alpha subunits of the heterotrimeric G proteins G12 and G13. Cell Signal *18*, 1051-1062.
Yuan, J., and Rozengurt, E. (2008). PKD, PKD2, and p38 MAPK mediate Hsp27 serine-82 phosphorylation induced by neurotensin in pancreatic cancer PANC-1 cells. J Cell Biochem *103*, 648-662.
Zaal, K.J., Smith, C.L., Polishchuk, R.S., Altan, N., Cole, N.B., Ellenberg, J., Hirschberg, K., Presley, J.F., Roberts, T.H., Siggia, E.*, et al.* (1999). Golgi membranes are absorbed into and reemerge from the ER during mitosis. Cell *99*, 589-601.
Zadra, G., Photopoulos, C., Tyekucheva, S., Heidari, P., Weng, Q.P., Fedele, G., Liu, H., Scaglia, N., Priolo, C., Sicinska, E.*, et al.* (2014). A novel direct activator of AMPK inhibits prostate cancer growth by blocking lipogenesis. EMBO molecular medicine *6*, 519-538.
Zhang, T., Braun, U., and Leitges, M. (2016). PKD3 deficiency causes alterations in microtubule dynamics during the cell cycle. Cell cycle *15*, 1844-1854.
Zhang, Y., Gao, X., and Garavito, R.M. (2011). Biochemical characterization of human dynamin-like protein 1. Journal of biochemistry *150*, 627-633.

Zhang, Z., Meszaros, G., He, W.T., Xu, Y., de Fatima Magliarelli, H., Mailly, L., Mihlan, M., Liu, Y., Puig Gamez, M., Goginashvili, A.*, et al.* (2017). Protein kinase D at the Golgi controls NLRP3 inflammasome activation. J Exp Med *214*, 2671-2693.
Zhou, G., Myers, R., Li, Y., Chen, Y., Shen, X., Fenyk-Melody, J., Wu, M., Ventre, J., Doebber, T., Fujii, N.*, et al.* (2001). Role of AMP-activated protein kinase in mechanism of metformin action. The Journal of clinical investigation *108*, 1167-1174.
Zuchner, S., Mersiyanova, I.V., Muglia, M., Bissar-Tadmouri, N., Rochelle, J., Dadali, E.L., Zappia, M., Nelis, E., Patitucci, A., Senderek, J.*, et al.* (2004). Mutations in the mitochondrial GTPase mitofusin 2 cause Charcot-Marie-Tooth neuropathy type 2A. Nature genetics *36*, 449-451.
Zunino, R., Braschi, E., Xu, L., and McBride, H.M. (2009). Translocation of SenP5 from the nucleoli to the mitochondria modulates DRP1-dependent fission during mitosis. J Biol Chem *284*, 17783-17795.

Olga BIELSKA

The role of PKD in mitochondrial fission during mitosis

Résumé

Au cours des deux dernières décennies, plusieurs études ont découvert et renforcé l'implication de la dynamique mitochondriale dans le cancer. Au cours de ma thèse, j'ai découvert un rôle inattendu des protéines kinases de la famille PKD dans la fission mitochondriale. La perte de l'activité PKD a conduit à un blocage de la fission mitochondriale et a entraîné une élongation significative des mitochondries par fusion continue. D'un point de vue mécanique, nous avons montré que les protéines PKD régule la dynamique mitochondriale en activant le facteur de fission mitochondrial (MFF) par phosphorylation de plusieurs sites. MFF agit comme un récepteur principal de la GTPase DRP1, qui resserre les mitochondries, et il est essentiel à une bonne division mitochondriale. Les trois membres de la famille PKD peuvent phosphoryler MFF. La phosphorylation de MFF est médiée par PKD et la fragmentation mitochondriale se produit spécifiquement pendant la mitose. Comme démontré dans plusieurs études mondiales sur les phosphoprotéomes, la phosphorylation du MFF est significativement augmentée dans les cancers très mitotiques. Ainsi, l'axe de signalisation PKD-MFF régulant la dynamique mitochondriale en mitose pourrait devenir une voie thérapeutique attrayante pour le traitement du cancer.

Résumé en anglais

Over the last two decades, multiple studies have uncovered and strengthen the implication of mitochondrial dynamics in cancer. During my thesis, I discovered an unanticipated role for the PKD kinase family in mitochondrial fission. Loss of PKD activity led to blockade of mitochondrial fission and resulted in a significant elongation of mitochondria by unopposed fusion. Mechanistically, we showed that PKDs regulated mitochondrial dynamics by activating the mitochondrial fission factor (MFF) through phosphorylation of multiple sites. MFF acts as a main receptor for the large GTPase DRP1, which constricts mitochondria, and it is critical for proper mitochondrial division. All three PKD family members could phosphorylate MFF. PKD-mediated MFF phosphorylation and mitochondrial fragmentation occurred specifically during mitosis. As MFF phosphorylation was found to be significantly upregulated in highly mitotic cancers, which was evidenced in several global phosphoproteome studies, the discovered PKD-MFF signaling axis regulating mitochondrial dynamics in mitosis could become an attractive therapeutic avenue for cancer treatment.